Master Thesis, Department of Geosciences

Palynofacies and palynology of the Cenomanian-Turonian deposits in ODP 174AX Bass River core, New Jersey

Depositional environment, vegetation history, petroleum potential and climate changes during the Oceanic Anoxic Event 2

Thomas Løkken Rustad

UNIVERSITY OF OSLO

FACULTY OF MATHEMATICS AND NATURAL SCIENCES

Palynofacies and palynology of the Cenomanian-Turonian deposits in ODP 174AX Bass River core, New Jersey

Depositional environment, vegetation history, petroleum potential and climate changes during the Oceanic Anoxic Event 2

Thomas Løkken Rustad

Master Thesis in Geosciences

Discipline: Geology

Department of Geosciences

Faculty of Mathematics and Natural Sciences

University of Oslo

September 2013

Tutors: Prof. Wolfram M. Kürschner and Prof. Henning Dypvik.

Front cover illustration: "Flygeøgler over Nordsjøen i midtjura" by R. W. Williams©

This work is published digitally through DUO – Digitale Utgivelser ved UiO

http://www.duo.uio.no

It is also catalogued in BIBSYS (http://www.bibsys.no/english)

Abstract

At the Cenomanian-Turonian (~94 Ma) boundary, sudden and major disruptions in the oceanic systems occurred. The disruptions led to the establishment of worldwide oceanic anoxia and deposition of organic-rich sediments. This event, the C-T Oceanic Anoxic Event (OAE2), is one of several OAEs occurring in the Cretaceous. OAEs are not very well understood and much research has been done since the concept was first proposed. However, the research has almost exclusively been concerned with the mechanisms for unleashing these events and the consequences in the marine environments. Little research has been done concerning the surrounding landmasses and what impact an OAE had on the terrestrial ecosystems.

Palynofacies and palynological analyses with emphasis on the terrestrial palynomorphs were performed on material from the Bass River core ODP 174AX in New Jersey. This material is also used in the PhD-project "Ocean biogeochemistry in the mid-Cretaceous: reconstructing the nutrient-biosphere-climate link" at Utrecht University. Geochemical data from this project were incorporated with the present thesis. The analyses determined the palaeoenvironment, vegetation history, source rock potential of the C-T deposits as well as identifying a possible connection between the OAE2 and climate changes.

The sediments were deposited on a stable, dysoxic, neritic shelf with a strong terrestrial signal from the proximal delta. On adjacent land the vegetation was open-canopied woodland typical for the mid-Cretaceous, southeastern North America, with wetlands surrounding the delta. The heavy influence of the delta or the location is hindering the establishment of anoxia and subsequent organic carbon burial, which is characteristic for OAE2 deposits. However, vegetation changes and geochemical data in the OAE2 interval in Bass River exhibit traits similar to the Plenus Cold Event. This event was probably caused by the rapid carbon burial and CO_2-drawdown during the OAE2.

Keywords: Palynolgy, palynofacies, petroleum potential, vegetation history, depositional environment, climate change, OAE2.

Acknowledgements

First and foremost I would like to thank my supervisors, Wolfram M. Kürschner and Henning Dypvik, this thesis would not have been possible to write without the guidance and support I received from them.

I would like to thank Niels van Helmond at Utrecht University who supplied Wolfram with the samples, subsequently giving me the opportunity to write this thesis, and for his endless supply of geochemical data and knowledge he willingly shared, my biggest regret will always be that I was unable to visit Utrecht University.

I would like to thank Shusheng Hu at Yale University for his assistance in identifying the many spores and pollens and their elusive botanical affinities.

A special thanks goes to Hans Arne Nakrem who found the wonderful illustration for my front page, and for the fact that he attempted to contact the illustrator for me just in case he might have had a more age relevant illustration.

I would like to thank Ragnar with his amazing proof-reading skills, the thesis would have been a sorry sight without you. Also I would thank Andreas, Petter, Thomas and Tord for their assistance in proof-reading and their helpful insights.

I would like to thank all the people from ZEB, especially those of room 217, 219 and the room with the annoying lock, I would not have gotten through the year without the fun coffee breaks and lunches in the kitchen.

Thanks also goes to Steven, Chris and Tess for making the long hours in front of the microscope so much more fun with witty conversations.

Finally I would like to thank my family for their boundless morale support throughout the years of education, and for always believing in me.

Thomas Løkken Rustad
Oslo, September 2nd, 2013

Contents

1. Introduction

The concept of Oceanic Anoxic Event (OAE) has been subject to much study the last four decades, ever since it was first proposed by Schlanger and Jenkyns (1976). This is largely because the trigger for such an event still remains uncertain. What is evident is that disturbances of the ocean system happen and that it creates worldwide oceanic anoxia. The OAEs also lead to organic carbon-rich deposits on a global extent in marine environments and therefore represent economically important petroleum source rocks. In this thesis one of the OAEs, the Cenomanian-Turonian (~94 Ma) Anoxic Oceanic Event (also known as OAE2 and Bonarelli Event), will be the subject of study.

1.1 Motivation

The marine nature of Oceanic Anoxic Events apparently has led to a skewness in the research and publications about these events. Even though many include a number of fields when conducting a study, such as lithostratigraphy, chemostratigraphy, biostratigraphy, palynology and palynofacies analysis and geochemical analyses (e.g. Sugarman et al., 1999; Miller et al., 2004; Takashima et al., 2009; Peyrot et al., 2011; Zobaa et al., 2011), terrestrial organisms and input are at best used to establish pollen zonation for age correlation. In geochemical papers (e.g Erbacher et al., 2002; Eleson and Bralower, 2005; Jenkyns, 2010; Sinninghe Damsté et al., 2010) terrestrial matter is hardly used; TEX86, organic δ^{13} carbon, TOC are almost explicitly derived from marine organic matter. Even in Palynofacies and palynology analyses (e.g. Zobaa et al., 2011; Götz et al., 2008) particulate organic matter of terrestrial origin are only applied in the palynofacies part; Any in depth analysis of palynomorphs are strictly of marine origin.

The consequences on land such as impact on terrestrial ecosystems during an OAE is seldom considered. One of the proposed driving mechanisms for triggering OAEs are increased continental weathering and subsequent terrestrial runoff and nutrient enrichment of oceanic systems (e.g. Jarvis et al., 2011; Monteiro et al., 2012), which will be considered in this thesis. However, only Eaton et al. (1997) has done study of the non-marine consequences, in this case

extinctions, of an OAE.

1.2 Purpose of the thesis

The main goal for this thesis is to do a palynological and palynofacies analysis of Cenomanian-Turonian Oceanic Anoxic Event deposits. The material studied comes from the New Jersey Coastal Plain on the east coast of North America and was collected from the Bass river core ODP 174AX (Figure 1.1).

Originally the core was drilled with the purpose to establish a high resolution chronostratigraphy, sequence stratigraphy and eustacy (Miller et al., 1998; Sugarman et al., 1999; Miller et al., 2002, 2004). Although these previous studies include interpretation of the depositional environment and biostratigraphy, they do not dwell upon any redox conditions and vegetation patterns. A palynologogical analysis was primary conducted to determine pollen zonations for the chronostratigraphy (See Miller et al., 1998 and reference within for more details). However, the previous interpretation of the depositional environment will be included in this study, to quality control and to have comparative data.

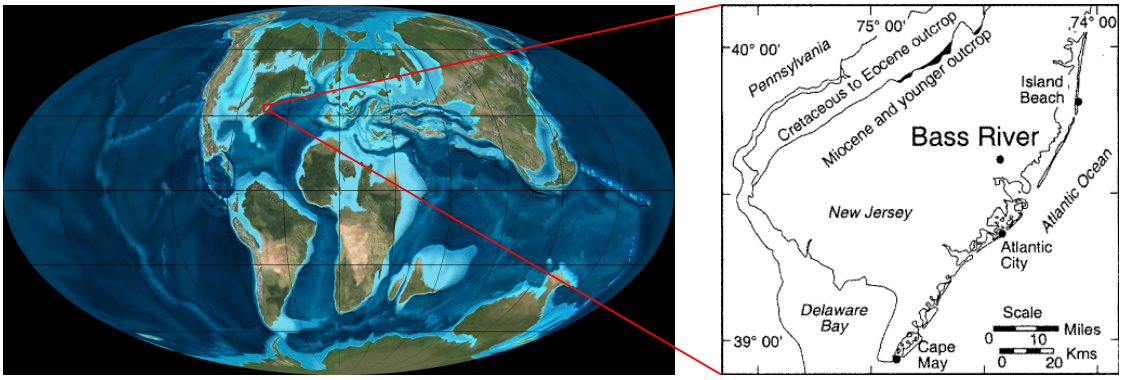

Figure 1.1 Location of the core ODP 174AX with approximate palynogeography to the left and present day to the right (Modified from Blakey and Colorado Plateau Geosystems Inc, 2013 and Sugarman et al., 1999)

A palynological approach allows the study of both the marine and terrestrial signal in one sample. As the neritic Cretaceous sediments were deposited close to the coast, the terrestrial signal is expected to be strong enough to show significant results.

Palynofacies analysis, as previously done by Götz et al. (2008) and Zobaa et al. (2011), will also be conducted to determine depositional environment and verify sea level changes. The analysis also enables assessment of the petroleum potential of the OAE2 black shales in the Bass River.

More specifically, this study is conducted to shed new light on the formation of black shales in the OAE2, in particular tackling the following research

questions:

1. What is the contribution of the terrestrial runoff to the increased OM accumulation of OAE2.
2. What kind of changes took place in the terrestrial ecosystems in association with the OAE2.
3. What is the depositional environment and redox conditions of the OAE2 on the New Jersey shelf?
4. What is the source rock potential of the black shales?

The study is in close collaboration with a current PhD project entitled "*Ocean biogeochemistry in the mid-Cretaceous: reconstructing the nutrient-biosphere-climate link*" at the Biomarine Science group at Utrecht University, The Netherlands. Whereas present thesis covers the palynofacies and terrestrial palynomorphs, the PhD project is combining a study of the marine palynomorphs and geochemical data. The PhD project is conducted by PhD student Niels van Helmond and supervised by Prof. H. Brinkhuis. Niels van Helmond provided the samples used in present thesis, as well as the results from the geochemical analyses, which has been applied as an independent correlations tools and quality control of the results.

2. Background

2.1 A palynological approach

Palynology is the study of organic microfossils, consisting of at least partly very resistant organic molecules, found in maceration preparation of sedimentary rocks (Traverse, 2007). In palynological analysis the focus is on the organic microfossils, the palynomorphs. In palynofacies the spectrum is broader, palynomorphs as well as all visible non-palynomorph palynological matter, collectively known as palynodebris, are included (Traverse, 2007).

2.2 The Cretaceous greenhouse world

The Cretaceous period spans from 145 to 66 Ma (Gradstein et al., 2012), and are characterised as a greenhouse world with high sea level and warm, predominantly ice-free climates (Jahren, 2002; Takashima et al., 2006; Kaufmann and Johnson, 2009). It began with a cool, temperate climate in the Early Cretaceous, followed by the warm to extremely warm mid- and Late Cretaceous (Kaufmann and Johnson, 2009).

The increase in temperature was largely caused by elevated global igneous activity. Increasing oceanic accretion and formations of Large Igneous Provinces (LIPs) contributed with outgassing of enormous amounts of CO_2 (Figure 2.1.A) (Takashima et al., 2006; Coiffard et al., 2012). Consequently the outgassing increased the temperature; global average ocean temperatures in the Cretaceous has been calculated to be ~6-12 °C higher than today (Kaufmann and Johnson, 2009; Price, 2009). Thus the North and South Polar and Sub-polar climatic zones was replaced in favour of a Cold, Mild and Warm Temperate zonation (Figure 2.1.B). Although evidence suggests an Antarctica with slush caps and developed ice in shorter colder periods, it is assumed that it was primarily ice free climates (Kaufmann and Johnson, 2009). The lack of permanent ice resulted in a low equator to pole thermal gradient and, combined with the elevated tectonic activity, a much higher sea level than today (Takashima et al., 2006; Price, 2009).

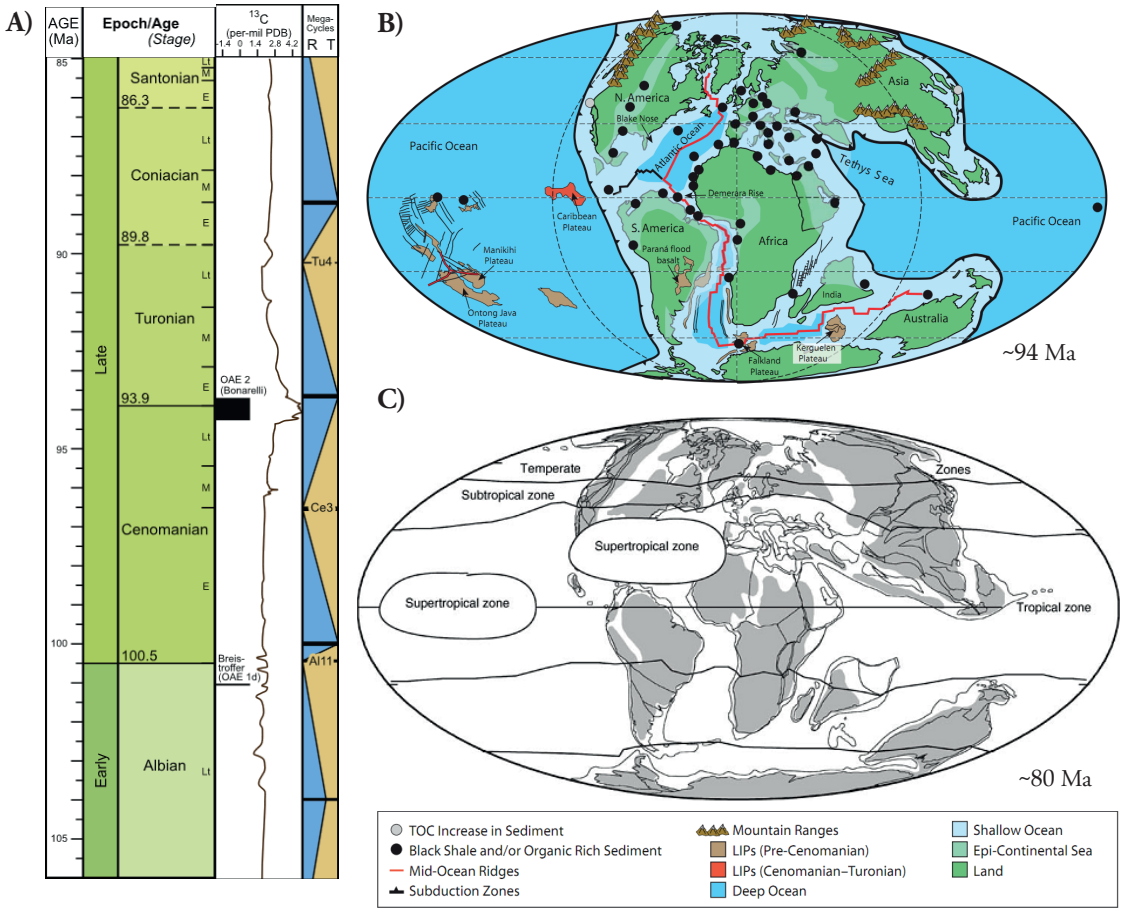

Figure 2.1 A) Time scale of mid-Cretaceous with global sea level megasequences and ^{13}C curve (modified from Gradstein et al., 2012). **B)** Distribution of black shales and/or increased TOC content in sediments, major LIPs and epicontinental seas at OEA2 (Takashima et al., 2006, see paper for further references). **C)** Climate zonation in the Cretaceous. Cold Mild, Warm temperate zones at the highest latitudes. Subtropical, Tropical and Supertropical zones expansion in the warmest periods (Kaufmann and Johnson, 2009, see paper for further references).

2.2.1 Climatology

The Cretaceous climate was largely controlled by sea level fluctuations relying on the atmosphere and ocean current for heat transfer. At highstand, continental seaways connected the Arctic Ocean with tropical oceans (Figure 2.1.B). These seaways brought tropical humidity and relatively high temperatures north and cool water south (Kaufmann and Johnson, 2009). This effective heat exchange kept Polar coastal areas, such as the northern Alaska, above freezing point and the average winter temperature of the Arctic Ocean at ~6 °C (Herman and Spicer, 1997).

At highstand in Cenomanian-Turonian the sea eustasy and temperature was at the Cretaceous maxima; the sea level was ~100-200 meter higher than the current sea level, submerging up to 40% of the continents, and had mean annual temperatures in the Arctic at 14 °C or higher (Figure 2.1.A) (Haq et al., 1987; Tarduno et al., 1998; Miller et al., 2005; Price, 2009). In the Northern Hemi-

sphere the Temperate zone stretched from the polar region to the Canadian-US border, followed by a subtropical zone extending down to the tropics in the southern part of the Gulf Coast states and north-central Mexico (Figure 2.1.B) (Kaufmann and Johnson, 2009). Areas close to the equator, such as Puerto Rico, Cuba, northern Colombia and Venezuela, periodically reached unusually high temperatures and salinities, creating a supertropical zone (Figure 2.1.B) (Kaufmann and Johnson, 2009). In the low latitudes (e.g. northern Africa, the Gulf of Mexico, South America, middle East) aridity indicators, such as evaporites, characterize a warm climate with low soil moisture (Price, 2009). At higher latitudes extensive coal deposits in Northern Eurasia and Eastern Europe as well as an abundance of coal in the US indicate prevailing year-round moist-wet conditions (Price, 2009).

2.2.2 Vegetation trends

The vegetation in Cretaceous is marked by the evolution of and rise of the dominion of flowering plants, the angiosperms. In Early Cretaceous the floras were dominated by ferns, conifers and cycads, with the early angiosperms comprising of small woody plants confined to disturbed, understorey sites in wet climate at low latitudes (Feild et al., 2004; Heimhofer et al., 2005; Feild et al., 2009). With the increasing temperature and humidity in Aptian-Albian, the angiosperms began to diversify and colonize the floodplain as understorey vegetation beneath coniferous canopy (Coiffard et al., 2012). The angiosperms also began to expand towards higher latitudes, reaching the poles by the end of Albian (Spicer et al., 1993). This initial low latitude radiation of angiosperms is common in North America (Lupia et al., 1999), Europe (Coiffard et al., 2012) and Australia (Nagalingum et al., 2002). By the Mid Cretaceous the angiosperms were both abundant and diverse, while many free-sporing bryphytes and ferns as well as some non-coniferous gymnosperms was on the decline (Lupia et al., 1999).

Throughout the Jurassic and Cretaceous the Northern Hemisphere was divided into the Siberian-Canadian and Indo-European provinces (Traverse, 2007). The provinces were based upon distinctive palynomorphs, restricted by geographic and stratigraphic distribution and with broadly latitudinal boundaries (Traverse, 2007). In Mid-Late Cretaceous he interior seaways in North America and Siberia formed effective barriers creating two provinces (Saward, 1992). They were the Normapolles province, stretching eastward from mid-continent North America to western Asia, and the *Aquilapollenites-Wodehouseia* province ranging east from eastern Asia to central North America (Traverse, 2007).

Wolfe and Upchurch (1987) performed analyses of physiognomy of leaf assemblages and structural adaptations of dicotyledonous woods. By doing this they were able to indicate North American Late Cretaceous vegetation and climate patterns.

At low latitudes the vegetation was open-canopy evergreen woodland and scrub adapted to low to moderate, evenly distributed rainfall throughout the year. The woodland probably had large massive trees, the tallest among them evergreen conifers, as well as wind-pollinating plants.

Climate at higher latitudes had mild seasonally variations. Although there were some large trees, the vegetation comprised mostly of small trees and shrubs, primarily evergreen conifers, forming humid, open woodlands (Wolfe and Upchurch, 1987; Spicer et al., 1993). These woodlands stretched to very high latitudes, evidence of rich fern, gymnosperm and angiosperm floras are found in Greenland, Siberia and Antarctica (Price, 2009). However, seasonality of light probably caused evergreen species to be replaced with deciduous vegetation (Wolfe and Upchurch, 1987).

2.2.3 Oceanic Anoxic Events

OAEs are characterised by a rapid onset, short duration ($\pm$0.5 m.y.), often significant positive shift in the organic and inorganic stable carbon isotopes ($\delta^{13}C/\delta^{12}C$ ratio), drop in carbonate content, and widespread distribution of organic carbon-rich deposits (Takashima et al., 2006; Sageman, 2009; Jenkyns, 2010). The deposits are often relatively thin but widespread intervals of shales, in many cases within thick limestone sequences, such as the Bonarelli horizon in Italy. The significant changes in stable carbon isotopes and other geochemical proxies suggest environments with elevated primary productions, benthic oxygen deficiency and widespread organic carbon burial (Schlanger and Jenkyns, 1976; Arthur et al., 1988; Jenkyns, 2010).

In total 9 possible Oceanic Anoxic Events with various geographic extent and evidence have been identified in the Phanerozoic, 6 of them in Cretaceous (Takashima et al., 2006; Sageman, 2009; Jenkyns, 2010). Only two have sedimentary records in all basins and thus can be called a worldwide Oceanic Anoxic Event: the early Aptian OAE (OAE1a) and the Cenomanian-Turonian (C/T) boundary OAE (also known as the Bonarelli Event and OAE2) (Leckie et al., 2002; Erbacher et al., 2002; Eleson and Bralower, 2005).

A consequence of the disturbances in the ocean system is evident in the fossil record. Some of the OAEs, such as OAE2, are also among the major Phanerozoic mass extinctions. The expansion of anoxic environments during OAE2 led to a

high turnover rate in marine microfossils. In less than 1 million years 20% of marine organisms in various environments became extinct (Takashima et al., 2006). Eaton et al. (1997) also noted that fresh-water vertebrates and riparian organisms (e.g. turtles) experience significant extinction in this period. The turnover in fresh water and riparian organisms is probably associated with loss of habitat because of eustatic changes. Other terrestrial organisms however, indicated no turnover rate above normal background rate.

OAEs are believed to be caused by the complex interplay of fundamental Earth processes, rather than one triggering mechanism (Kump and Arthur, 1999; Barclay, 2011). Processes such as volcanism, rates of continental weathering, oceanic overturn and stratification, and nutrient available led to the large-scale changes in the geochemical cycles that marks the OAEs (Barclay, 2011). Because of the multiple mechanisms involved in the OAEs, the circumstances surrounding the OAEs remain uncertain (Barclay, 2011). Kump and Arthur (1999) were able to successfully recreated the same amount of carbon burial, some with identical isotope signature, by combining different sets of mechanisms. Therefore are the forcing mechanisms for each OAE not necessarily the same, and thus the OAEs must be considered individually in terms of driving mechanisms (Barclay, 2011).

The Oceanic Anoxic Event 2

Across the C-T boundary (~94 Ma) sudden warming of deep water disrupted the sluggish circulating oceans and collapsed the vertical stratification (Huber et al., 1999). Warming of deep sea water led to upwelling of nutrient rich deep oceanic water to the surface. The oceanic disruptions marked the onset of the OAE2, which lasted for approximately 500 k.y. (Sageman et al., 2006).

The disruption of the oceanic systems has largely been connected to a large-scale magmatic activity before the onset of OAE2 (Turgeon and Creaser, 2008; Adams et al., 2010; Barclay, 2011; Jenkyns, 2010). Increased volcanic outgassing led to high atmospheric CO_2 concentration, and subsequently a warmer climate (Barclay, 2011). Deep water warming can also have caused release and oxidation of buried methane hydrates (Takashima et al., 2006). Released gas hydrates would have depleted the oxygen solubility in deep ocean settings and further increased the CO_2 concentration in the atmosphere (Takashima et al., 2006). Additionally, warmer climate would lead to an intensifying of chemical weathering on the continents (Barclay et al., 2010). Increased weathering would bring more nutrients, such as phosphate, into the oceans from fluvial inputs (Schlanger and Jenkyns, 1976; Jenkyns, 2010; Monteiro et al., 2012).

Nutrient enrichment led to enhanced primary production, which in turn

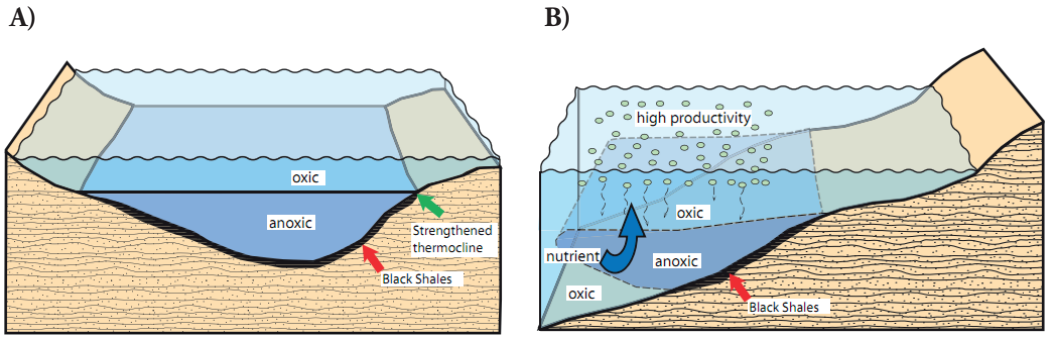

Figure 2.2 Representative models for black shale depositions: **A)** The stagnant ocean model. **B)** The oxygen minimum zone model

caused an expansion of the oxygen minimum zone (OMZ) (Huber et al., 1999; Takashima et al., 2006). Rapid expansion of the OMZ is one of two proposed models for the OAEs, the second being stagnant ocean model (Figure 2.2) (see Takashima et al., 2006 and references therein for further details). Modelling of the expansion of oceanic anoxia during the OAE2 suggest an increase from ~5% before the onset to at least ~50% during the OAE2 (Monteiro et al., 2012).

2.3 The study area

2.3.1 Regional geology

Bass River lies within the boundary of the New Jersey Coastal Plain (Figure 2.3.A), which is part of the greater Atlantic Coastal Plain. The Atlantic Coastal Plain is a seaward thickening sedimentary wedge that lies atop the Paleozoic crystalline basement. It stretches along the east coast of the US, from Florida to Long Island (Bally and Palmer, 1989).

The sediments began to accumulate as a consequence of the rifting and break up of the supercontinent Pangaea in the Mesozoic. By Triassic the North American plate had started to break up and drift away from the African and European plate (Nystuen et al., 2008). In Mid Jurassic the rifting had ended and the subsequent subsidence, caused by thermal cooling of the continental crust, commenced. Following the subsidence, the newly formed Central Atlantic Ocean began to submerge the Canadian and North American continental margins (Bally and Palmer, 1989). In turn, shallow marine sediments began to onlap progressively atop the post-rift unconformity (Figure 2.3.B). Now the Atlantic Coastal plain was fully formed and part of the eastern North American passive margin, stretching from the Bahamas to Baffin Bay in Canada (Bally and Palmer, 1989).

Throughout the upper Cretaceous the strata of New Jersey Coastal Plain has

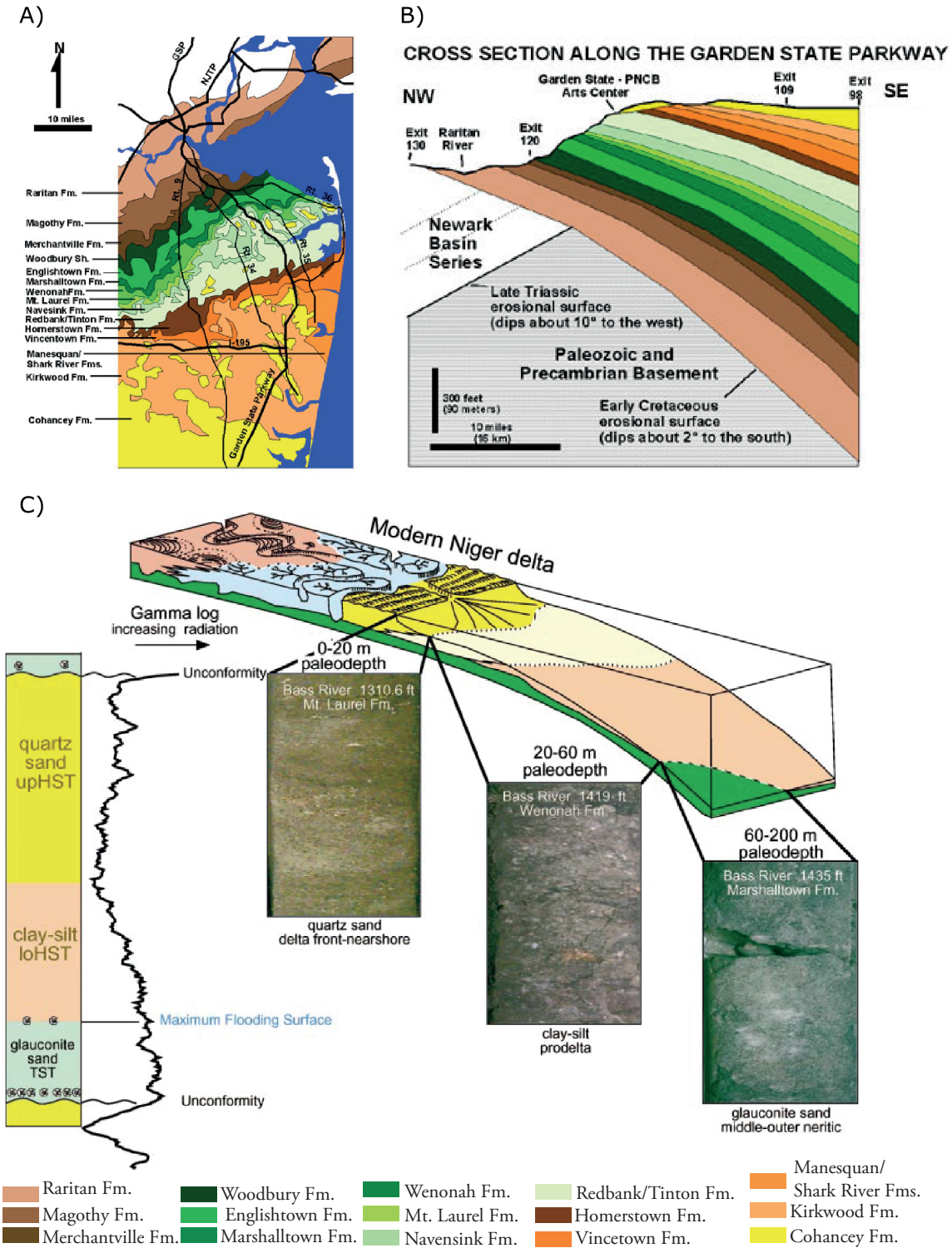

Figure 2.3 A) Geologic map of the Coastal Plain in eastern New Jersey and New York City (U.S. Geological Survey, 2013). **B)** Generalised cross section of the Coastal Plain along with a portion of the Garden State Parkway in eastern New Jersey (U.S. Geological Survey, 2013). **C)** Anatomy of a New Jersey Upper Cretaceous sequence with a facies model for the modern Niger River Delta (Miller et al., 2004).

been noted to have transgressive-regressive cycles (Miller et al., 2004). In general the facies is deltaically influenced marine-shelf facies, where transgressive shelf glauconite beds are overlain by prodelta silts and delta-front sands (Miller et al., 2004). A modern analogue to this type of depositional environment is the wave-dominated Niger Delta (Figure 2.3.C) (Miller et al., 2004).

2.3.2 The Bass River Formation

The stratigraphy of the New Jersey Coastal Plain consists of different sedimentary formations. They are divided by age and overlying unconformily atop the pre-Cretaceous basement (Figure 2.4). The formations range from the oldest, basal Potomac formation from Early Cenomanian to recent glacial and fluvial deposits (Stanford et al., 2004; U.S. Geological Survey, 2013). Together the formations cover an unbroken record, excluding the hiatuses, of the past 100 million years of sediment deposition in the region.

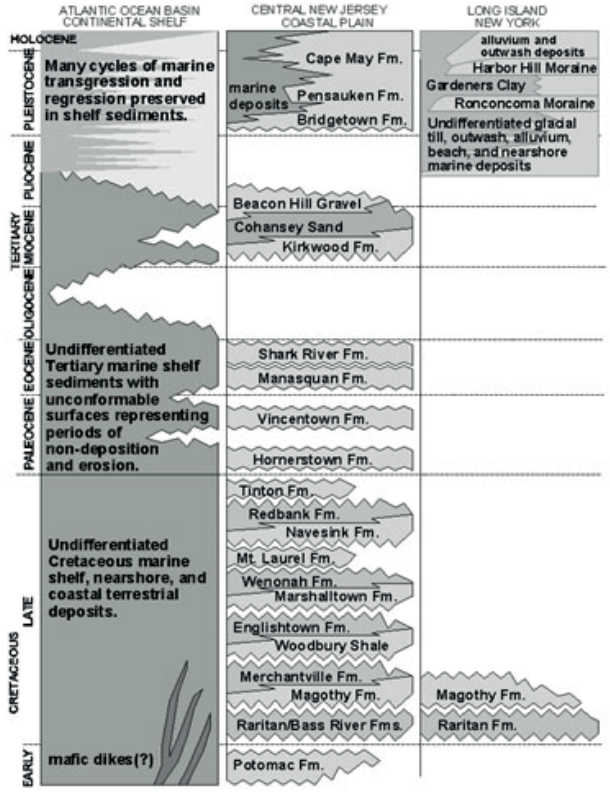

Figure 2.4 The Cretaceous and Cenozoic stratigraphy of the coastal plain of The New York Bight region (U.S. Geological Survey, 2013)

Unconformily atop the Potomac Formation lie the lateral equivalents Bass River and Raritan Formation (U.S. Geological Survey, 2013). Both are deposits from the Late Cenomanian to Early Turonian. The Raritan formation is found in

outcrops (Figure 2.3.B), meanwhile the Bass River Formation can only be found subsurface. The Raritan Formation contains both fluvial and marine sediments and the Bass River Formation is fully marine (Miller et al., 2004; U.S. Geological Survey, 2013). Miller et al. (2004) defined 3 sequences, Bass River I, II, III, within the Bass River Formation. In the Bass River borehole only the uppermost sequence, Bass River III, was recognised, from 1806.4 ft to the total core depth of 1956.4 ft (Miller et al., 2004).

The Bass River III in ODP 174AX consists of prodeltaic micaceous, silty clay deposits with a sedimentation rate exceeding 31 m/m.y. (Miller et al., 2004). At the base it is slightly glauconitic and at the top it contains mica and shells, which reflects open shelf and prodelta environments interfingering (Figure 2.5) (Miller et al., 2004). Paleodepths range from inner to middle-neritic with some intervals of prodelta and delta front/nearshore deposits (Miller et al., 2004). The total variation of the waterdepth within the sequence was relatively small (~20 m) (Miller et al., 2004).

Benthic foraminiferal biofacies indicate several distinct parasequences bound by flooding surfaces, from inner to middle neritic palaeodepths (Figure 2.5, Sugarman et al., 1999). The four parasequences had shallowing upwards trends and durations of ~350-460 k.y. (Sugarman et al., 1999).

Based on organic δ^{13} carbon and δ^{13}C data from the foraminiferas, the Oceanic Anoxic Event 2 begins at 1945 ft (Sugarman et al., 1999; Bowman and Bralower, 2005), and ends around 1900 ft (van Helmond, 2013). The Cenomanian-Turonian boundary are defined by the nannofossil zone CC10 and CC11 transition, in Bass River III this is placed at 1935.5 ft (Sugarman et al., 1999).

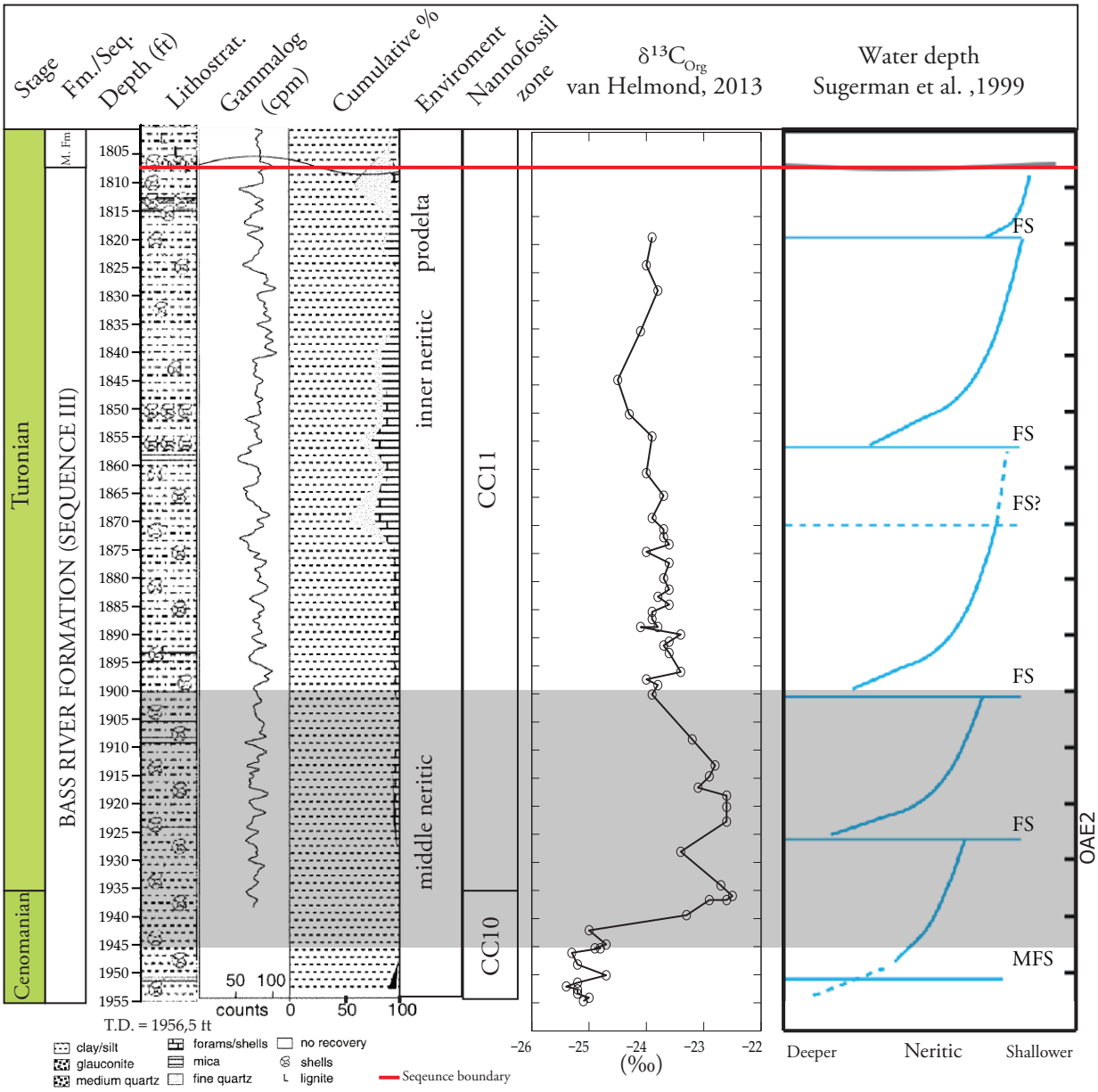

Figure 2.5 The Cenomanian-Turonian section in the Bass River core ODP 174AX, New Jersey displaying: Stage; formation; core depth in feet; generalised lithology and sequence boundary (red line); downhole gamma log; cumulative percent of clay-silt, fine sand, medium to coarse sand, glauconite, shells and mica; palaeoenvironment; nannofossil zonations; organic ^{13}Carbon content and generalised water depth (M. Fm. = Magothy Formation) (After Sugarman et al., 1999, Miller et al., 2002, Miller et al., 2004 and van Helmond, 2013). The OAE2 inteval is highlighted in gray.

3. Material and methods

3.1 Samples

Bass River Core ODP174AX was chosen because of the high sedimentation rate, the position of the core, coastal plain and shelf facies, and the excellent preservation of marine and terrestrial palynomorphs as well as biomarkers. In addition there is a high abundance of foraminifera (van Helmond, 2013), which altogether allows high resolution studies on sediments that contains both terrestrial and marine input.

Samples were acquired from the core by Niels van Helmond in connection with his PhD project. In total 71 samples were taken for palynological analysis (see Appendix B for full list of samples). In addition samples were taken for geochemical analyses, conducted by the Laboratory of Palaeobotany and Palynology at Utrecht University, The Netherlands, such as TEX86, $CaCO_3$, TOC and $\delta^{13}C$ content (see Appendix C for full list of data).

3.2 Slide preparation

Palynological processing and slide preparation was done by the Laboratory of Palaeobotany and Palynology at Utrecht University (van Helmond, 2013). The processing was done according to their standardised quantitative methods. Between 3 and 14 g of sediments was slightly crushed (5mm>) and a known amount of *Lycopodium* marker spores was added to the sediment sample. The marker spores are added in order to enable quantification of the palynomorph counts.

The samples were treated with ~30% hydrochloric acid (HCl) to dissolve carbonates, subsequently followed by ~38% hydrofluoric acid (HF) treatment for dissolution of silicates. After decantation of the solution, ultrasonic separation was employed. For sieving of the samples a 15 µm nylon mesh was used and the residues were mounted on slides for microscopic analysis.

3.3 Geochemical proxies

Geochemical proxies and palynological and palynofacies analyses goes hand in hand. Some geochemical proxies, such as organic matter content (wt% total organic carbon, TOC), amount of carbonate (wt% $CaCO_3$) and the isotopic composition of organic matter ($\delta^{13}C_{org}$) provide indications of palaeoenvirnment and palaeoclimate. These proxies are a useful addition, in terms of comparative data and data enhancement, and quality control of the analyses.

The geochemical analyses was performed by the Laboratory of Palaeobotany and Palynology at Utrecht University, the Netherlands. Following proxies were used in this thesis: TOC, $CaCO_3$, Titanium, Aluminium and $\delta^{13}C_{org}$ content, and the TEX_{86} index. The Ratio between Titanium and Aluminium are an indication of aeolian terrestrial input (Bertrand et al., 1996; Rachold and Brumsack, 2001). The TEX_{86} index are a sea surface temperature proxy but it needs calibration. In this study it was calibrated with a logarithmic function for TEX_{86}^{H} proposed in Kim et al., 2010. These authors suggest that the TEX_{86}^{H} calibration were the best suited for high index values.

3.4 Analysis

The palynofacies and palynological analysis are both conducted with a light microscope. For each slide at least 300 organic particles were categorised and counted followed by identification of at least 300, if possible, sporomorphs for the palynofacies and palynological analyses (More details in Sections 3.5 and 3.6). As mentioned in Section 1.2, the palynological analysis will emphasise on the terrestrial input, the sporomorphs. Thus only the sporomorphs were identified and accounted for.

In addition to light microscopy, several slides with the highest content of amorphous organic matter were chosen for fluorescent light analysis. Particulate organic matter can react to the exposure to fluorscent light, depends on the origin of the material, and thus are a useful property to utilize when conducting a palynofacies analysis.

The components can be presented as relative (%) and absolute (g^{-1}) abundance. The relative abundance is the components' percentages of the total sum. The absolute abundance is the concentration of pollen per gram dry sample, and is calculated by the use of the *Lycopodium* marker spores.

The results were calculated and plotted in diagrams by the use of the software Tilia and Microsoft Office Excel, graphs plotted in MATLAB and all figures and graphs were annotated with Adobe Illustrator.

3.5 Palynofacies

The presence of organic particles other than palynomorphs in maceration residue slides was noted early on. Thus over the years many have done systematic studies on all particulate organic matter (POM), both palynomorphs and palynodebris, and attempted to classify the different groups of particles. The classifications have been subjective and with a certain scientific goal in mind, which have resulted in a range of different classifications (Traverse, 2007).

In this study the methodology and classification are modified after Tyson (1995) and modernised with Traverse (2007) (Table 3.1) (see Sections 3.5.1 to 3.5.3 for further details). These authors' approach on palynofacies is well suited to the purpose of this thesis: The results with this classification can be readily applied to determination of petroleum potential, depositional environment, terrestrial influx and redox conditions.

The distinctive, total assemblage of all POM observed in a sample is called palynofacies. Like other facies, a palynofacies represents a specific sedimentary depositional environment (Powell et al., 1990).

Table 3.1 Classification of sedimentary organic matter, see text for further descriptions (based on Tyson, 1995 and Traverse (2007))

	GROUP		CONSTITUTENT
STRUCTURED	Phytoclast		Opaque phytoclast Translucent woody tissue Cuticles Plant tissue
	Palynomorph	Green algea	Prasinophytes
		Sporomorph	Spores Bissaccate pollen non-bissacate pollen
		Marine palynomorph	Acritarchs Dinoflagellate cysts
		Zoomorph	Foraminiferal linings
STRUCTURELESS	Amorphous organic material		Degraded terrestrial organic matter Degraded aquatic organic matter

3.5.1 Phytoclasts

Phytoclasts are remains and debris from higher plants (Tyson, 1995). The phytoclast group can be divided into two major groups, the translucent and the opaque phytoclasts.

Translucent phytoclasts

The translucent phytoclasts are subdivided into wood remains, cuticles and plant tissue.

The wood particles are woody tissue from plants. They have brown translucent material, often observed with biostructures such as holes or stripes in them.

The cuticles are leaf cuticles (Tyson, 1995). They appear translucent, light coloured and retain their cellular structure which make them easily recognisable.

The plant tissue is from the cellulose, non-woody part of the plant (Tyson, 1995). They are brown translucent material, but unlike the wood remains they also have cellular structure.

Opaque phytoclasts

The opaque phytoclasts (opaques) are oxidised or carbonised wood, including charcoal (Tyson, 1995). The charcoal originate from forest fires, and the wood has been postdepositionally oxidised or carbonised with burial. The opaques are completely black and can be divided in two by their form, the equidimensional (length:width < 3) and blade-shaped (length:width > 3) (Tyson, 1995).

3.5.2 Amorphous organic matter

The amorphous organic matter (AOM) are either of aquatic or terrestrial origin (Tyson, 1995). The aquatic AOM can originate from organic aggregates or faecal pellets from zooplankton and bacteria (Tyson, 1995). The terrestrial AOM can be resins secreted from or a result of biodegredation of higher plants (Tyson, 1995). AOM appear like completely structureless, translucent, often grey, bubbly mass in the microscope.

3.5.3 Palynomorphs

The palynomorph group encompasses all organic microfossils. The components can be derived from either plants or animals, such as the sporomorphs, dinoflagellate cysts, acritarchs, zoomorphs and algae and algae remains.

Sporomorphs

Sporomorphs, the pollen and spores, are the terrestrial constituent of the palynomorphs. They are a product of the life-cycle of embryophytic plants (Traverse, 2007). The embryophytes are plants that produce true embryos, the spore

producing Bryophytes and ferns, and the pollen producing gymnosperms and angiosperms (Traverse, 2007).

To distinguish the different pollen and spores in palaeopalynology they are identified by morphology.

Spores can be subdivided by the number of laesurae, the 'scar' which shows the contact between spores (Traverse, 2007), either monolete, trilete or alete.

Pollen grains on the other hand are much more morphologically diverse. The nature of pollination varies among the seed plants. Air sacs, monosaccate or bisaccate, are often used to increase buoyancy and thus also the dispersal area. Those without sacs simply use other means for pollen dispersal. In the palynofacies analysis the pollen grains are simply divided into bisaccate and non-bisaccate.

Dinoflagellate cysts

The dinoflagellate are motile, one-celled phytoplankton . They are completely marine organisms and an important primary producer (Traverse, 2007). The dinoflagellates uses two flagella for propulsion.

Dinoflagellates have a non-motile stage in life were they lose the flagellas. They then produce a resting cyst, consisting of decay-resisting organic material, of one or more layers (Traverse, 2007). These cysts can be fossilised and be recognised by the plated surface, apical and antapical horn and processes.

Acritarchs

Like the dinoflagellates the acritarchs are single-celled organisms. Their biological affinity however, is unknown (Traverse, 2007). Most are believed to be resting cysts of phytoplankton, or at least of algae origin. In general acritarchs occur in marine settings, but fresh- and brackish water species have been found (Traverse, 2007). Acritarchs mean "of undecided or doubtful origin" and thus encompass fossil remains with a wide range of different morphologies (Traverse, 2007).

Zoomorphs

The most common of the zoomorphs found in marine POM-assemblages are foraminiferal linings. They are the chitinous inner test of microforaminifera (Traverse, 2007). Although all morphologies occur, foraminiferal linings are almost always planispiral. Typically they have a brown colour and are often translucent at the edges (Tyson, 1995).

Algae

Both freshwater and marine algae and algae parts can be found in palynological slides. They vary in size and shape depending on genus and species. Often they retain their colonial structure, have a lustrous colour and appear clearly under fluorescent light (Tyson, 1995; Traverse, 2007).

3.5.4 Palynofacies analysis

Palynofacies analysis is the study of all organic matter in a sample slide. It can be used as an indicator for depositional environment and an alternative or addition to geochemical analysis in regards for petroleum potential. The relative distribution of the POM in a slide can be applied to facies recognition and palaeoenvironment reconstruction. Significant palynofacies parameters and ratios are described and summarised from Tyson (1995) in Table 3.2.

Table 3.2 Paleoenvironmental significance of palynofacies end-members and proxies used (modified after Tyson, 1995)

PARAMETER	SIGNIFICANCE OF HIGH VALUES
Opaque:other phytoclats ratio	Distal depositional environments, low TOC content indicate oxic conditions.
	Local high influx of charcoal due to wildfires and subsequently increase of runoff.
	Postdepositional oxidation or local reworking from mature sediments, such as beaches, of phytoclasts.
Equdimensional:lath-shaped opaque phytoclast ratio	Low transportation distance. Proximal to fluvio-deltaic source.
Marine:terrestrial palynomorph ratio	Indicate distal setting
Bisaccate:spores ratio	Depositional environment adjacent to land with conifers
	Low absolute abundance of bisaccates; Distal depositional environments away from terrestrial sources or mainly aeolian transportation of sporomorphs.
AOM fluorescence	High amount of fluoresenct AOM indicate marine origin.
Frequency of foraminiferal linings	A normal marine shelf or slope. Can be areas with high productivity and benthic foraminferal biomass.
	Can also be basinal environment with redepositional influx of shallow water carbonate debris.

The relative abundance of the different categories in an assemblage reflects distinct palynofacies.

High relative amount of phytoclasts can indicate a large magnitude of the input of terrestrial organic matter such as a close proximity of fluvio or deltaic sources. In this case the TOC content is medium to high and the phytoclast assemblage is mixed (Tyson, 1995). However, if the TOC content is low and the

phytoclasts are small and opaque the environment is oxidising where the other components are selectively destroyed (Tyson, 1995).

In cases with high relative abundance of AOM, the environment is at least periodically dysoxic to anoxic and has a high preservation rate (Tyson, 1995). Such characteristics are common for a distal depositional environment .

The indications of high relative abundance of palynomorphs depends on the distribution of the different internal components.

When there is a dominance of sporomorphs, the environment can be oxidising, with low AOM content and moderate proximity to river outlets, or hypersaline which causes low production of plant debris and plankton (Tyson, 1995). If the sporomorphs consist of bisaccates and small pollen the environment is distal, stably stratified and the dinoflagellates cyst production are low (Tyson, 1995).

If the dominant components are planktonic they indicate a oxidised environment with high productivity but low AOM preservation. It could be distal shelf area, with either or both distance from any fluvio-deltaic sources and poorly vegetated adjacent land areas (Tyson, 1995).

With this as a background, Tyson (1995) developed a terniary diagram for the relative % between AOM, phytoclasts and palynomorphs, the marine palynofacies APP-diagram Figure 3.1. The diagram apply POM-assemblages to palynofacies, and the defined fields indicate petroleum inclination and depositional environment, including redox conditions (see Table 3.3).

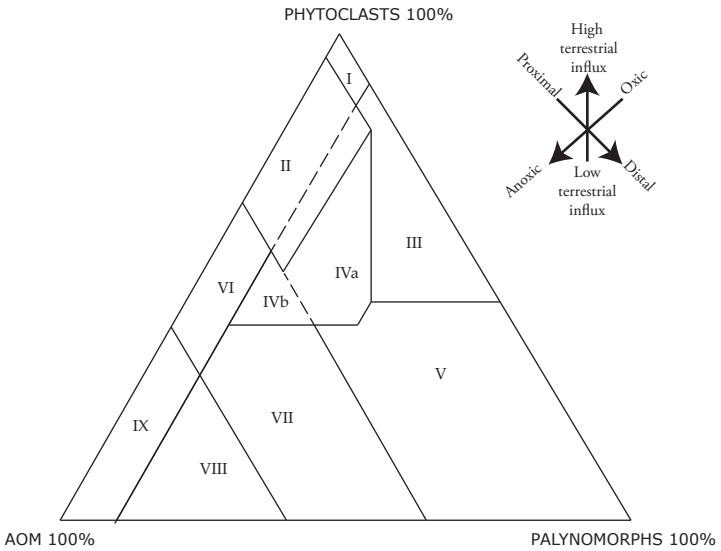

Figure 3.1 Terniary APP-diagram. See Table 3.3 for field explanation (modified after Tyson, 1995)

Table 3.3 Marine palynofacies fields related to the APP-diagram (Figure 3.1) (modified after Tyson, 1995)

PALYNOFACIES FIELD	ENVIRONMENT	PETROLEUM INCLINATION
I	Highly proximal shelf or basin	Gas prone
II	Marginal dysoxic-anoxic basin	Gas prone
III	Heterolithic oxic shelf ('proximal shelf')	Gas prone
IVa	Dysoxic-suboxic shelf or basin transition	Mainly gas prone
IVb	Suboxic-anoxic shelf or basin transition	Mainly gas prone
V	Mud-dominated oxic shelf ('distal shelf')	Gas prone
VI	Proximal suboxic-anoxic shelf	Oil prone
VII	Distal dysoxic-anoxic 'shelf'	Oil prone
VIII	Distal dysoxic-anoxic shelf	Oil prone
IX	Distal suboxic-anoxic basin	Highly oil prone

3.6 Palynology

3.6.1 Taxonomic identification

Spore and pollen grains are products of plant taxa with a distinct morphology. Because of the length of the desired interval of the core, sampling rate, time available and low availability of literature covering this period and area, the level of identification were kept at major morphologically sporomorph groups. Only the most abundant sporomorphs were identified down to at least genus, or if possible species. Although this choice reduces the resolution it became evident as work progressed that pyritisation of the sporomorphs caused problems when attempting to identify them.

The major morphological groups chosen are based on the work of Christopher (1979) on the Raritan and Magothy Formation and displayed in Table 3.4.

3.6.2 Sporomorph EcoGroups

Plants are sensitive indicators for continental environments. They have specific demands on temperature, moisture and soil. Consequently, this makes it possible to interpret sporomorph assemblages in terms of palaeovegetation, ecology and climate (Abbink et al., 2001; Traverse, 2007).

To conduct such reconstructions the sporomorphs need to have a known botanical affinity from a near living relative (Abbink et al., 2001). When working with Quaternary-recent samples this is not a problem; almost all spores and pollen can be appointed with a botanical affinity and ecology. To older sediments on the other hand, this is proven a challenge.

Table 3.4 Morphologic groups, their origin and short description, used for the sporomorph identification in this study (modifed after Christopher, 1979; Traverse, 2007). *= Monosulcate pollen grain can either be produced by gymnosperms or seed ferns

ORIGIN	MORPHOLOGIC GROUP	DESCRIPTION
Ferns and fern allies	Spores	The spores can be identified by their number of laesurae.
Gymnosperms	Monosaccate	Pollen with a single saccus
	Bisaccate	Pollen with two sacci
	Inaperturate	Pollen with no haptotypic features
	Monosulcate*	Pollen with a single colpus
Angiosperms	Tricolpate and tricolporate	Pollen with three colpi without; tricolpate, or with three pores; tricolporate. The colpi are 120 \degree apart viewed from pole. The tricolporate have the pores or other modifications equatorial oriented in each colpi.
	Normapolles and other triporate	Pollen with three equatorial, more or less isodiametric germinal aperture.

*= Monosulcate pollen grain can either be produced by gymnosperms or seed ferns

With increase of sedimentary age the sporomorphs will increasingly represent extinct plant taxa with uncertain botanical affinity and ecological preferences (Abbink et al., 2001). In addition, other influencing aspects must be considered: The nature of pollen and spore production and dispersal.

Plants have different reproduction strategies. Early plants relied on wind and water pollination and developed various means for maximum dispersal. Such strategies can be by producing great amounts of sporomorphs and with morphological adaptations, such as airsacs, for increased travel distance. With the advent of angiosperms insect pollination came as a new strategy, which is effective with relative little amount of pollen.

The various strategies results in different plants producing different amounts of sporomorphs. Differences in sporomorph production can bias the assemblage; the most abundant sporomorph doesn't necessarily need to be the dominant. It could also mean the parental plant produced greater amounts of sporomorphs compared to other plants.

Differences in morphology amongst sporomorphs causes a varied range of travel distance, which must also be considered, especially in marine settings. For example, bisaccate pollen grains have, with their increased buoyancy, the ability to travel greater distances than large and heavy spores. The phenomenon is known as the Neve's effect and is reflected in sporomorph assemblages (Figure 3.2) (Traverse, 2007).

Nevertheless, Abbink et al. (2001) noted that palaeocommunities should be distinctive habitat-bound and characterised by taxa generally favouring the same ecological conditions. Based on this principle Abbink et al. (2001) pre-

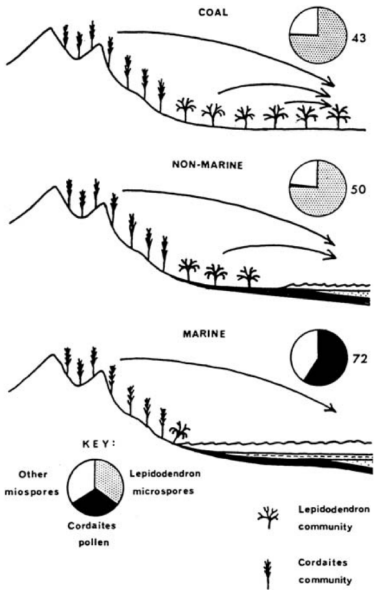

Figure 3.2 Illustration of Neve's effect, where the proportion of upland sporomorphs increases with the distance to shore (Chaloner and Muir, 1968)

sented the conceptual Sporomorph EcoGroup model. The model assigns spores and pollen into different Sporomorph EcoGroups (SEGs). A SEG represents a particular palseocommunity type, a sporomorph source community reflecting vegetation with specific stress and disturbance conditions (Abbink et al., 2001).

For the Jurassic-Early Cretaceous Abbink et al. (2001) defined six distinct SEGS based on plant survival strategies: Upland, lowland, river, pioneer, coastal and tidally influenced (Table 3.5). Although the Bass River Formation is from Late Cretaceous these SEGs are assumed to still be applicable. Many of the same spores and pollen grain are still extant, and eastern North America and Europe belonged to the same palynofloral province throughout the Jurassic and Cretaceous (Traverse, 2007).

In the Jurassic and Early Cretaceous the angiosperms had yet to emerge, and therefore were not considered in the original SEG model by Abbink (1998); Abbink et al. (2001, 2004). This will have to be taken into consideration when assigning taxa into SEGs.

SEG analysis

A SEG analysis enables the establishment of a relative, composite palaeohumidity and palaeotemperature curve for the given interval and SEG (Abbink et al., 2001). Amongst the SEGs, the coastal and lowland are the most receptive to climate change (Abbink et al., 2001) and they will be the main focus in this study.

Table 3.5 Sporomorph EcoGroups (after Abbink et al., 2001)

SEG	REFLECTION	DESCRIPTION
Upland SEG	upland communities	Vegetation on higher terrain well above groundwater level that is never submerged by water.
Lowland SEG	lowland communities	Vegetation on plains and/or in freshwater swamps; the plains may periodically be submerged by freshwater; there is no influence of sea salt, except, perhaps, under extreme circumstances.
River SEG	riverbank communities	Vegetation on riverbanks which are periodically submerged and subject to erosion
Pioneer SEG	pioneer communities	Vegetation at unstable and recently developed ecospace ,e.g. vegetation growing at places that had been submerged by the sea for a longer period.
Coastal SEG	coastal communities	Vegetation growing immediately along the coast, never submerged by the sea but under a constant influence of salt spray.
Tidally influenced SEG	tidally influenced communities	Vegetation influenced by daily tidal changes regularly submerged at high tide.

The analysis is done by calculating of the abundance of warmer and drier elements (in % of total lowland/coastal association); wetter and drier elements (in % of total lowland/coastal association); warm:cold and dry:wet ratios (Abbink et al., 2001). Ideally this should be calculated for both lowland and coastal, but if this is not possible one should suffice.

4. Results

4.1 Palynofacies

In total between 308-427 (avg. 352) particulate organic particles (POM) were identified and counted for each slide (see Appendix D for the complete list of data). The results are displayed in Figures 4.1 to 4.4.

Throughout the studied section the phytoclasts are dominating the total sum of particulate organic matter (TPOM) (Figure 4.3). Of the phytoclasts, the most abundant are the opaques, ranging between 20 and 65% (avg. 39%) of TPOM. The second most abundant are woody remains with 10-30% (avg. 21%), the cuticles and plant tissues are minor contributors with up to 16% (avg 8%) of TPOM (Figure 4.3. Colour on the POM varied between light yellow to yellow in all samples. Additionally, although the degree of abundance varied, clusters of pyrite and pyritisation of TPOM were present in all samples.

The relative abundances of palynomorphs fluctuate greatly in the assemblages throughout the Bass River Formation, spanning between 1-51% (avg 17%) (Figure 4.3. Of the palynomorphs, the aquatic are the dominant group with up to 34% (avg. 11%) of TPOM. Foraminiferal linings are the greatest contributors with 1-18% (avg. 5%), closely followed by dinoflagellate cysts (dinocysts) with 0-13% (avg. 5%). The acritarchs and other algae remains are small contributors with prasinophytes between 0-4% (avg. 1%) and acritarchs up to 1%. The relative abundance of terrestrial palynomorphs are between 1-18% (avg. 6%) of TPOM. Within the terrestrial group the bisaccates are ranging between 1-9% (avg. 3%), other pollen 0-5% (avg. 2%) and spores 0-3% (avg. 1%) of TPOM.

Amorphous organic matter (AOM) is, like the palynomorphs, fluctuating in relative abundance, ranging from 6 to 27% of TPOM. In the fluorescent light analysis the AOM reacted little to none to the exposure to fluorescent light.

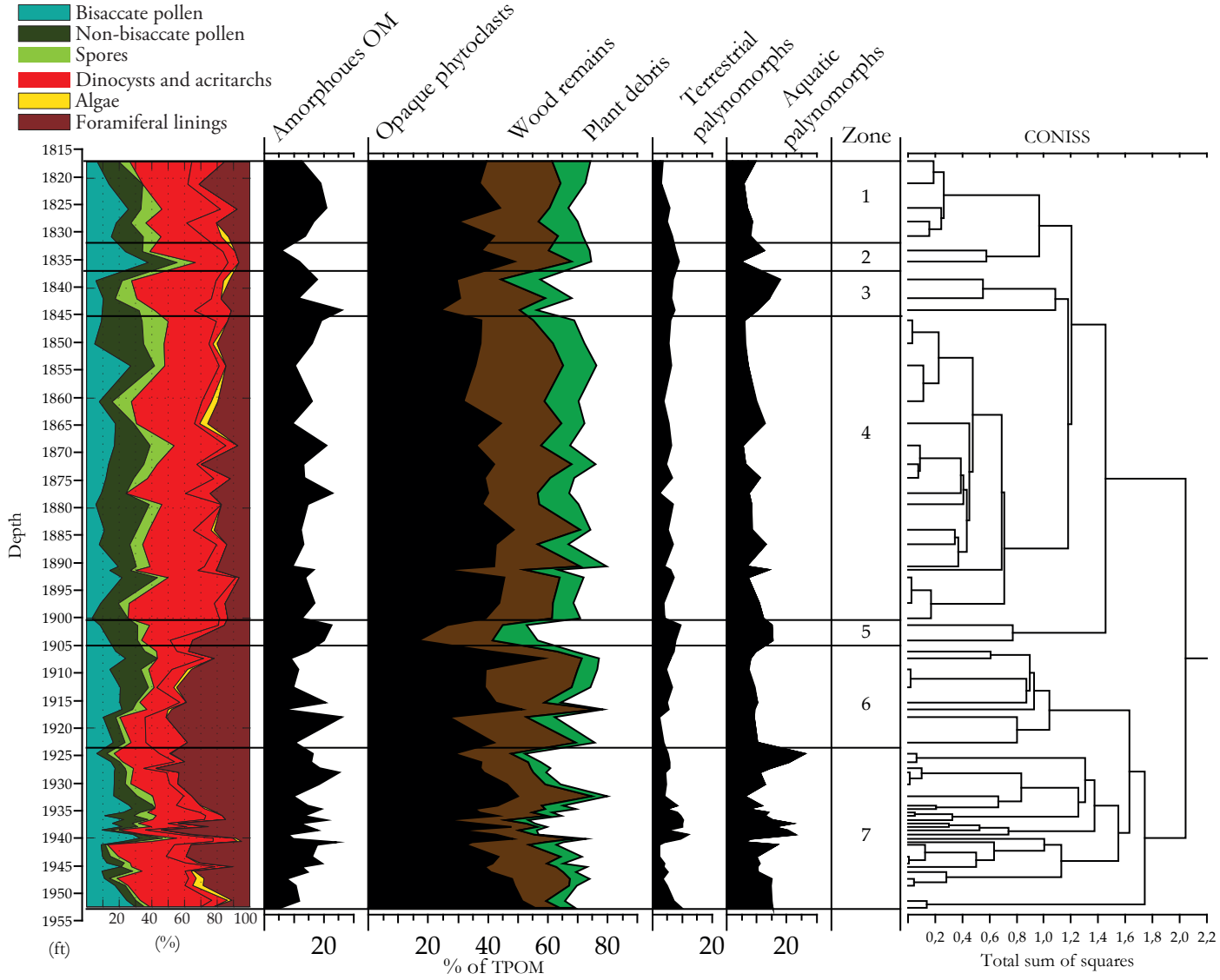

Figure 4.1 Diagram with relative distribution of all palynomorphs correlated with the stacked groups of organic detritus. The cluster analysis was the basis for the determination of palynofacies zonations.

A statistical cluster analysis was performed in Tilia with the TPOM data. The results from the analysis enabled the definition of in total 7 distinct palynofacies assemblage zones throughout the Bass River Formation (Figures 4.1, 4.3 and 4.4), which is described in Section 4.1.1.

In addition, the AOM, palynomorphs and phytoclasts were plotted against each other in the ternary APP-diagram (Figure 4.2.A) (modified after Tyson, 1995) and the AOM correlated with the TOC content (Figure 4.2.B). Based on the APP-diagram the marine facies for the Bass River fluctuate between field II and IVa, with three outliers in field III.

The correlation shows that there is a clear connection between the AOM and TOC, the peaks of TOC and AOM almost always coincide with each other (Figure 4.2).

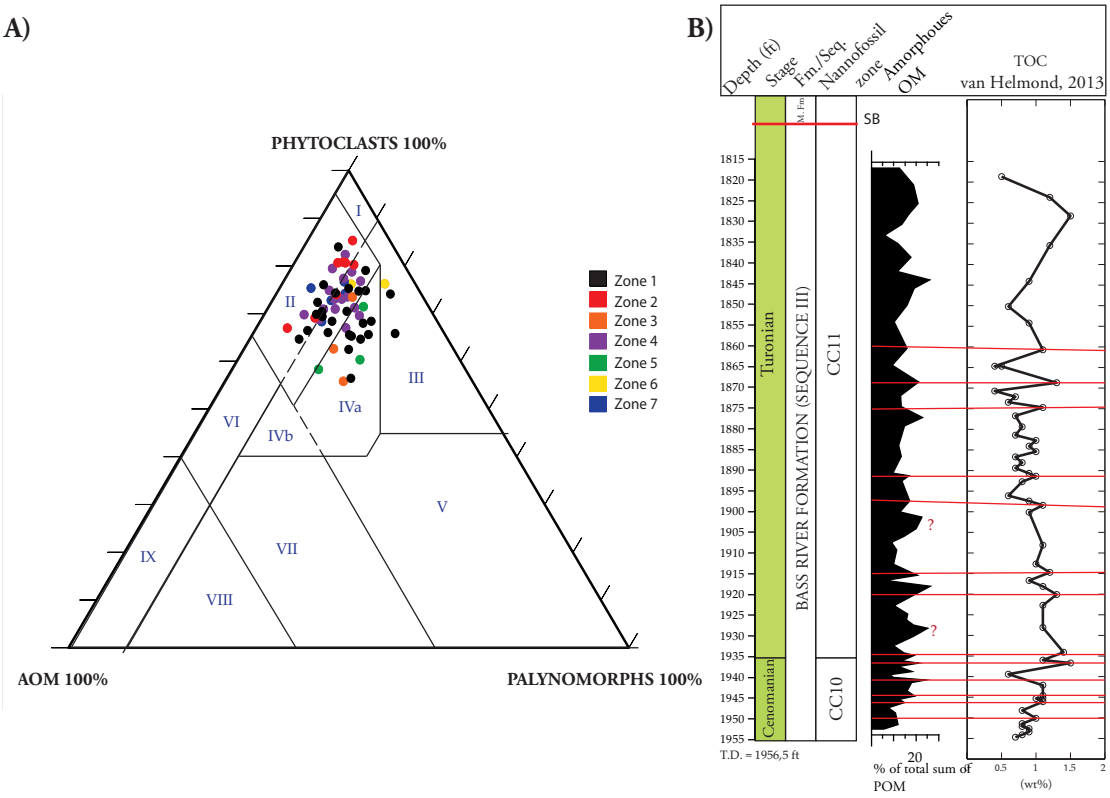

Figure 4.2 A) The palynofacies data plotted in the ternary AOM-Phytoclast-Palynomorph diagram (see Table 4.1 for descriptions of the fields) (modified after Tyson, 1995). **B)** Correlation betweeen the AOM and TOC content in the Bass River Formation.

Table 4.1 Description of the 3 marine palynofacies displayed by the POM assemblages in the Bass River Formation (Figure 4.2) (modified after Tyson, 1995)

PALYNOFACIES FIELD	ENVIRONMENT	PETROLEUM INCLINATION
II	Marginal dysoxic-anoxic basin	Gas prone
III	Heterolithic oxic shelf ('proximal shelf')	Gas prone
IVa	Dysoxic-suboxic shelf or basin transition	Mainly gas prone

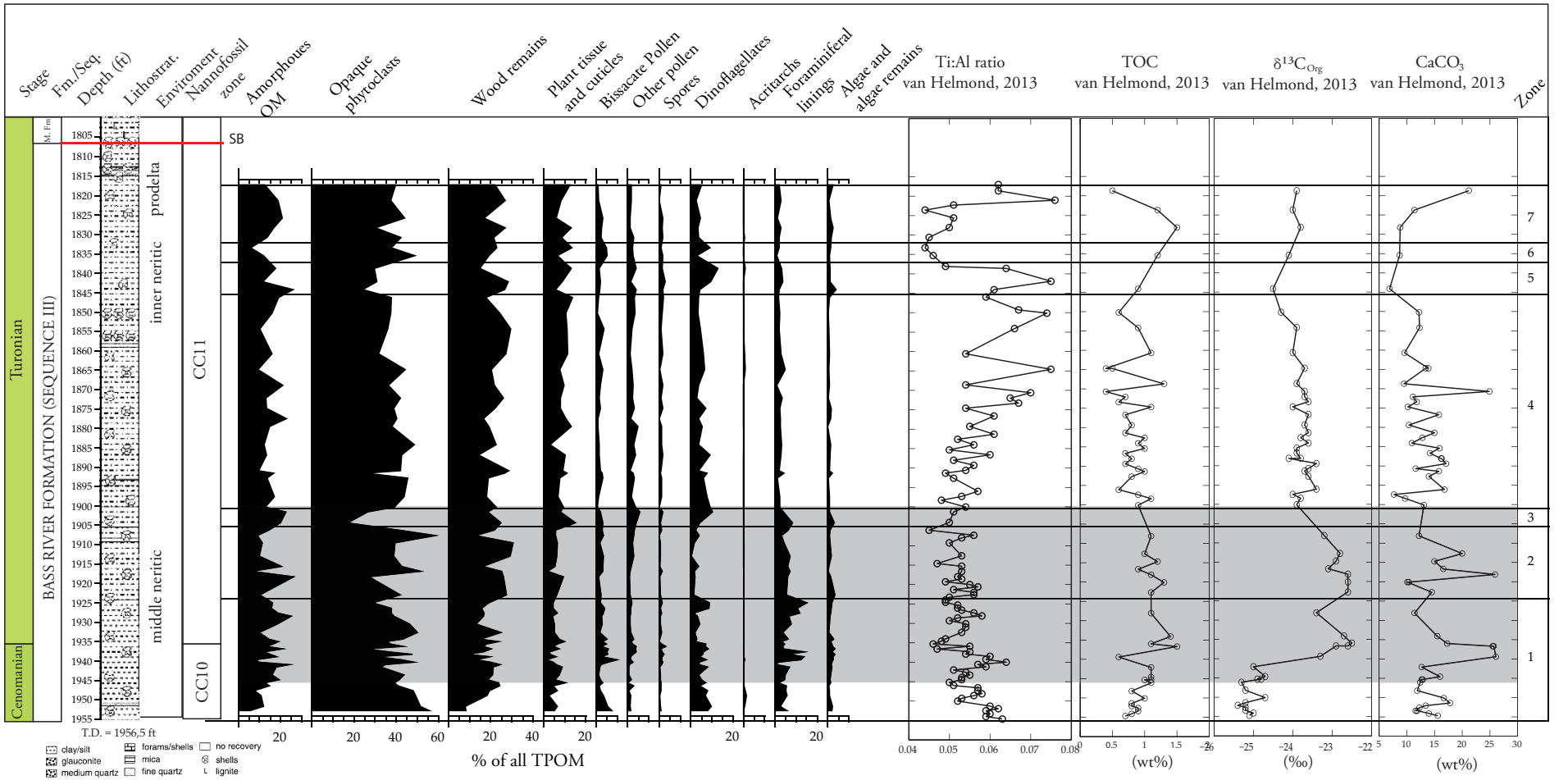

Figure 4.3 Diagram of total amount of particulate orangic matter (TPOM) and cluster analysis zonations from this study, correlated with literature data and geochemical proxies. The detritus groups and zonation are plotted against lithostratigraphy (modified after Sugarman et al., 1999; Miller et al., 2002, 2004), geochemical data (van Helmond, 2013) and generalised water depth (modified after Miller et al., 2002). The OAE2 interval is highlighted in grey.

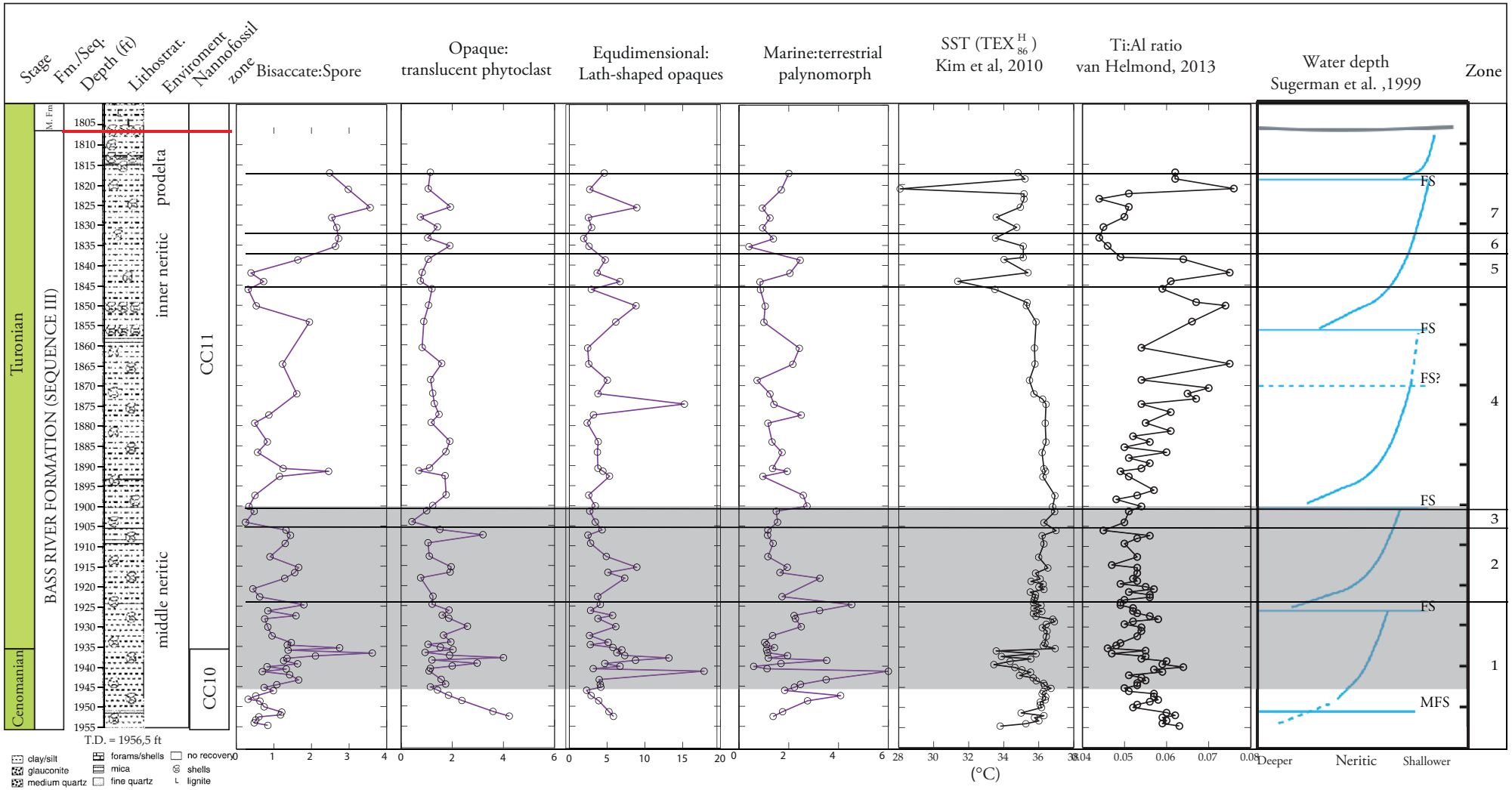

Figure 4.4 Diagram with POM ratios and palynofacies zonations from this study plotted against lithostratigraphy (modified after Sugarman et al., 1999; Miller et al., 2002, 2004), geochemical data (van Helmond, 2013) and generalised water depth (modified after Miller et al., 2002). The OAE2 interval is highlighted in grey.

4.1.1 Palynofacies zones

Palynofacies zone 1 (1956.5-1924 ft)

The basal palynofacies zone is characterised by high fluctuations, especially around 1945 feet, of the different groups of POM (Figure 4.3). There is an overall dominance of phytoclasts with an average relative abundance of 64%, especially opaques (avg. 41%). At the upper boundary is marked by a drop in phytoclasts, down to 52%, and sudden rise and fall of global peak of foraminiferal linings at 15% and local peak dinoflagellate cysts at 9% (Figure 4.3).

The POM ratios and geochemical data show a similar trend (Figures 4.3 and 4.4). They fluctuate strongly, especially at the OAE2 onset, at around 1945 feet, where the marine:terrestrial and equidimensional:lath-shaped phytoclast ratios reach the global maxima (Figure 4.4). The bissaccate:spore and opaque: translucent phytoclast ratios reach the global maxima slightly above the other two (Figure 4.4). After the peaks they decline towards the upper boundary (Figure 4.4).

A positive excursion of the organic $\delta^{13}C$ content marks the onset of OAE2, from -25 to -23‰(Figure 4.3). The carbonate content has its global maximum right after the onset, before declining towards the upper boundary (Figure 4.3). The TOC content remains the least affected staying stable at ~1 wt%, except for a quick rise and fall, down to ~0.5 wt%, at the beginning of OAE2 (Figure 4.3).

Palynofacies zone 2 (1924-1905 ft)

The 2nd palynofacies zone from the base is characterised by a more stable assemblage, only minor fluctuations in the phytoclasts, AOM and palynomorphs (Figure 4.3). Phytoclasts continue to dominate ranging between 62-77% of TPOM. There is a slight, overall increase in wood particles and the palynomorphs portion become stable (Figure 4.3). At the upper boundary the marine and terrestrial palynomorphs begin to increase in abundance (Figure 4.3). The AOM reaches a local maximum of 26% right after the lower boundary before it decreases towards the top (Figure 4.3). At the upper boundary, the opaque phytoclasts reaches the global maximum at 59% before it drops abruptly down to 17% (Figure 4.3). All palynomorphs, AOM, plant tissue and cuticles begin display a slight increase when approaching the upper boundary (Figure 4.3).

Both the Equidimensional:lath-shaped phytoclast and marine:terrestrial palynomorph ratios display an upwards declining trend (Figure 4.4). The remaining two ratios fluctuate more, and have a sudden drop at the upper boundary (Figure 4.4). The Ti:Al ratio continues to fluctuate but also have generally an

upwards declining trend (Figure 4.4).

TOC content remains stable at ~1 wt% whereas the organic $\delta^{13}C$ shows a negative excursion through the palynofacies zone (Figure 4.3). The carbonate content has a slight drop to 10 wt% before it increases rapidly to 25 wt%, followed by a gradual decline towards the upper boundary (Figure 4.3).

Palynofacies zone 3 (1905-1900 ft)

The 3rd palynofacies zone is characterised by the global minimum of opaque phytoclasts at 17% and local maxima of AOM (23%), plant tissue and cuticles (15%), wood remains (25%), and all palynomorphs (25%) (Figure 4.3). Towards the uppper boundary all palynomorphs except dinocysts, AOM, plant tissue and cuticles fall in relative abundance (Figure 4.3). Opaque phytoclasts and dinocysts begins to increase towards the upper boundary, with a local maximum of dinocysts (10%) close to the boundary (Figure 4.3).

Throughout the palynofacies zone the TOC and $\delta^{13}C$ content display an upward negative excursion, which is marking the end of the OAE2 (Figure 4.3). The bisaccate:spore and equidimensional:lath-shaped opaques remain low before a slight rise at the upper boundary (Figure 4.4). Opaque:translucent, marine:terrestrial and Ti:Al ratios as well as the carbonate content increase in the zone (Figures 4.3 and 4.4).

Palynofacies zone 4 (1900-1845.5 ft)

Palynofacies zone 4 is characterised by the end of the OAE2 at the base and a stable assemblage with only minor fluctuations in the POM groups (Figure 4.3). The phytoclasts stabilise and continue to dominate with relative abundance at ~70% throughout the palynofacies zone (Figure 4.3). The remaining percentages are divided, close to equally, between the AOM, terrestrial and marine palynomorphs (Figure 4.1).

After an initial negative excursion, the $\delta^{13}C$ content rises slightly and stabilises at ~-24‰(Figure 4.3). The TOC content fluctuates between ~0.5-1 wt%, and the carbonate content between ~10-15 wt%, with a local maximum of ~25 at 1870 ft (Figure 4.3).

The opaque:translucent, equidimensional:lath-shaped and marine:terrestrial ratios all remain stable with low values, although the equidimensional:lath-shaped ratio display a sudden local peak at 1880 ft (Figure 4.4). The bisaccate:spore ratio increases at the base before declining and stabilising (Figure 4.4). Towards the upper boundary the bisaccate:spore ratio have a slight increase before suddenly dropping again. Overall, although with great oscillation, the

Ti:Al ratio have an upwards increasing trend towards the top where a decline marks the boundary (Figure 4.4).

Palynofacies zone 5 (1845.5-1837 ft)

Palynofacies zone 5 is characterised by a drop in phytoclasts, especially opaques, and the global maximum of dinocysts at 13% (Figure 4.3). The terrestrial palynomorphs remain steady at ~6.5%, whereas the wood remains (28%), plant tissue and cuticles(13%) have local maxima after an initial drop (Figure 4.3). Following the local maxima, they decline again just to rise along with the opaques towards the upper boundary (Figure 4.3). Initially, the AOM has a local peak (26%) before declining, followed by another minor peak (18%) close to the upper boundary (Figure 4.3).

The TOC, δ^{13}C, carbonate and opaque:translucent ratio all have a slight increase through the palynofacies zone (Figure 4.3 and **??**). The bisaccate:spore ratio have a local minimum before it increases rapidly towards the upper boundary (Figure 4.4). Both the marine:terrestrial and Ti:Al ratios display the same trend with an initial increase before a rapid drop towards the upper boundary (Figure 4.4).

Palynofacies zone 6 (1837-1832 ft)

The 6th palynofacies zone contains the global minimum of AOM at 6% and a peak in bisaccate pollen (5%) and dinoflagellates (9%) (Figure 4.3). The TOC and δ^{13}C continues to follow a gradual rise, whereas the carbonate content flats out and the Ti:Al ratio drops (Figure 4.3). The equidiminsional:lath-shaped and marine:terrestrial ratios reach a global minima, the latter rises slightly again towards the upper boundary (Figure 4.4).

Palynofacies zone 7 (1832-1817.05 ft)

The topmost palynofacies zone is characterised by an increase in AOM, up to 21%, phytoclasts keeping steady at ~70% and the remaining percentages are split between the marine and terrestrial palynomorphs, the former being slightly higher (Figures 4.1 and 4.3).

The TOC content falls continuously down from 1 wt% to the global minimum at 0.5 wt% (Figure 4.3). The amount of carbonate increases from 10 to 20%, and the δ^{13}C , along with the marine:terrestrial palynomorph ratio, are stable (Figures 4.3 and 4.4). The remaining POM ratios are low at the base before a local maxima at 1825.5 ft, followed by an upward declining trend (Figure 4.4).

Finally, the Ti:Al ratio is low at the lower boundary, before it increases to the global maximum right before the upper boundary (Figure 4.4).

4.2 Palynology

Overall, 250-352 (avg. 310) sporomorphs were identified for each slide (see Appendix E for complete list of data). Six slides had insufficient identifiable sporomorphs and were therefore below the preferred limit of 300. A lack of identifiable sporomorphs was either caused by a general absence of adequate sporomorphs or because of pyritisation of sporomorphs causing identification problems, or both (Figure 4.5). Lycopodium spores were only counted from 1895-1954 (TD) because of the focus on the OAE2 interval.

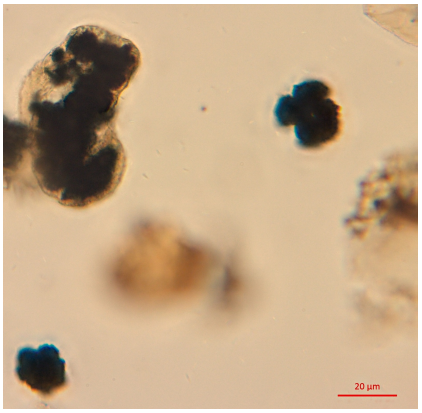

Figure 4.5 Illustration of pyrite clusters as well as pyritisation of a bisaccate.

In total 27 genera and species were identified in addition to the major morphological sporomorph groups (Table 4.2), and the distribution of relative abundances of these are displayed in Figures 4.6 and 4.7. The sporomorph assemblages reveal a rich microflora, dominated by coniferous pollen grains ranging between 4-59% (avg. 33%); spores ranging between 11-49% (avg. 29%); and pulses of high relative abundance of angiospermid pollen, especially Normapolles pollen grains, ranging between 3-72% (avg. 21%) Figures 4.6 and 4.7.

The taxa were systematically described and botanical affinities were allocated to them (Sections 4.2.1 and 4.2.2) and absolute abundances of the sporomorphs were calculated across the OAE2 interval. Afterwards the taxa was assigned, if possible, to Sporomorph EcoGroups and Lowland temperature and humidity curves were calculated (Section 4.2.5 and figure 4.10).

A cluster analysis was performed in Tilia in order to divide the relative abundances into palynofloral zones, in total five, defined by distinct sporomorph assemblages (Figures 4.6 and 4.7).

Table 4.2 List of the identified taxa and major morphological groups in the Bass River Formation.

SPORES	POLLEN
Cicatricosisporites spp	*D. rarus*
Taurocusporites spp	*Phyllocladidites* sp
Lycopodiumsporites sp	*Abietineaepollenites* indet.
Todisporites sp	*A. grandialatus*
Appendicisporites spp	*A. microreticulatus*
C. minor	*A. microsaccus*
C. australis	*R. rugosus*
A. Kerguelensis	*Tsugapollenites* sp
Concavisporites sp	*Inaperturopollenites* indet.
Clavatipollenites sp	I. dubius
Spores indet.	*I. hiatus*
	I. rugosus
	I. atlanticus
	Normapolles indet.
	Complexiopollis spp
	A. verrucosus
	Bisaccate indet.
	Monosulcate indet.
	Tricolpate, tricolporate, triporate indet.

4.2.1 Systematic description

Spores

Genus: *Alsophilidites* (Cookson, 1947) ex Potonié, 1956

Alsophilidites kerguelensis COOKSON, 1947

Plate 1, Figure 1

Description: Psilate, trilete spore with laesurae reaching equator. The equatorial contour is triangular and with broadly rounded apices.

Genus: *Appendicisporites* Weyland and Krieger, 1953

Appendicisporites spp.

Plate 1, Figures 5, 6

Description: Trilete spores with long straight laesurae and triangular, somewhat convex equatorial contour. The exine is striate with ridges.

Genus: *Cicatricosisporites* Potonié and Gelletich, 1933

Cicatricosisporites spp.

Plate 1, Figures 10, 11

Description: Trilete spores with long, straight laesurae, characterised by striate and ridged exine in various degrees, forming a crisscross patttern.

Genus: *Concavisporites* Pflug, 1953

Concavisporites spp.

Plate 1, Figures 7, 8

Description: Trilete spore with long laesurae bordered by margo and extending to equator. The equator contour is triangular and concave.

C. australis Couper, 1953

Plate 1, Figure 4

Description: Trilete spore with rounded-triangular equatorial contour. Equatorial countour is straight and the laesurae is straight, bordered by margo and extends $^2/_3$ to margins. The exine is otherwise psilate.

Genus: *Cyathidites* Couper, 1953

Cyathidites minor Couper, 1953

Plate 1, Figures 2, 3

Description: Psilate, slightly concave trilete spore with triangular equatorial contour and broadly rounded apices. The laesurae is well defined, straight and extends $^2/_3$ to margins.

Genus: *Lycopodiumsporites* Delcourt, Potonié and Sprumont, 1955

Lycopodiumsporites sp.

Plate 1, Figure 12

Description: Coarsely reticulate trilete spore with short laesurae and rounded-triangular equatorial contour.

Genus: *Todisporites* Couper, 1953

Todisporites sp.

Not illustrated

Description: Trilete spore with circular equatorial contour and straight, short and well defined laesurae.

Genus: *Taurocusporites* Stover, 1962

Taurocusporites sp.

Plate 2, Figure 9

Description: Trilete spore with triangular to semicircular equatorial contour. The laesurae extends almost to the margins and the exine is heavily ornamented.

Undifferentiated trilete spores

Not illustrated

Description: Any trilete spore with distinctive laesurae but further identifying impossible.

Monosulcates

Genus: *Clavatipollenites* Couper, 1958

Clavatipollenites sp.
Plate 4, Figures 3 and 4
Description: Distinctly reticulate, small monosulcates.

Undifferentiated Monosulcates
Plate 4, Figure 5
Description: Any pollen grain with one sulcus, but further identifying impossible.

Bisaccates

Genus: *Abietineaepollenites* Delcourt, Potonié and Sprumont, 1955
Abietineaepollenites grandialatus Groot and Penny, 1960
Plate 2, Figure 1
Description: Large reticulate bisaccate pollen grain with large bladders and scabrate body. The breadth and length of body close to equal.

Abietineaepollenites microreticulatus Groot and Penny, 1960
Plate 2, Figure 7
Description: Finely reticulate bisaccate pollen grain with large bladders. The pollen grain has slightly more length than breadth.

Abietineaepollenites microsaccus Groot, Penny and Groot, 1961
Not illustrated
Description: Bisaccate pollen grain with a distinctly scabrate body that has greater length than breadth. The bladders are small and coarsely reticulate.

Genus: *Dacrydiumpollenites* Groot, Penny and Groot, 1961
Dacrydiumpollenites rarus Groot, Penny and Groot, 1961
Plate 2, Figures 3, 4
Description: Bisaccate pollen grain with rugulate body and striate bladders. The body are larger than the bladders, and the pollen grain have a slightly less length than breadth.

Genus: *Phyllocladidites* (Cookson, 1947) ex Couper, 1953
Phyllocladidites sp.
Plate 2, Figure 2
Description: Crudely reticulate, scabrate bisaccate pollen grain. The pollen grain is without a distinct exine cap. Instead it has frills at the periphery.

Genus: *Rugubivesiculites* Pierce, 1961
Rugubivesiculites rugosus Pierce, 1961
Plate 2, Figures 5-6

Description: Bisaccate pollen grain with small bladders almost undistinguishable and a body with a round outline and rugulae.

Undifferentiated bisaccates
Not illustrated
Description: Any indistinguishable bisaccate pollen grains.

Monosaccates

Genus: *Tsugaepollenites* (Potonié and Venitz, 1934) ex Potonié, 1958
Tsugaepollenites sp.
Not illustrated
Description: Monosaccate pollen grain characterised by a circular equatorial contour with distinct frill around the circumference.

Inaperturates

Genus *Inaperturopollenites* Thomson and Pflug, 1953
Inaperturopollenites atlanticus Groot, Penny and Groot, 1961
Plate 4, Figure 2
Description: Inaperturate pollen grain with irregular contour, thin, clearly scabrate exine and numerous folds.

Inaperturopollenites dubius Thomson and Pflug, 1953
Plate 4, Figure 1
Description: Small inaperturate, spherical or ellipsoidal, strongly folded pollen grain. The exine is thin and psilate to slightly scabrate.

Inaperturopollenites hiatus (Potonié, 1931) Thomson and Pflug, 1953
Not illustrated
Description: Inaperturate, spherical pollen grain split open. The exine is psilate and thin.

Inaperturopollenites rugosus Groot, Penny and Groot, 1961
Not illustrated
Description: folded, inaperturate pollen grain with oval to irregular contour and distinctly scabrate exine.

Undifferentiated *Inaperturopollenites*
Not illustrated
Description: Indistinguishable *Inaperturopollenites* pollen grains.

Tricolpates, tricolporates, triporates

Genus: *Atlantopollis* Krutzsh in Góczán, Groot, Krutzsch and Pacltová, 1967
Atlantopollis verrucosa Góczán, Groot, Krutzsch and Pacltová, 1967
Plate 3, Figures 7, 8
Description: Small, strongly verrucate Normapolles pollen grain with less developed pore structures compared to *Complexiopollis*.

Genus: *Complexiopollis* Krutzsch, 1959
Complexiopollis spp.
Plate 3, Figures 1-6
Description: Normapolles pollen grain with straight to triangular equatorial contour. The exine varies between species, from thin and unsculptured to thick and distinctly ornamented.

Undifferentiated Normapolles
Not illustrated
Description: Any indistinguishable triporate pollen grains with internally complex pore structure.

tricolpates
Plate 3, Figures 10-11
Description: Any indistinguishable tricolpate pollen grains without pores.

Undifferentiated tricolpates and tricolporates
Not illustrated
Description: Pollen grains with apparent tricolpate that may or may not have pores.

tricolporates
Plate 3, Figures 12
Description: Any indistinguishable tricolporate pollen grains.

triporates
Not illustrated
Description: Any indistinguishable triporate pollen grains.

4.2.2 Palynoflora

The palynoflora in the Bass River Formation in core ODP 174AW consists of spores from hornworts (Anthocerotophyta), ferns and fern allies (Pteridophyta and Lycophyta), seed ferns (Pteridospermaphyta), conifers (Coniferophyta) and other gymnosperms, and angiopsperms (Figure 4.7). Their botanical affinities were determined by previous studies on the identified taxa and morphological

groups (see Appendix F for full list of references).

Liverworts, hornworts and mosses (Hepatophyta, Anthocerotophyta and Bryophyta)

Only the species of the genus *Taurocusporites* is a possible hornwort.

Ferns and fern allies (Pteridophyta and Lycophyta)

Ferns are represented by the families Schizaeaceae (*Cicatricosisporites* spp.), *Appendicisporites* spp.), Cyatheaceae (*C. minor*, *C. australis*, *Alsophilidites* spp.), Osmundaceae (*Todisporites* sp.) and Matoniaceae (*Concavisporites*). The only genus with affinity towards fern allies are *Lycopdodiumsporites* sp., which is thought to be in the Lycopodiaceae family. Undifferentiated trilete spores are also, although tentatively, included within the ferns and fern allies.

Seed ferns (Pteridospermaphyta)

The only possible candidates for being seed ferns are the monosulcate pollen grains. Monosulcate pollen grains are produced by either the seed ferns Cycadales, gymnospermid Ginkgoaceae or the angiosperms, such as *Clavatipollenites* spp.. Because monosulcate pollen grains were classified as either monosulcate or *Clavatipollenites* sp., the presence of Cycadales and Ginkgoaceae species remain unknown.

Conifers (Coniferophyta)

Conifers are the most dominant group of the gymnosperms in the sporomorph assemblages. The families represented are Araucariaceae (*I. atlanticus*), Podocarpaceae (*D. rarus*, *Phyllocladidites* sp.), Pinaceae (*Abietineaepollenites* spp., *Tsugapollenites* sp.) and Taxodiaceae-Cupressaceae (*Inaperturopollenites* spp.).

Other gymnosperms

As mentioned above, the undifferentiated monosulcates can be produced by the gymnospermid Ginkgoaceae.

Angiosperms

The angiospermid pollen grains are characterised by abundance of Normapolles, mainly by the genera *Complexiopollis* and *Atlantopollis*. These are wind pollinating angiosperms of the family Fagales. Other minor contributors are of the family Chloranthaceae (*Clavatipollenites*) and undifferentiated tricolpate, tricolporate and triporate pollen grains of unknown angiospermid origin.

4.2.3 Palynofloral zones

Palynofloral zone 1 (1956.5-1927.5 ft)

The basal Palynofloral zone 1 is characterised by heavy fluctuation of angiosperms, especially the Normapolles pollen grains, and otherwise dominance of conifers (avg. 47%) (Figures 4.6 and 4.7). The angiosperms increases quickly at the base until they reach the global maximum of relative abundance at 72% right before the onset of OAE2 (Figure 4.7). At the OAE2 boundary there is a rapid decrease before the angiosperms recover (up to 46%) (Figure 4.7). After the recovery there is an overall upwards drop in angiosperms, down to ~12%, before a sudden peak up to 47% at the upper boundary (Figure 4.7). The *Inaperturopollenites* spp. display a trend similar to the angiosperms, whereas the majority of spores and other conifers show the opposite (Figures 4.6 and 4.7).

The sea surface temperature (SST) shows warm temperatures which begin to drop at the onset of OAE2 (Figure 4.7). Following the initial drop the temperature displays high oscillation between warmer and colder temperatures, before stabilising at temperatures close to the same level as before the onset (Figure 4.7).

Palynofloral zone 2 (1927.5-1905 ft)

The 2nd palynofloral zone is characterised as a stable period. After the peak of angiosperms at the lower boundary they drop below 10% to an average of ~6% (Figure 4.7). *Inaperturopollenites* spp. continue to display the same trends as the zone below (Figure 4.6). The main portion of the assemblages are conifers with ~51% followed by spores with average of ~31% (Figures 4.6 and 4.7). The temperature in floral zone 2 is generally slightly colder than the zone below, with a local maximum close to the upper boundary (Figure 4.7).

Palynofloral zone 3 (1905-1895 ft)

The 3rd palynofloral zone is characterised by a sudden rise of angiosperms at the lower boundary, from 7 to 47% (Figure 4.7). After the initial peak the angiosperms have an upward declining trend, while the conifers increase (Figure 4.7). The ferns display a slight rise toward the upper boundary (Figure 4.7). This rise is mostly caused by an increase in abundance of *Appendicisporites* spp. (Figure 4.6). The temperature show an initial drop at the base before recovering to previous level (Figure 4.7). At the upper boundary the temperature falls to the level of the previous palynofloral zone (Figure 4.7).

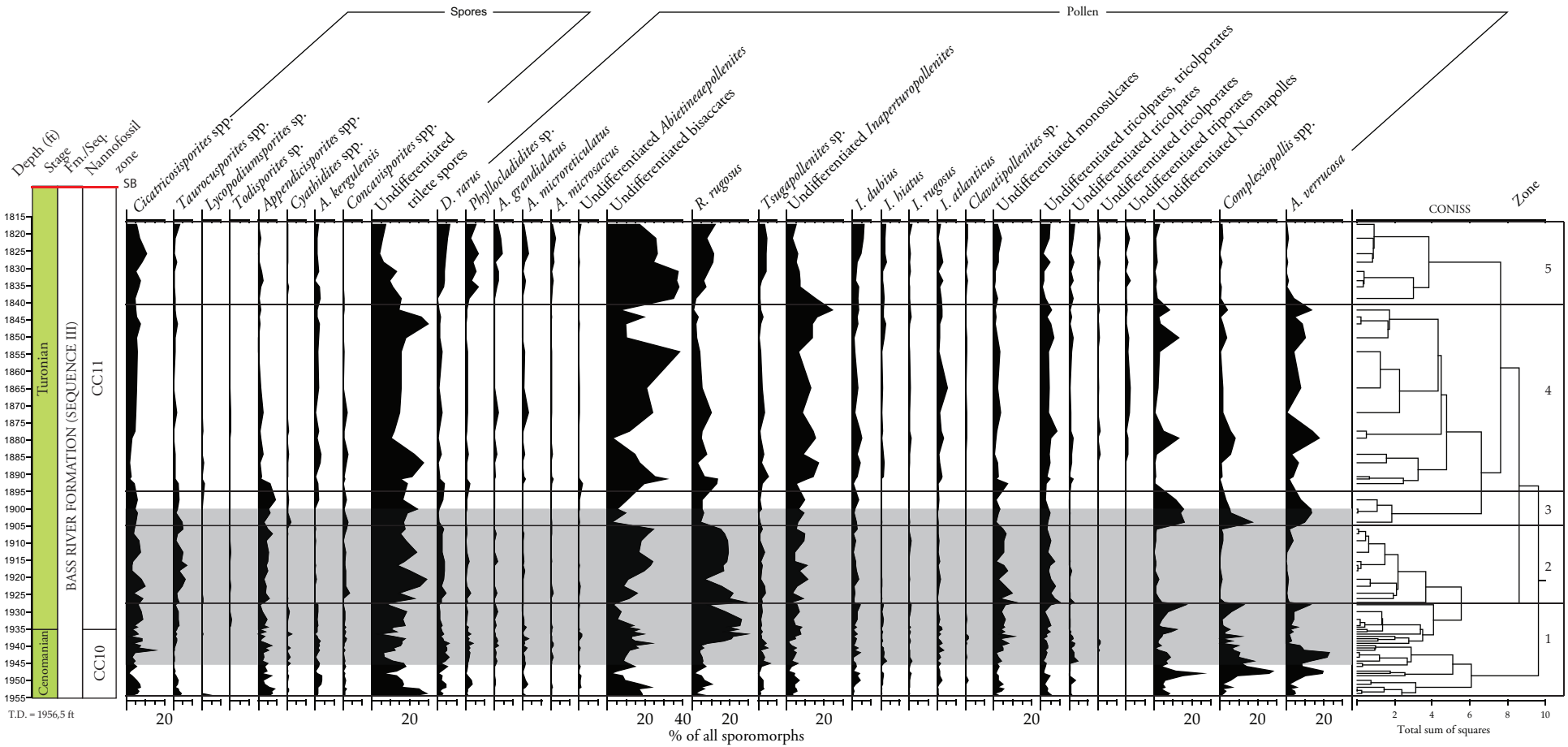

Figure 4.6 The relative distribution of all identified sporomorphs in the Bass River Formation. The cluster analysis was the basis for the determination of the palynofloral zonations. The OAE2 interval is highlighted in grey.

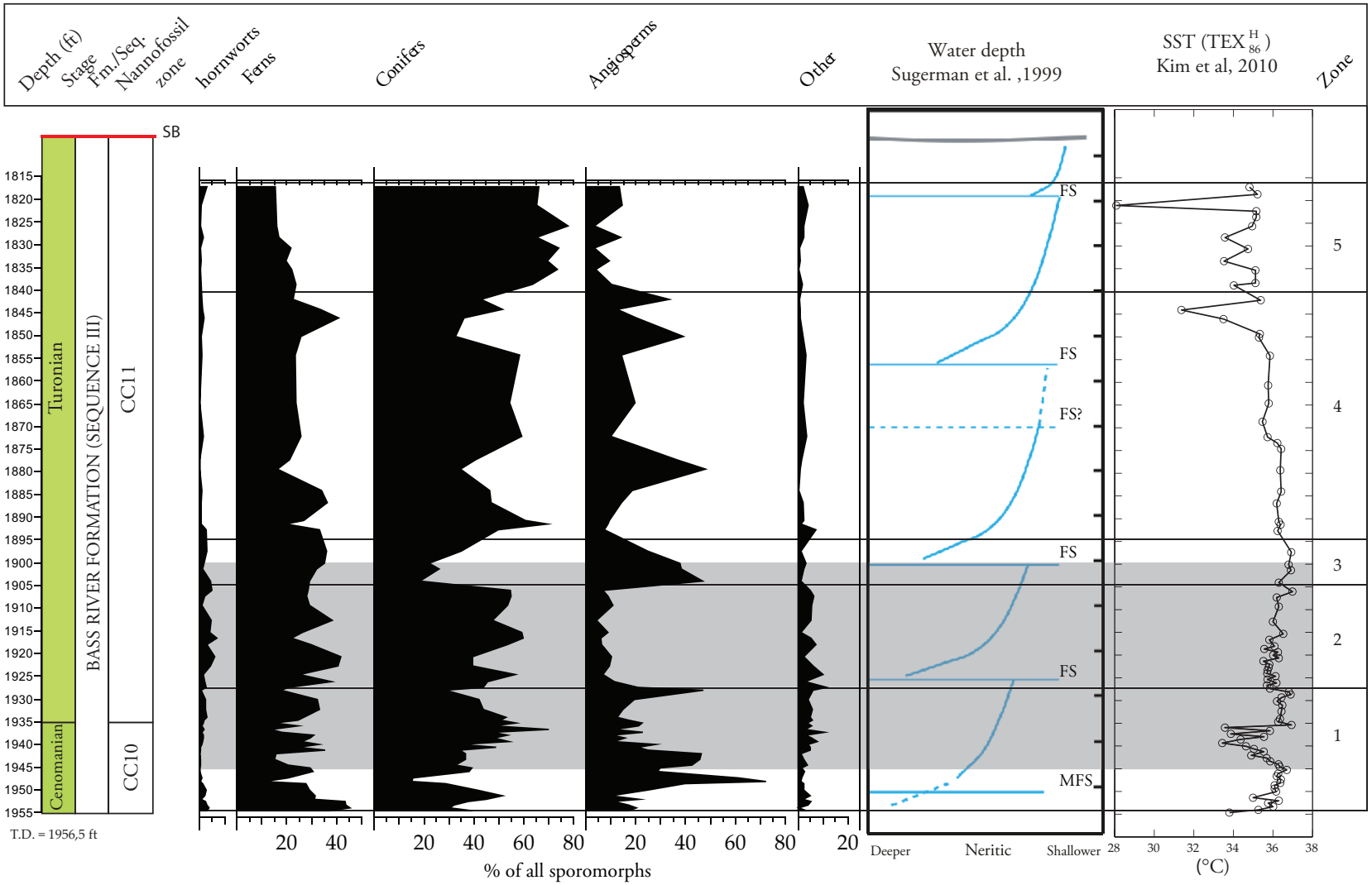

Figure 4.7 The relative distribution of plants in the Bass River Formation with sporomorph zonations, generalised water depth (modified after Miller et al., 2002) and sea surface temperature (van Helmond, 2013). The OAE2 interval is highlighted in grey.

Palynofloral zone 4 (1895-1841 ft)

Palynofloral zone 4 is characterised by a vegetation consisting of mainly conifers (avg.~50%), with pulses of high-abundances peaks (up to 48%) of angiosperms, and a stable fern population at ~27% (Figure 4.7). Among the conifers there is a small overall increase of *Inaperturopollenites* spp. (Figure 4.6). The temperature display a gradual decline, at an increasing rate, towards the top (Figure 4.7). At the upper boundary the assemblages and temperature curve show increasing fluctuations and alternating dominances between angiosperms and conifers (Figures 4.6 and 4.7).

Palynofloral zone 5 (1841-1817.05 ft)

The topmost palynofloral zone is characterised by a slightly fluctuating temperature, a stable and clear predominance of conifers (avg. ~70%), ans low abundance of angiosperms (avg. <10%) (Figures 4.6 and 4.7).

4.2.4 Absolute abundances of the OAE2

Absolute abundances for the OAE2 interval in the Bass River Formation was calculated in Tilia and overlain by the relative abundances and correlated with generalised sea level and SST calibrated TEX_{86} (Figure 4.8).

Overall, the relative and absolute abundance curves follow each other, although they are changed in terms of surface area. The bisaccates for instance, are greatly reduced while the contributors with minor relative abundances are amplified. However there are sections of the absolute that does not follow the relative curve. These deviations correlate with the shifts in the lycopodium spike, temperature changes and/or sea level change.

4.2.5 Sporomorph EcoGroup Model (SEG)

The palynological data obtained were used to reconstruct palaeoecosystems with the application of Sporomoprph EcoGroup (SEG) modelling. The resulting model contained 3 palaeocommunities, the Upland, Lowland and (Lowland) Wetland SEG (Table 4.3 and figure 4.9).

The Upland SEG consists exclusively of all the conifers except for the *Inaperturopollenites* spp. (Table 4.3). *Phyllocladidites* sp., *Tsugapollenites* sp. and *D. rarus* are only tentatively assigned to Upland under the assumption that most conifers thrived there (Table 4.3).

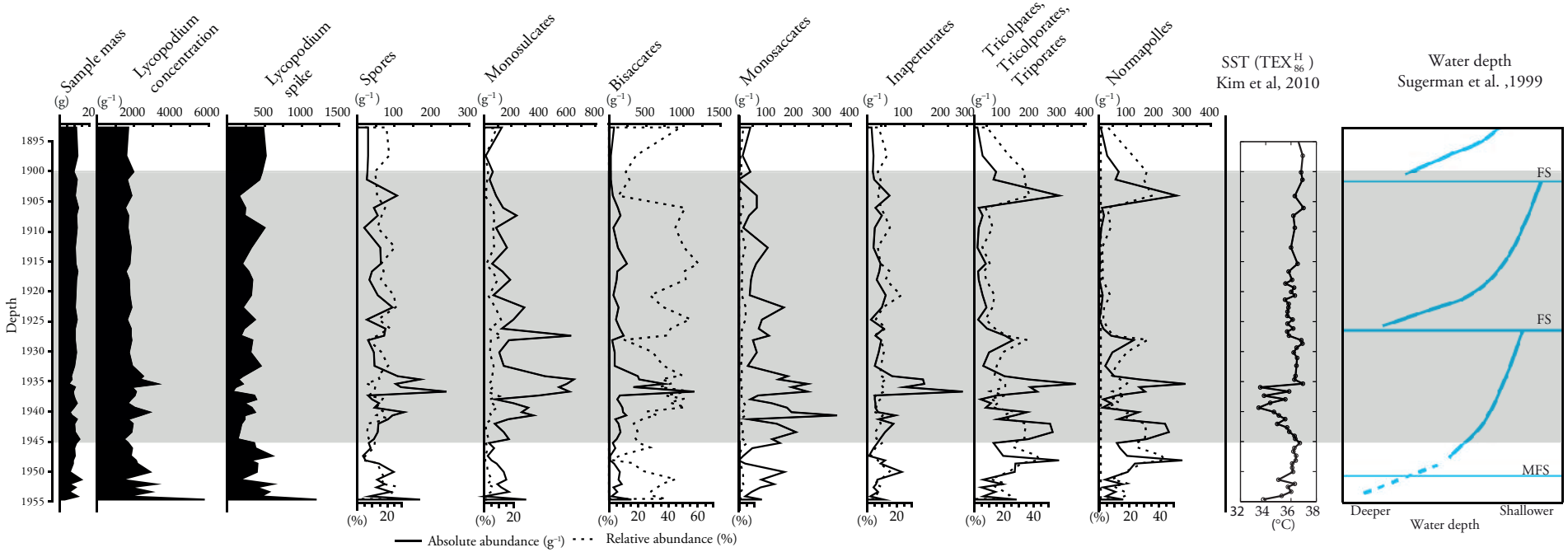

Figure 4.8 The sample mass, lycopodium concentration, lycopodium spike (number of counted lycopodium), relative and absolute abundance of the major morphological sporomorph groups during the OAE2 plotted against TEX_{86} calibrated sea surface temperature (van Helmond, 2013) and generalised sea level (modified after Miller et al., 2002). The OAE2 interval is highlighted in grey.

The Lowland SEG was split in two, in order to differentiate between the Wetland taxa and the other Lowland taxa. This was done to enhance changes in the vegetation. The Wetland taxa are coniferous *Inaperturopollenites* spp. and *Cyathidites* spp. ferns (Table 4.3). Remaining taxa in the Lowland SEG are comprised of the following ferns and fern allies: *Appendicisporites* spp., *Cicatricosisporites* spp., *Concavisporites* sp., *Todisporites* sp. and *Lycopdodiumsporites* sp as well as hornworts (*Taurocusporites* sp.) (Table 4.3).

Of the angiosperms, the Normapolles producing Fagales are included in the Lowland SEG. According to Wolfe and Upchurch (1987) the southeastern North American mid-Cretaceous palynoflora has a close resemblance to the vegetation of New Caledonia. In the flora of New Caledonia, wind pollinating angiosperms occur especially in the lowlands Wolfe and Upchurch (1987), which is why the Fagales species are placed in the Lowland SEG.

The resulting SEG model was included with the palynofloral zonations and correlated with the SST calibrated TEX_{86} and generalised water depth (Figure 4.9). Based on the Lowland data, warm:cold and dry:wet ratio curves were calculated and plotted with the palynofloral zonations and correlated with geochemical data (Figure 4.10). The ratio curves were plotted logarithmically to enhance the changes.

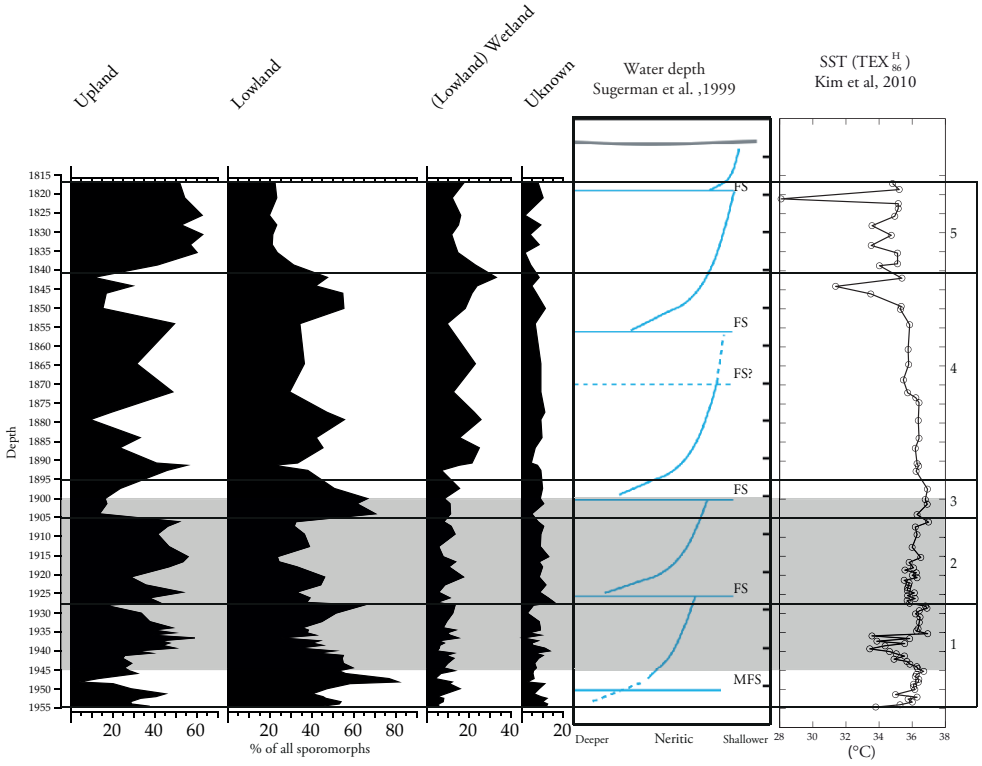

Figure 4.9 The relative abundance the different SEGs plotted against TEX_{86} calibrated for sea surface temperature (van Helmond, 2013) and generalised water depth (modified after Miller et al., 2002). The OAE2 interval is highlighted with grey.

Table 4.3 The SEG and climate indications of the sporomorphs with references

SPOROMORPH	CLIMATE INDICACTION	SEG	REFERENCES
Anthocerotophyta			
Taurocusporites sp.	-	Lowland	Gary et al., 2009
Pteridophyta			
Appendicisporites spp.	Warmer, wetter	Lowland	Peyrot et al., 2011
Cicatricosisporites spp.	Warmer, wetter	Lowland	Abbink, 1998
Concavisporites spp.	Warmer, drier	Lowland	Abbink et al., 2004
Cyathidites spp.	Warmer, drier	(Lowland) Wetland ; brackish swamp and back mangrove	Gary et al., 2009
Todisporites sp.	Warmer, wetter	Lowland	Gary et al., 2009
Undifferentiated spores	Cooler, drier	Lowland	Gary et al., 2009
Lycophyta			
Lycopdodiumsporites	Warmer?	Lowland	Gary et al., 2009
Coniferophyta			
Abietineaepollenites spp.	Cooler, temperate	Upland	Kimyai, 1966
D. rarus	Cooler, temperate	Upland	
Inaperturopollenites spp.	Warmer, wetter	(Lowland) Wetland ; Freshwater swamp	Götz et al., 2011
Phyllocladidites sp.	Cooler, temperate	Upland	
Rugubivesiculites rugosus	Cooler, temperate	Upland	Kimyai, 1966
Tsugapollenites sp.	Cooler, temperate	Upland	
Undifferentiated bisaccates	Cooler	Upland	Gary et al., 2009
Anthophyta			
A. verrucosus	Warmer, drier	Lowland*	Friis et al., 2003
Complexiopollis spp.	Warmer, drier	Lowland*	Friis et al., 2003
Undifferentiated Normapolles	Warmer, drier	Lowland*	Friis et al., 2003
*See text for further explanation			

Overall, there are major fluctuations in dominance between the Lowland and Upland communities, whereas the Wetland SEG remains relatively stable throughout the Bass River Formation Figure 4.9. The Wetland taxa do display a general increase in abundance post-OAE (Figure 4.9).

The warm and cold taxa, and thus the warm:cold ratio, more or less reflect the SST, although with deviations, especially post-OAE (Figure 4.10). The wet and dry taxa as well as the dry:wet ratio are more ambiguous, sometimes mirroring the temperature curves, but at other times showing a opposite trend (Figure 4.10).

Palynofloral zone 1 (1956.5-1927.5 ft)

The basal palynofloral zone displays in general a dominance of Lowland taxa with an average of 49%, and reaching the global peak at 82% right before the onset of the OAE2 (Figure 4.9). After the peak and onset, the Lowland taxa is gradually displaced by more Upland taxa, before a rapid increase towards the upper boundary, peaking at 60% (Figure 4.9).

Both the temperature and humidity curves show an increase in warmth and aridity towards the OAE2 onset, displaying their global peaks simultaneously with the Lowland taxa (Figures 4.9 and 4.10). Following the onset of OEA2 there is an overall increase in humidity, whereas the warm:cold curve fluctuate heavily (Figure 4.10).

Palynofloral zone 2 (1927.5-1905 ft)

The lower boundary of palynofloral zone 2 is defined by a sudden drop in warm taxa and an increase of wetter taxa (Figure 4.10). Throughout the palynofloral zone the temperature and humidity remain stable at the same level, with only minor fluctuations (Figure 4.10). The upper boundary is marked by a sudden increase in warm and dry taxa (Figure 4.10).

Although there are minor fluctuations between the Lowland and Upland taxa the vegetation is stable with ~40% of Lowland and ~40% of Upland taxa, the remaining 20% split between the Wetland and unknown taxa (Figure 4.9).

Palynofloral zone 3 (1905-1895 ft)

The 3rd palynofloral zone is characterised by a stable population of warm and dry taxa, until the end of the OAE2 (Figure 4.10). From the ending of OAE2 and toward the upper boundary the colder and wetter taxa increases slightly (Figure 4.10).

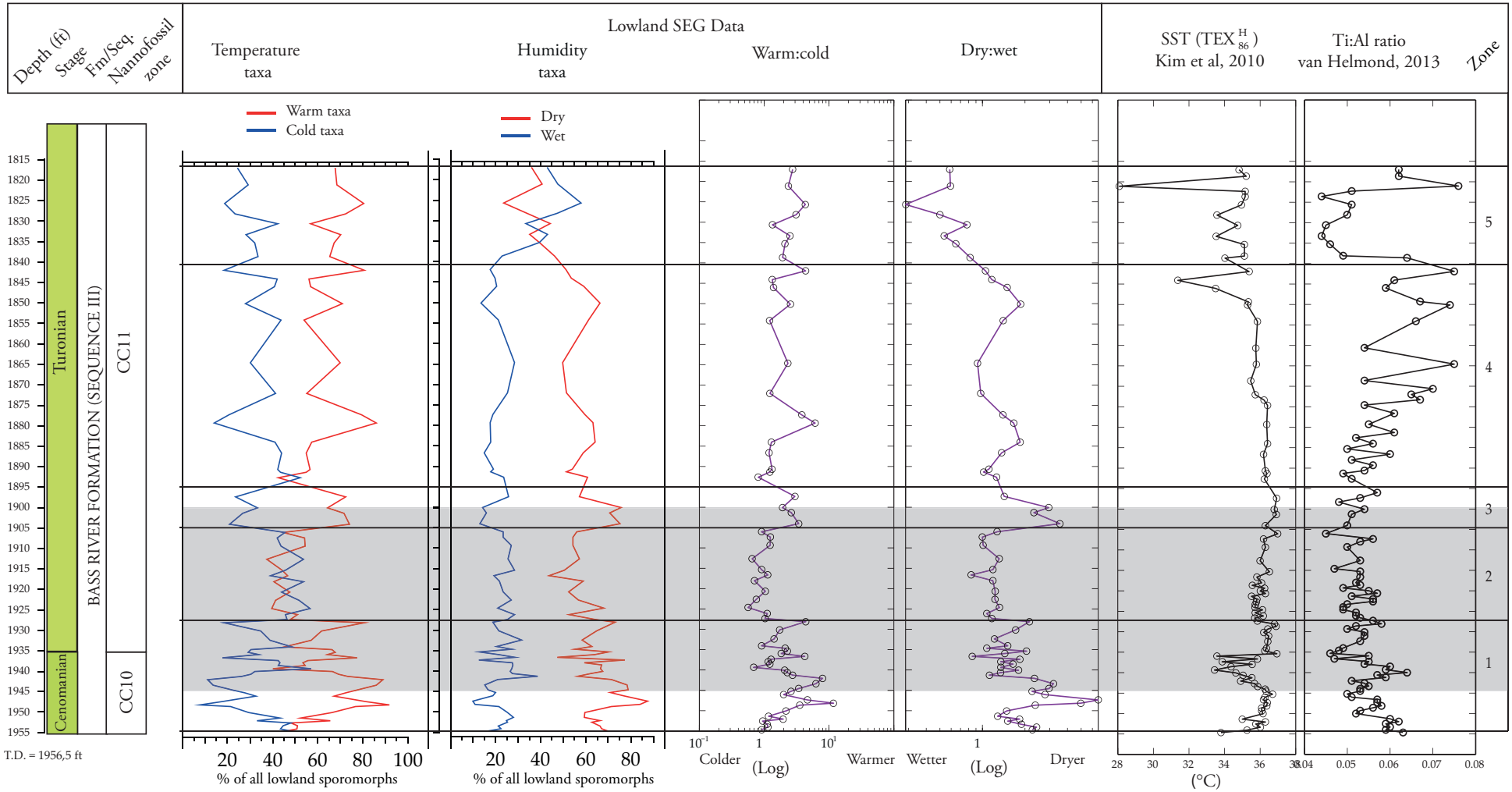

Figure 4.10 Logarithmic Lowland climate ratio curves of the Bass River Formation with palynofloral zonations plotted against $TEX_8 6$ calibrated for sea surface temperature, TOC and organic δ^{13}carbon content (van Helmond, 2013). The OAE2 interval is highlighted with grey.

In the SEG model there is a sudden increase of the Lowland taxa at the lower boundary (Figure 4.9). After the initial rise, the Lowland taxa have an upwards decreasing trend, whereas the Upland taxa increases (Figure 4.9). The Wetland taxa remain stable at the same level until the upper boundary, which is defined by a slight drop in swamp taxa.

Palynofloral zone 4 (1895-1841 ft)

Palynofloral zone 4 is characterised by a period of more Upland taxa and an overall increase in Wetland taxa. The Wetland taxa increase from an average of ~10% in lower part (below the lower boundary of palynofloral zone 4) to ~20% in the upper part of the core (Figure 4.9). The Lowland taxa continue the decline from the lower palynofloral zone before stabilising at ~40% (Figure 4.9). The upper boundary is marked by a global maximum of Wetland taxa and a local maximum of Lowland taxa (Figure 4.9).

Among the warm-cold and dry-wet taxa it is more stable, reflecting the sea surface temperature (Figure 4.10). The humidity curve has a local maximum in aridity after the initial trend towards wetter taxa (Figure 4.10). After the aridity peak the taxa becomes gradually more humid, followed by another rise towards dryer taxa (Figure 4.10). After the second arid peak, the taxa display a trend towards wetter preferences again, which continues well into the topmost palynofloral zone (Figure 4.10). The earm-cold taxa have minor fluctuations, but remain with a general ratio of 2:1 in favour of warmer taxa throughout the 4th and 5th palynofloral zones (Figure 4.10). There is one exception with a local warm maximum, at 1880 ft, with a ratio of ~1:6 in favour of warm taxa (Figure 4.10).

Palyfloral zone 5 (1841-1817.05 ft)

The topmost palynofloral zone is characterised by a severe drop in Lowland taxa, down to an average of 25%, in favour of Upland taxa (Figure 4.9). The Upland communities are now dominating with an average of 50% (Figure 4.9) and the Wetland taxa, after an initial drop, stabilize at ~20% (Figure 4.9).

The warm:cold ratio continues the same pattern as in floral zone 4 (Figure 4.10), whereas the humidity curve show a rise in wet taxa, which reaches a global maximum with a 2:1 ratio in favour of wet taxa (Figure 4.10). After the maximum there is an increase of dryer taxa, which continues towards the top of the Bass River Formation.

5. Discussion

5.1 Paleoenvironmental reconstruction

Distinct assemblages of the particulate organic matter (POM) can provide implications of the depositional environments, redox conditions and sea level changes (Tyson, 1995). Each of these subjects will be discussed in detail in Sections 5.1.1 to 5.1.3.

The overall indications of the palynofacies analysis are displayed in Figure 5.1. The Cenomanian-Turonian sediments in the Bass River ODP 174 AX were deposited in a neretic shelf environment with proximity to a highly influential delta (Figure 5.1). With the exception of two flooding events (Figure 5.1), the environment was stable throughout the formation. The water column was most likely dysoxic and underneath the ocean floor anoxia may have been present.

5.1.1 Depositional environment

In the Bass River Formation the POM assemblages are characterised by a rich, mixed composition, with generally a high percentage of phytoclasts, low to intermediate percentages of AOM, terrestrial and marine palynomorphs (Figures 4.1, 4.3 and 4.4).

The Presence of both marine and terrestrial palynomorphs in addition to the high abundance of phytoclasts (Figure 4.3) imply a marine environment with proximity to a fluvio-deltaic source(s) (Tyson, 1995). Because the phytoclats have a slightly higher percentage of opaques phytoclasts (Figure 4.3), which is predominantly equidimentional (Figure 4.4), the environment is probably on a continental shelf.

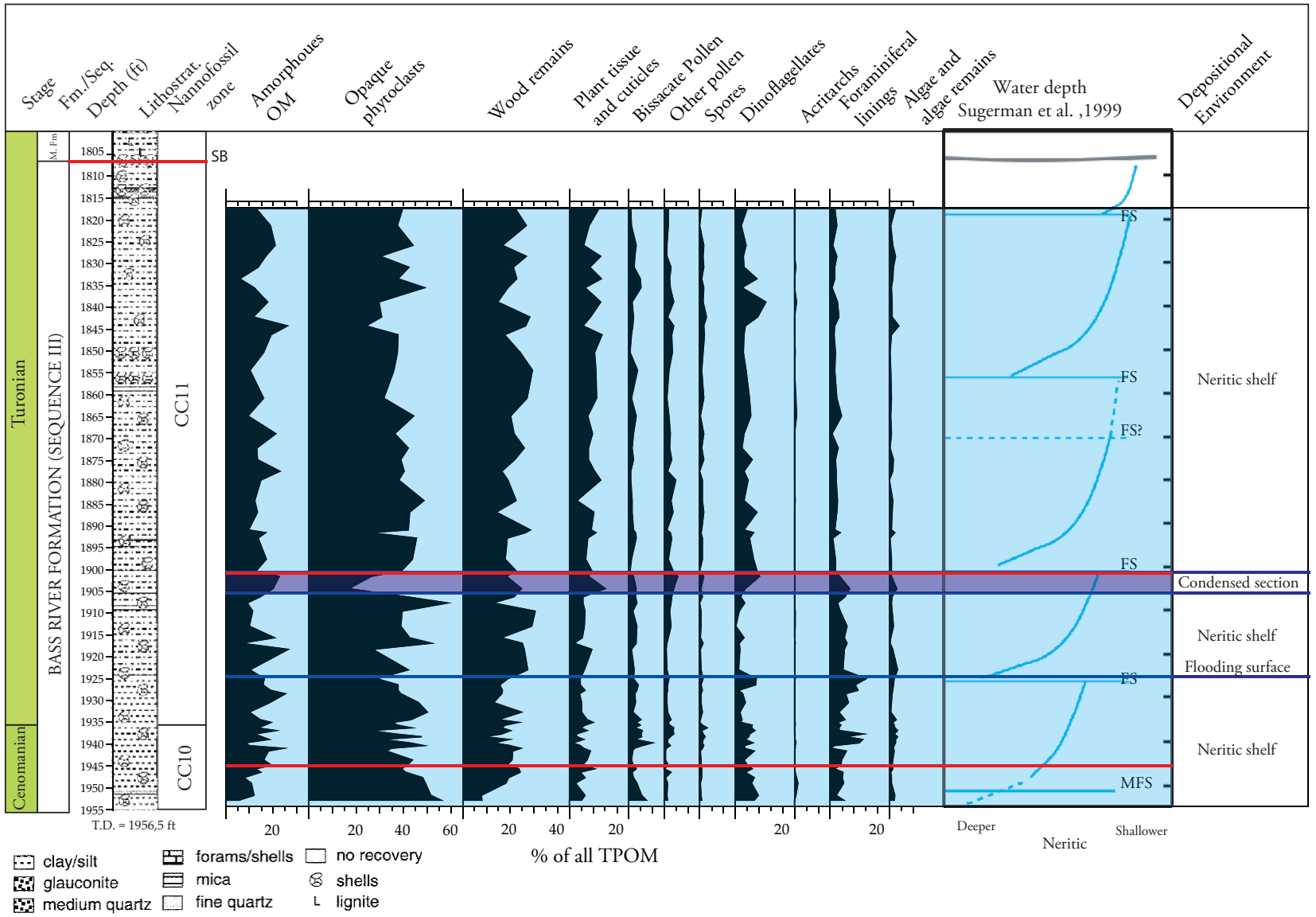

Figure 5.1 Diagram showing the stage, formation, depth, lithostratigraphy, nannofossil zonations, distribution of TPOM correlated with the generalised water depth (modified after Miller et al., 2002); and interpreted depositional environment of the Bass River Formation. The OAE2 boundaries are highlighted in red.

The terniary APP diagram further confirms this by indicating field II and IVa, in addition to the three outliers in field III (Figure 4.2.A), which denotes fluctuation between shelf to basin transition or marginal basin environment (Table 3.3) (Tyson, 1995). This general trend supports the earlier interpretations, a neretic shelf environment with proximity to a delta, done by Miller et al. (1998); Sugarman et al. (1999); Miller et al. (2004) on the ODP 174AX core.

5.1.2 Flooding surfaces

There are three major and one minor deviations to the general depositional trend in the Bass River Formation. The major occur in palynofacies zones 3, 5 and 6, and the minor deviation occurs at the upper boundary of zone 1 (Figures 4.1, 4.3 and 4.4).

The minor deviation is represented by a peak in marine palynomorphs (Figure 4.3) and the marine:terrestrial ratio (Figure 4.4), which together denote a flooding surface (Tyson, 1995). A drop in the Lowland taxa at the same boundary imply a loss of habitat and therefore a sea level rise (Figure 4.9). Although the bisaccate:spore ratio (Figure 4.4) suggests the opposite (Tyson, 1995), the flooding surface is confirmed by a close correlation to a flooding surface described by Sugarman et al. (1999) (Figure 4.4).

Zone 3 displays similarities to the upper boundary of zone 1 (Figure 4.1). However, it encompasses a section of 5 feet rather than just a boundary (Figure 4.3). In addition, the zone has an increase of AOM; a slight drop in the phytoclasts (Figure 4.3); and the Lowland taxa declines throughout the section with a complete drop at the upper boundary (Figure 4.9). All these trends indicate a flooding surface with higher preservation rate (Tyson, 1995). The unchanged marine:terrestrial ratio (Figure 4.4), can be explained by that the individual groups of marine palynomorphs peak at different depths (Figure 4.3), and can therefore be disregarded. The upper boundary of the zone also correlates with the second flooding surface from Sugarman et al. (1999).

Because of the thickness (Figure 4.1), drop in opaque in favour of translucent phytoclasts (Figure 4.4), peaks of marine palynomorphs and AOM (Figure 4.3), zone 3 may be a condensed section. Condensed sections are slowly accumulated fine-grained sedimentary rocks enriched in organic material, most commonly deposited during transgression (Schlumberger, 2013), such as in this case. A drop in the lycopodium spike during the interval (Figure 4.8) indicates a decrease in sedimentation rate. Changes in the lycopodium spike is caused by climate change and/or decrease of sedimentation rate, in this case the latter is most likely. The enrichment of marine and plant detritus (Figure 4.3) further

implies a condensed section. Additionally the decrease of opaque phytoclasts in favour of translucent denotes more reducing conditions, which is another characteristic of condensed section. This is because translucent phytoclasts tend to oxidise to opaque phytoclasts under normal marine conditions (Tyson, 1995).

The last discrepancy is the combined palynofacies zones 5 and 6 (Figure 4.1). The results display ambiguous signals, with peaks of dinoflagellate cysts that does not correlate with any of the other results (Figures 4.3 and 4.4) or the uppermost flooding surface from Sugarman et al. (1999). However, both the Titanium:Alum-inium (Ti:Al) ratio and sea surface temperatures (SST) display heavy fluctuations in this interval, indicating climate changes. The significant drop in the Ti:Al ratio implicate climate changes. This is because Ti:Al ratio can be applied in stratigraphic profiles as an indicator of aeolian source strength (Bertrand et al., 1996; Rachold and Brumsack, 2001).

There is no evidence of the two uppermost flooding surfaces described by Sugarman et al. (1999). Miller et al. (2004) commented that the parasequences observed in the formation were minor, ~20 m, which could explain the absence. This can be because the eustatic changes were below resolution, too sparse sampling rate, especially in the upper part of the formation, and/or the sea level changes simply were too small to affect the POM and sporomorph assemblages.

5.1.3 Redox conditions

In addition to determining the depositional environment, the terniary AAP diagram (Figure 4.2) indicates the oxygen supply in the water column. Field II suggests dysoxic to anoxic, field IVa dysoxic-suboxic and three outliers in field III denotes oxic conditions (Figure 4.2.A, Table 3.3). Occurrence of foraminiferal linings, pyrite and shells, mainly molluscs (Miller et al., 1998), throughout the formation further complicates the matter. These occurrences indicate opposing signals in terms of the oxygen supply because pyrite is typically abundant in anoxic, clastic environments (Tyson, 1995; Batten, 1996), whereas benthic organisms such as foraminifera and molluscs are dependent on oxygen on the ocean floor (Doyle and Lowry, 1996; Armstrong and Brasier, 2005).

Foraminiferal linings are the inner test linings of chitinous benthic foraminifera (Traverse, 2007), which require the presence of oxygen in the water at the ocean bottom (Armstrong and Brasier, 2005). The occurrences of oxygen dependent molluscs (Doyle and Lowry, 1996) further imply oxic conditions on the ocean bottom. Both the foraminfera and shell could be allochthonous, brought with the sediments from the delta into anoxic environments. However, if the water column is only dysoxic the molluscs and foraminifera could be autochthonous,

because of species known to be adapted to reduced oxygen conditions (Doyle and Lowry, 1996; Armstrong and Brasier, 2005).

The TOC and AOM peaks correlations (Figure 4.2.B) is an indication of at least increased preservation rate (Tyson, 1995), and confirm reducing conditions in the environment. If the origin(s) of the AOM is determined, more implications will become available.

None of the AOM particles reacted to the florescent light, which is typical for degraded terrestrial, organic detritus mediated by anaerobe microorganisms (Tyson, 1995; Batten, 1996; Pacton et al., 2011). Absence of marine AOM could mean that it is anoxic conditions and anaerobe bacteria are degrading the OM but terrestrial debris is diluting the composition of POM (Tyson, 1995), and/or the high sedimentation rate is preventing anaerobe, marine algae to grow, or the water column is oxic-dysoxic and degradation is secondary, occurring after deposition, within anoxic sediments beneath the ocean bed. Of the these the last is most likely, given the complete absence of marine AOM.

Summarised, the indications of the terniary APP diagram are ranging between dysoxic-anoxic (Figure 4.2) (Tyson, 1995). Combined with the oxic outliers in the diagram (Figure 4.2) (Tyson, 1995) and the other implications previously mentioned, the water column was probably dysoxic rather than anoxic. Not even during the OAE2 are there any significant changes that promotes evidence of more anoxic conditions (Figure 4.3). Degradation of the terrestrial, organic detritus, pyrite generation and pyritisation of organic matter would then have been secondary, taking place below the ocean bottom, within sediments with anoxic conditions.

The pattern of anoxic sediments and dysoxic water column may have been caused by a combination of high primary production and the sedimentation rate and the fluvial influence of the delta.

In the mid-Cretaceous there was a possible nutrient enrichment in the surface water, before and during the OAE2 (Takashima et al., 2006; Barclay et al., 2010; Barclay, 2011; Monteiro et al., 2012). A proposed theory for the nutrient enrichment is that upwelling, because of subsea volcanism, and increased chemical weathering on the continents led to enrichment of nutrient in the photic zone and subsequently enhanced the primary production (Takashima et al., 2006; Barclay et al., 2010; Barclay, 2011; Monteiro et al., 2012). Because of the warm climate and low thermal gradient, sluggish circulation, stagnation and stratification in the oceans were common in the mid-Cretaceous especially in the Atlantic Ocean (Huber et al., 1999; Trabucho Alexandre et al., 2010). These conditions promote deposition of organic rich sediments (Tyson, 1995; Batten, 1996; Trabucho Alexandre et al., 2010).

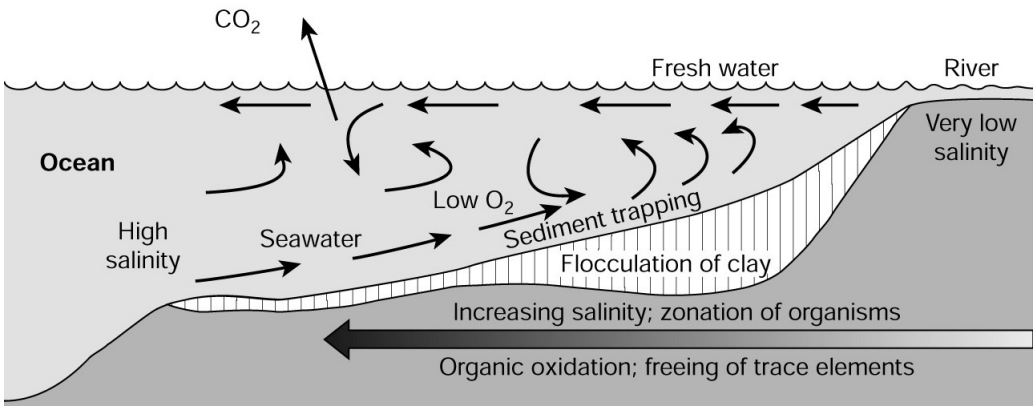

Figure 5.2 Illustration of the possible circulation on the New Jersey shelf outside the Bass River delta in the Cenomanian-Turonian. The freshwater intermixed with stagnant, oxygen depleted oceanic water, preventing anoxia to form (modified after Cheng, n.d.).

However, in the Cenomanian-Turonian the Bass River delta was prograding despite of the rising sea level (Miller et al., 2002, 2004). This indicates both a high sedimentation rate and fluvial influence on the marine environment. A strong fluvial influx may therefore have prevented stratification and supplied with oxygen-rich freshwater leaving the water column possibly dysoxic (Figure 5.2).

A consequence of the high sedimentation rate is rapid burial (Nichols, 2009). Combined with reducing conditions it could have enforced genesis of pyrite and degeneration of the organic matter within the deposited sediments. This would completely deplete the sediments for the remaining oxygen, which would further amplify the two processes.

Another possibility for the absence of anoxia could simply be that the depositional environment was too shallow for the expanding OMZ during the OAE2 to reach.

5.2 Source rock potential

Palynofacies analysis has been proven to be able to provide valuable source rock information (Tyson, 1995; Traverse, 2007; Zobaa et al., 2011). Coupled with geochemical data, the palynofacies analysis can give an accurate assessment of petroleum potential of sedimentary rocks (Tyson, 1995; Batten, 1996).

The total organic carbon (TOC) content is in general relatively low (Figure 4.3). This is not necessarily a limiting factor because sedimentary rocks with similar content of TOC can be able to produce petroleum (Tyson, 1995; Batten, 1996). But this is dependent on the origin of the organic material.

In the Bass River Formation the terrestrial organic material is dominating throughout the formation (Figure 4.1), which is especially illustrated in the ter-

niary APP diagram (Figure 4.2.A). Tyson (1995) defined the fields II, III and IVa to be gas prone in terms of petroleum potential (Table 3.3).

However, the colour of the particulate organic matter in Bass River implies that the sediments are thermal immature, below the oil and gas window (Tyson, 1995). Considering that the phytoclasts consist mainly of opaque phytoclasts (Figure 4.1), which are already oxidised (Tyson, 1995), immaturity of sediments and low amount of TOC, gas generation is unlikely.

5.3 Vegetation history

5.3.1 Palynoflora

The composition of terrestrial palynomorphs in the Bass River Formation display a rich flora with high diversity of conifers and ferns (Figure 4.6). Angiosperms are less diverse and mainly dominated by *Atlantopollis verrucosa* and *Complexipollis* spp. (Figure 4.6). Such dominance of these angiospermid species are characteristic for the pollen Zone IV of Christopher (1982), the same zone to which Miller et al. (1998) assigned the Bass River Formation to.

The microflora of Bass River is a typical mid-Cretaceous assemblage observed in southeastern North America (Wolfe and Upchurch, 1987), as well as sharing similar traits as floras in the Iberian peninsula in Europe (Diéguez et al., 2010). This is not unreasonable, given that all sites belong to the Normapolles palynofloral province (Traverse, 2007).

According to Wolfe and Upchurch (1987) the flora in southeastern North America were open-canopy vegetation (e.g. woodland) rather than a dense tropical forest (Figure 5.3). The open woodland consisted of mainly evergreen conifers, interfingering angiosperms and understorey of ferns (Wolfe and Upchurch, 1987), which resembles the general floral trends displayed in the Bass River Formation (Figure 4.6).

There are some deviations from the Wolfe and Upchurch (1987) model in the Bass River palynological assemblages (Figures 4.6 and 4.10). Open-canopy vegetation was probably promoted by dryness, which would explain the presence of wind pollinating plants such as Fagales (Wolfe and Upchurch, 1987). However, in Bass River, the hygrophobic (arid-preferring) taxa such as the Fagales, are not dominant, but closer to equal to the xerophobic (humid-preferring) taxa in abundance (Figure 4.10).

Instead of a dominance, the hygrophobic taxa display high-abundance pulses (Figure 4.10), which is probably because of the presence of the delta. The fluvial influx into the delta would promote wetlands, which in this case are swamps

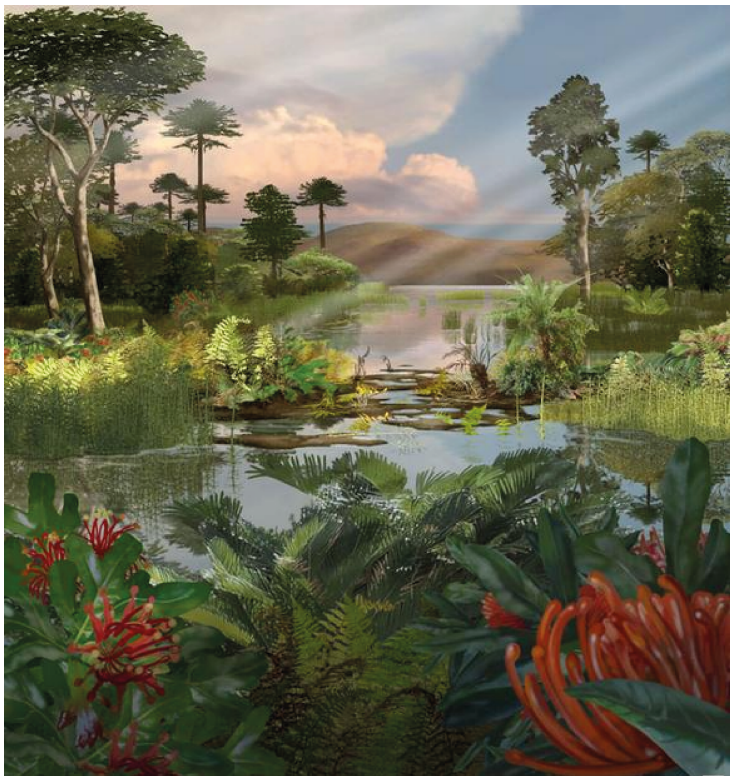

Figure 5.3 Illustration of a Late Cretaceous plant community. Pictured: Angiosperms, gymnosperms, Nothofagus, araucarians, podocarps, cycads, proteacea, flowering plants, Stenocarpus (Carr, 2013).

and/or mangrove forests (Figure 4.9). The high-abundance pulses of Normapolles pollen grains may therefore represent more arid periods, which would both promote blooms of the hygrophobic plants and diminish the fluvial influence and wetlands.

The results yielded 5 distinct palynofloral zones, which represent changes in the vegetation (Figure 4.7). Each zone represents plant assemblages of different climate preferences: The unstable, arid pre- and early OAE2 period; the stable, cold and humid middle OAE2 period; the extremely arid latest and post-OAE2 period; the warm and dry post-OAE2 period; and warm and humid post-OAE2 period (Figure 4.10). These changes and causes for changes are discussed in detail in Section 5.3.2.

5.3.2 Vegetation changes and causes

At the base, zone 1 is characterised by the onset of the OAE2 and instability in the vegetation, especially right after the onset. The assemblages display heavy fluctuations between the SEGs and warm-cold and arid-humid taxa (Figures 4.9 and 4.10). These changes coincides nearly always with variations in the SST (Figures 4.7 and 4.10). The upper boundary is additionally coinciding with the lowest flooding surface (figures 4.7 and 4.9) (Miller et al., 2004).

Palynofloral zone 2 displays a stable period in the vegetation, which coincides with the SST (Figure 4.7). The upper boundary is define by a sudden change in the vegetation, but is unrelated to the SST, which does not change (Figures 4.7 and 4.9). But the upper boundary of the palynofloral zone 2 is parallel to the upper boundary of palynofacies zone 3, marking the beginning of the condensed section and flooding surface (Figures 4.3, 4.7 and 4.9).

The 3rd palynofloral zone is characterised by the end of the OAE2 and dramatic change in the vegetation. This is not reflected in the SST but coincides with the flooding surface at the upper boundary of the zone (Figures 4.3, 4.7 and 4.9) (Miller et al., 2004). There is also a spike in aridity in this zone, which could indicate climate changes as well.

Palynofloral zone 4 is generally stable in the SST and vegetation (Figures 4.7 and 4.9). However, there are several high-abundance pulses of angiosperms that are opposing the signal from sea level and SST variations (Figures 4.7 and 4.9). This could be because the peaks of relative abundances are not necessarily peaks but caused by the percentage effect: the angiosperms increase simply because the other components in the total sum decreases. The lycopodium spores were not counted in the samples above 1895 feet because it was considered unnecessary, and absolute abundances could therefore not be calculated. However, an interval of high relative abundance of conifers coincides with the humidity curve, which is a ratio and therefore not affected by the percentage effect (Figures 4.7 and 4.10). This could indicate that the changes in vegetation are related to humidity variations.

The uppermost zone 5 displays the same problems as the 4th. The lower boundary is characterised by a sudden increase in conifers, which remains dominant throughout the zone (Figure 4.7). This is in contrast to the rising SST and with no apparent sea level change (Figure 4.7). Another prominent change in the interval is the rise in the humidity curve (Figure 4.10) and a rapid drop in the Ti:Al ratio (Figure 4.7). The Ti:Al ratio an indicator for aeolian transportation (Bertrand et al., 1996; Rachold and Brumsack, 2001). A drop in this ratio could mean more humid climate, wetter environments would reduce wind transportation of particles, as displayed in the humidity curve. Therefore are the changes in this zone probably related to a more humid climate.

Altogether, the results from the palynological analysis suggest that the driving mechanisms for the vegetation changes are sea level variations and climate changes. This is not surprising because of the dependency most plants have on specific climatic conditions and habitats (Abbink et al., 2001 and references therein). A sea level change could have severe impacts on plant coastal and lowland communities by changing the land area, and therefore also the habi-

tats. Changes in the climate could alter or remove the plant habitats. Those plants unable to adapt would vanish and new, more adaptive plants would prosper in the vacancy.

5.4 The C-T Oceanic Anoxic Event (OAE2)

In the Bass River Formation the Cenomanian-Turonian Oceanic Anoxic Event is defined by the characteristic positive excursion of $\delta^{13}C_{org}$ at the onset and reverse excursion at the end (Figure 4.3) (Schlanger and Jenkyns, 1976; Bowman and Bralower, 2005; Jenkyns, 2010). These boundaries are overlapped by climate changes at the lower Figure 5.1 and the upper boundary is coinciding with a flooding surface (Figure 5.1) and climate changes. These simultaneous happenings could be either related or coincidences. Although the former is most likely, the results merely state that whatever triggered the OAE2 was connected to climate changes, and what ended it also were linked to sea level and climate changes.

One of the many proposed mechanisms for triggering the OAE2 is increased chemical weathering on the continents induced by the warming of the climate (Schlanger and Jenkyns, 1976; Jenkyns, 2010; Monteiro et al., 2012). This will be discussed in Section 5.4.1.

Because of the complex signal mentioned above, the palynological and palynfacies analysis reveal only one possible consequence for the vegetation related to OAE2, which is discussed in detail in Section 5.4.2.

5.4.1 Terrestrial runoff

One of the proposed triggers for OAE2 is increased terrestrial runoff before the OAE2 onset. This was because the warming of the climate, probably in the relation of the increased volcanic activity, enhanced the chemical weathering (Schlanger and Jenkyns, 1976; Jenkyns, 2010; Monteiro et al., 2012). The weathered material was then brought into the oceans from fluvial inputs, fuelling the primary production (Schlanger and Jenkyns, 1976; Jenkyns, 2010; Monteiro et al., 2012).

The palynofacies analysis, however, do not indicate an increase in terrestrial runoff before the onset of the OAE2 (Figures 4.1, 4.3 and 4.4). Considering the absence of anoxia in the Bass River Formation this could mean that either the increase of terrestrial runoff was a secondary mechanism that amplified the established anoxia or it could be a triggering mechanism and therefore explain the absence of consistent anoxia in Bass River.

5.4.2 The Plenus Cold Event

In the OAE2 interval in Bass River there are 2 distinct periods of colder, both displayed in the SST and Lowland temperature curve, slightly more humid period (Figure 5.4.A). Both periods are defined by a lower boundary marked by a positive excursion in $\delta^{13}C_{org}$ and an upper boundary displaying a negative excursion (Figure 5.4.A).

These 2 periods can be related to the Plenus Cold Event. Gale and Christensen (1996) described a cold period shortly after the OAE2 onset in France, calling it the Plenus Cold Event (PCE). Similar cold periods were described in Newfoundland (Sinninghe Damsté et al., 2010) and southwestern Utah (Barclay et al., 2010) and were linked to the PCE. These sites displayed a specific $\delta^{13}C_{org}$ and temperature signature during the PCE, a rise in $\delta^{13}C_{org}$ and subsequent cooling, which is similar to the signal of the cold periods in this study.

A theory has been proposed concerning the apparent connection between the positive $\delta^{13}C_{org}$ excursion and temperature drop. The theory suggests that the sudden and rapid burial of organic carbon after the onset of the OAE2 led to a temporary negative feedback in the short term carbon cycle (Sinninghe Damsté et al., 2010; Barclay et al., 2010; Jarvis et al., 2011). The forced CO_2-drawdown from the atmosphere consequently led to a cooling of the climate (Barclay et al., 2010; Sinninghe Damsté et al., 2010; Jarvis et al., 2011). Barclay et al. (2010) presented a quantitative pCO_2 terrestrial proxy record that revealed two significant pulses of drawdown correlating with the $\delta^{13}C_{org}$ peaks (Figure 5.4.B).

Because of the difference in resolutions of the $\delta^{13}C_{org}$ data, correlation between data from present study and Barclay et al. (2010) was only illustrative. However, the similarities suggest that the two cold periods displayed in this study are related to the PCE.

5.5 Comparison to other OAE sites

The Bass River site is somewhat unique compared to the other sites that has been studied in connection with the OAE2. While Bass River was a clastic environment, the carbonate content is negligible (Figure 4.3), other sites have been deep marine (Sinninghe Damsté et al., 2010; Zobaa et al., 2011), carbonate platform (e.g. Götz et al., 2008; Takashima et al., 2009) or epicontinental (e.g. Curiale et al., 1992; Bowman and Bralower, 2005) settings.

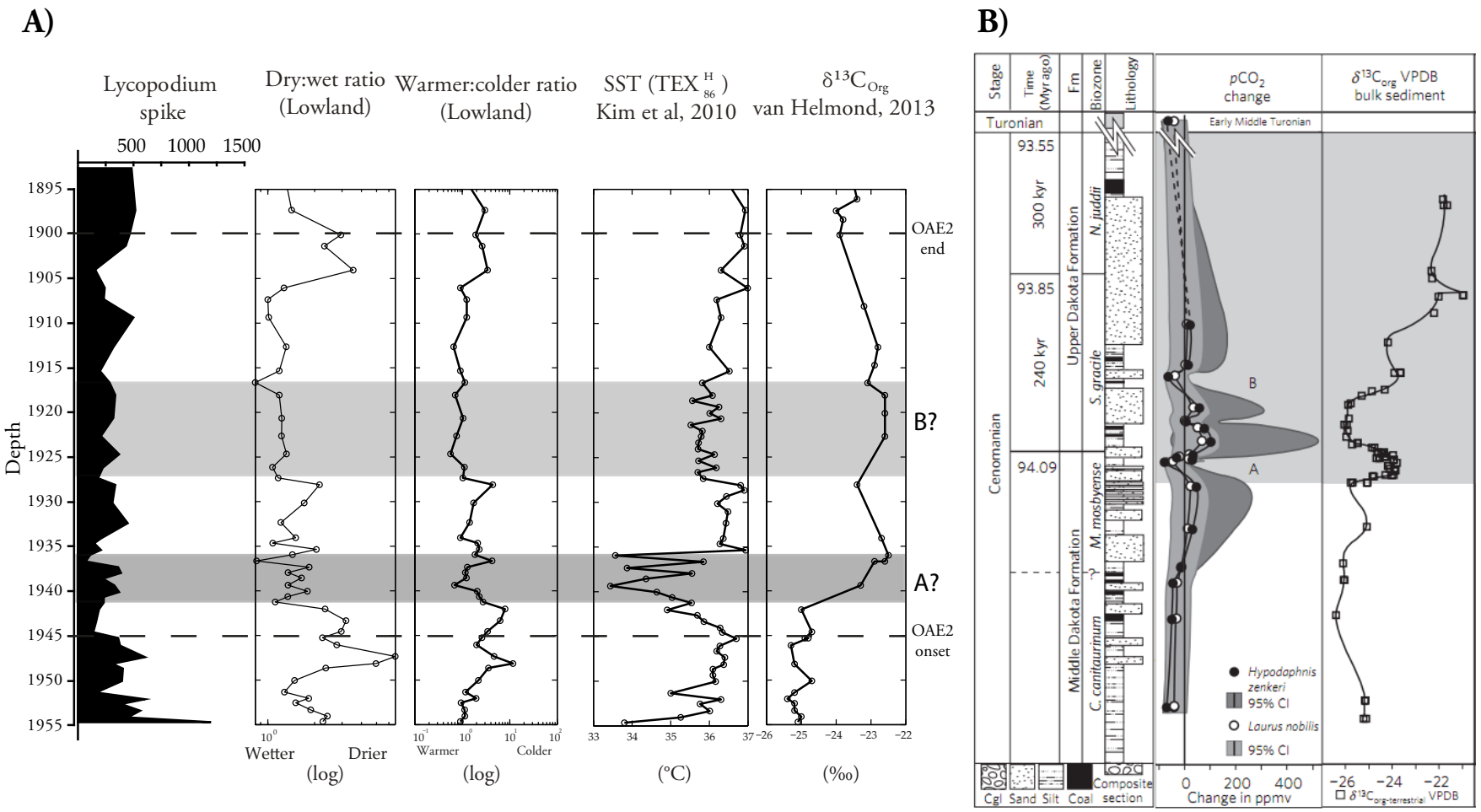

Figure 5.4 A) Display of palynological (this study) and geochemical data (van Helmond, 2013) from Bass River across the OAE2 interval. Lycopodium spike, SEG Lowland humidity and temperature curve, sea surface temperature calibrated from the TEX_{86} index, and $\delta^{13}C_{org}$. The two possible OAE2 cold events, A and B, proposed by Barclay et al. (2010) are highlighted in gray. The boundaries of the OAE2 are marked with dashed lines **B)** The original high resolution atmospheric palaeo-pCO_2 reconstruction across the OAE2 interval from southwestern Utah done by Barclay et al. (2010) (modified from Barclay et al., 2010)

Although the Bass River site displays the OAE2 $\delta^{13}C_{org}$ signature, none of the other characteristics of the OAE2 observed at other sites are evident; The TOC content is almost unaffected during the OAE2 interval and there are no signs of anoxia.

Only one other site displays the same pattern, the Morelos Formation in southern Mexico (Elrick et al., 2009). This site has a completely different depositional environment, nearshore carbonate deposits, but both the Bass River and Morelos formation display absence of anoxia and increased terrestrial runoff. This could mean that because of the relatively shallow setting both sites were above the expanded oxygen minimum zone, and/or the lack of increased terrestrial runoff did not trigger anoxia on these sites, or the increased runoff were a secondary mechanism, only amplifying the anoxic expansion, and not triggering the OAE.

5.6 Signification of the analyses

This thesis has shown that terrestrial palynomorphs from marine settings can yield additional, useful data on the circumstances surrounding the Oceanic Anoxic Events. Such an analysis is of course limited by the abundance of terrestrial palynomorphs in the sediments, which is evident in Zobaa et al. (2011). The authors used the palynomorphs only as a secondary supplement because of the inadequate and unreliable representation in the samples.

Nonetheless, the present study demonstrates the high potential of a terrestrial palynological analysis when adequate abundances are available. By using models such as the SEG model proposed by Abbink (1998), the terrestrial palynological analysis can be used as an independent supplement and correlation tool for other marine and geochemical derived data.

6. Conclusion

This study was first and foremost conducted to shed light on the impact the Cenomanian-Turonian Anoxic Event had on the terrestrial ecosystems. Because of the absence of such studies in connection to research on the OAEs, as of yet, it would also demonstrate the possibilities as a supplement and independent correlation tool for marine derived data. Given the presence of terrestrial organic matter in many marine settings, it could be of interest for future researches concerning the OAEs.

The Palynological and palynofacies analyses, coupled with the geochemical data, of the retrieved samples from the Bass River Formation in the ODP 174AX core yielded the following conclusions:

1. The composition of particulate organic matter in the Bass River Formation indicates that the sediments were deposited offshore on the neritic part of the shelf, with at least two flooding events.
2. There is evidence of dysoxic conditions in the depositional environment, but the presence of benthic organisms throughout the formation implies absence of anoxia, even during the OAE2.
3. The dysoxic conditions may be a result of an intermixing of sediment-, and nutrient-rich freshwater and stagnant, stratified oceanic water depleted of oxygen, on the shelf. This is, however, only speculations and need further investigation.
4. The palynofacies analysis indicates periodic elevated preservation rate and anoxia in the deposited sediments beneath the ocean bottom. This is probably because of the high terrestrial input of organic detritus diluting the total amount of particulate organic matter and the rapid burial caused by the high sedimentation rate.
5. The Bass River Formation have generally a low amount of immature organic carbon content, which is principally terrestrial derived and therefore mainly gas prone.
6. On the adjacent land the vegetation consisted of an open woodland, comprising of primary conifers and hygrophobic Normapolles producing an-

giosperms with an understorey of ferns. Evidence of wetlands on the coastal plain and within the delta is reflected by the presence of freshwater and brackish swamp and mangrove forest taxa.

7. The vegetation changes are mainly driven by either climate or sea level variations (by changing the area of the coastal plain) or a combination of the two.
8. There is no apparent evidence of an increase of terrestrial runoff before the onset of the OAE2 in the particulate organic material.
9. Two colder periods are displayed in the geochemical and palynological data during the OAE2. These periods may be related to the proposed theory of sudden and rapid carbon burial leading to CO_2 drawdown and causing a temporary cold period.
10. If it is viable, a terrestrial, palynological analysis can serve as a supplement and independent correlations tool for marine and geochemical derived data.

7. References

Abbink, O. A. (1998), *Palynological investigations in the Jurassic of the North Sea region*, LPP Foundation.

Abbink, O., Targarona, J., Brinkhuis, H. and Visscher, H. (2001), "Late Jurassic to earliest Cretaceous palaeoclimatic evolution of the southern North Sea", *Global and Planetary Change* , Vol. 30(3), Elsevier, pp. 231–256.

Abbink, O., Van Konijnenburg-Van Cittert, J. and Visscher, H. (2004), "A sporomorph ecogroup model for the Northwest European Jurassic-Lower Cretaceousi: concepts and framework", *Netherlands Journal of Geosciences-Geologie en Mijnbouw* , Vol. 83(2), Veenman Drukkers, pp. 17–31.

Adams, D. D., Hurtgen, M. T. and Sageman, B. B. (2010), "Volcanic triggering of a biogeochemical cascade during Oceanic Anoxic Event 2", *Nature Geoscience* , Vol. 3(3), Nature Publishing Group, pp. 201–204.

Armstrong, H. and Brasier, M. (2005), *Microfossils*, Wiley.

Arthur, M. A., Dean, W. E. and Pratt, L. M. (1988), "Geochemical and climatic effects of increased marine organic carbon burial at the Cenomanian/Turonian boundary", *Nature* , Vol. 335(6192), Nature Publishing Group, pp. 714–717.

Bally, A. and Palmer, A. (1989), *The Geology of North America: An Overview*, Geological Society of America.

Barclay, R. S. (2011), "Testing The Driving Mechanisms For Ocean Anoxic Event 2 (94Ma) Using pCO2 Estimates And Carbon Isotopes Derived From Fossil Plant Material In The Dakota Formation Of Southwestern Utah ", PhD thesis, Northwestern University, Evanston, Illinois.

Barclay, R. S., McElwain, J. C. and Sageman, B. B. (2010), "Carbon sequestration activated by a volcanic CO2 pulse during Ocean Anoxic Event 2", *Nature Geoscience* , Vol. 3(3), Nature Publishing Group, pp. 205–208.

Batten, D. (1996), Palynofacies and petroleum potential, *in* J. Jansonius and D. C. McGregor, eds, 'Palynology, principles and applications', Vol. 3, American Association of Stratigraphic Palynologists Foundation, College Station, TX, pp. 1065–1084.

Bertrand, P., Shimmield, G., Martinez, P., Grousset, F., Jorissen, F., Paterne, M., Pujol, C., Bouloubassi, I., Menard, P. B., Peypouquet, J.-P. et al. (1996), "The glacial ocean productivity hypothesis: the importance of regional temporal and spatial studies", *Marine Geology* , Vol. 130(1), Elsevier, pp. 1–9.

Blakey, R. and Colorado Plateau Geosystems Inc (2013), 'Mollewide Plate Tectonic Maps', `http://cpgeosystems.com/index.html`. Retrieved (31.05.13) from `http://cpgeosystems.com/90moll.jpg`.

Bowman, A. R. and Bralower, T. J. (2005), "Paleoceanographic significance of high-resolution carbon isotope records across the Cenomanian–Turonian boundary in the Western Interior and New Jersey coastal plain, USA", *Marine geology* , Vol. 217(3), Elsevier, pp. 305–321.

Carr, K. (2013), 'Late cretaceous plant community', `www.karencarr.com/`. Retrieved (31.08.13) from `http://www.karencarr.com/portfolio-images/Dinosaurs-and-ancient-life/Cretaceous/Australian-Museum/Australian-Museum-Late-Cretaceous-plant-community/411`.

Chaloner, W. and Muir, M. (1968), Spores and floras, *in* D. G. Murchison and T. S. Westall, eds, 'Coal and coal-bearing strata', Oliver and Boyd, Edinburgh, pp. 127–146.

Cheng, W. (n.d.), 'Oceans', `http://www.ic.ucsc.edu/~wxcheng/`. Retrieved (31.08.13) from `http://www.ic.ucsc.edu/~wxcheng/envs23/lecture6/FG04_09.JPG`.

Christopher, R. A. (1979), "Normapolles and triporate pollen assemblages from the Raritan and Magothy Formations (Upper Cretaceous) of New Jersey", *Palynology* , Vol. 3(1), American Association of Stratigraphic Palynologists, pp. 73–121.

Christopher, R. A. (1982), "The occurrence of the Complexiopollis-Atlantopollis Zone (palynomorphs) in the Eagle Ford Group (Upper Cretaceous) of Texas", *Journal of Paleontology* , Vol. 56(2), JSTOR, pp. 525–541.

Coiffard, C., Gomez, B. and Daviero-Gomez, V. (2012), Deciphering early angiosperm landscape ecology using a clustering method on cretaceous plant

assemblages, *in* J. Tiefenbacher, ed., 'Perspectives on Nature Conservation - Patterns, Pressures and Prospects', InTech.

Cookson, I. C. (1947), *Plant microfossils from the lignites of Kerguelen Archipelago*, BANZAR Expedition Committee.

Couper, R. A. (1953), *Upper Mesozoic and Cainozoic spores and pollen grains from New Zealand*, Vol. 22, RE Owen, Government Printer.

Couper, R. A. (1958), "British Mesozoic microspores and pollen grains. A systematic and stratigraphic study", *Palaeontographica* , Vol. 103B, Schweizerbart'sche Verlagsbuchhandlung, pp. 75–179.

Curiale, J., Cole, R. and Witmer, R. (1992), "Application of organic geochemistry to sequence stratigraphic analysis: Four Corners Platform Area, New Mexico, USA", *Organic geochemistry* , Vol. 19(1), Elsevier, pp. 53–75.

Delcourt, A., Potonié, R. and Sprumont, G. (1955), *Les spores et graines de pollen du Wealdien du Hainaut*.

Diéguez, C., Peyrot, D. and Barrón, E. (2010), "Floristic and vegetational changes in the Iberian Peninsula during Jurassic and Cretaceous", *Review of Palaeobotany and Palynology* , Vol. 162(3), Elsevier, pp. 325–340.

Doyle, P. and Lowry, F. (1996), *Understanding fossils: an introduction to invertebrate palaeontology*, Wiley.

Eaton, J. G., Kirkland, J. I., Hutchison, J. H., Denton, R., O'Neill, R. C. and Parrish, J. M. (1997), "Nonmarine extinction across the Cenomanian-Turonian boundary, southwestern Utah, with a comparison to the Cretaceous-Tertiary extinction event", *Geological Society of America Bulletin* , Vol. 109(5), Geological Society of America, pp. 560–567.

Eldrett, J. S., Greenwood, D. R., Harding, I. C. and Huber, M. (2009), "Increased seasonality through the Eocene to Oligocene transition in northern high latitudes", *Nature* , Vol. 459(7249), Nature Publishing Group, pp. 969–973.

Eleson, J. W. and Bralower, T. J. (2005), "Evidence of changes in surface water temperature and productivity at the Cenomanian/Turonian Boundary", *Micropaleontology* , Vol. 51(4), Micropaleontol Project, pp. 319–332.

Elrick, M., Molina-Garza, R., Duncan, R. and Snow, L. (2009), "C-isotope stratigraphy and paleoenvironmental changes across OAE2 (mid-Cretaceous) from shallow-water platform carbonates of southern Mexico", *Earth and Planetary Science Letters* , Vol. 277(3), Elsevier, pp. 295–306.

Erbacher, J., Mosher, D., Bauldauf, J. and Malone, M. (2002), "LEG 207 Scientific Prospectus: Demerara Rise: Equatorial Cretaceous and Paleogene Paleoceanographic Transect, Western Atlantic", *Ocean Drilling Program Scientific Prospectus* , Vol. 107, 207: College Station, TX (Ocean Drilling Program), pp. 1–66.

Feild, T., Chatelet, D. and Brodribb, T. (2009), "Ancestral xerophobia: a hypothesis on the whole plant ecophysiology of early angiosperms", *Geobiology* , Vol. 7(2), Wiley Online Library, pp. 237–264.

Feild, T. S., Arens, N. C., Doyle, J. A., Dawson, T. E. and Donoghue, M. J. (2004), "Dark and disturbed: a new image of early angiosperm ecology", *Paleobiology* , Vol. 30(1), Paleontological Society, pp. 82–107.

Friis, E., Crane, P. and Pedersen, K. (2011), *Early Flowers and Angiosperm Evolution*, Cambridge University Press.

Friis, E. M., Pedersen, K. R. and Schönenberger, J. (2003), "Endressianthus, a New Normapolles-Producing Plant Genus of Fagalean Affinity from the Late Cretaceous of Portugal", *International journal of plant sciences* , Vol. 164(S5), JSTOR, pp. S201–S223.

Gale, A. S. and Christensen, W. K. (1996), "Occurrence of the belemnite Actinocamax plenus in the Cenomanian of SE France and its significance", *Bulletin of the Geological Society of Denmark* , Vol. 43, GGeological Society of Denmark, pp. 68–77.

Gary, A. C., Wakefield, M. I., Johnson, G. W. and Ekart, D. D. (2009), Application of fuzzy C-means clustering to paleoenvironmental analysis: Example from the Jurassic, Central North Seas, UK, *in* 'Geologic Problem Solving with Microfossils: A Volume in Honor of Garry D. Jones', jones, g.d. and demchuk, t.d. and gary, a.c. and sepm edn, Society for Sedimentary Geology (SEPM).

Góczán, P., Groot, J. J., Krutzsch, W. and Pacltová, B. (1967), "Die Gattungen des "Stemma Normapolles Pflug 1953b" (Angiospermae)", *Palaont. Abhandlungen, ser. B.* , Vol. 2(3), pp. 427–633.

Götz, A. E., Feist-Burkhardt, S. and Ruckwied, K. (2008), "Palynofacies and sea-level changes in the Upper Cretaceous of the Vocontian Basin, southeast France", *Cretaceous Research* , Vol. 29(5), Elsevier, pp. 1047–1057.

Götz, A. E., Ruckwied, K. and Barbacka, M. (2011), "Palaeoenvironment of the Late Triassic (Rhaetian) and Early Jurassic (Hettangian) Mecsek Coal For-

mation (south Hungary): implications from macro-and microfloral assemblages", *Palaeobiodiversity and Palaeoenvironments* , Vol. 91(2), Springer, pp. 75–88.

Gradstein, F. M., Ogg, J. G. and Schmitz, M. (2012), *The Geologic Time Scale 2012, 2-volume set*, Elsevier.

Groot, J. J. and Groot, C. R. (1962), "Plant microfossils from Aptian, Albian and Cenomanian deposits of Portugal", *Comm. Geol. Survey Portuga* , Vol. 46, pp. 133–184.

Groot, J. J. and Penny, J. S. (1960), "Plant microfossils and age of nonmarine Cretaceous sediments of Maryland and Delaware", *Micropaleontology* , Vol. 6(2), Micropaleontol Project, pp. 225–236.

Groot, J. J., Penny, J. S. and Groot, C. R. (1961), "Plant microfossils and age of the Raritan, Tuscaloosa and Magothy Formations of the eastern United States", *Palaeontographica Abteilung B* , Vol. 108(3-6), Schweizerbart'sche Verlagsbuchhandlung, pp. 121–140.

Haq, B. U., Hardenbol, J. and Vail, P. R. (1987), "Chronology of fluctuating sea levels since the Triassic", *Science* , Vol. 235(4793), American Association for the Advancement of Science, pp. 1156–1167.

Heimhofer, U., Hochuli, P., Burla, S., Dinis, J. and Weissert, H. (2005), "Timing of Early Cretaceous angiosperm diversification and possible links to major paleoenvironmental change", *Geology* , Vol. 33(2), Geological Society of America, pp. 141–144.

Herman, A. B. and Spicer, R. A. (1997), "New quantitative palaeocolimate data for the Late Cretaceous Arctic: evidence for a warm polar ocean", *Palaeogeography, Palaeoclimatology, Palaeoecology* , Vol. 128(1), Elsevier, pp. 227–251.

Huber, B. T., Leckie, R. M., Norris, R. D., Bralower, T. J. and CoBabe, E. (1999), "Foraminiferal assemblage and stable isotopic change across the Cenomanian-Turonian boundary in the subtropical North Atlantic", *The Journal of Foraminiferal Research* , Vol. 29(4), CFFR, pp. 392–417.

Jahren, A. H. (2002), "The biogeochemical consequences of the mid-Cretaceous superplume", *Journal of Geodynamics* , Vol. 34(2), Elsevier, pp. 177–191.

Jarvis, I., Lignum, J. S., Gröcke, D. R., Jenkyns, H. C. and Pearce, M. A. (2011), "Black shale deposition, atmospheric CO2 drawdown, and cooling during the

Cenomanian-Turonian Oceanic Anoxic Event", *Paleoceanography* , Vol. 26(3), Wiley Online Library, pp. n/a–n/a.

Jenkyns, H. C. (2010), "Geochemistry of oceanic anoxic events", *Geochemistry, Geophysics, Geosystems* , Vol. 11(3), Wiley Online Library, pp. 1–30.

Kaufmann, E. G. and Johnson, C. C. (2009), Cretaceous warm climates, *in* V. Gornitz, ed., 'Encyclopedia of Paleoclimatology and Ancient Environments', Springer, pp. 213–217.

Kim, J.-H., Van der Meer, J., Schouten, S., Helmke, P., Willmott, V., Sangiorgi, F., Koç, N., Hopmans, E. C. and Damsté, J. S. S. (2010), "New indices and calibrations derived from the distribution of crenarchaeal isoprenoid tetraether lipids: Implications for past sea surface temperature reconstructions", *Geochimica et Cosmochimica Acta* , Vol. 74(16), Elsevier, pp. 4639–4654.

Kimyai, A. (1966), "New plant microfossils from the Raritan Formation (Cretaceous) in New Jersey", *Micropaleontology* , Vol. 12(4), JSTOR, pp. 461–476.

Krutzsch, W. (1959), "Einige neue Formgattungen und -Arten von Sporen und Pollen aus der mitteleuropaischen Oberkreide und dem Tertih "ars", *Palaeontographica Abteilung B* , Vol. 195(5-6), Schweizerbart'sche Verlagsbuchhandlung, pp. 125–157.

Kump, L. R. and Arthur, M. A. (1999), "Interpreting carbon-isotope excursions: carbonates and organic matter", *Chemical Geology* , Vol. 161(1), Elsevier, pp. 181–198.

Leckie, R. M., Bralower, T. J. and Cashman, R. (2002), "Oceanic anoxic events and plankton evolution: Biotic response to tectonic forcing during the mid-Cretaceous", *Paleoceanography* , Vol. 17(3), American Geophysical Union, p. 1041.

Lupia, R., Lidgard, S. and Crane, P. R. (1999), "Comparing Palynological Abundance and Diversity: Implications for Biotic Replacement during the Cretaceous Angiosperm Radiation", *Paleobiology* , Vol. 25(3), Paleontological Society, pp. 305–340.

Miller, K. G., Browning, J. V., Sugarman, P. J., McLaughlin, P. P., Kominz, M. A., Olsson, R. K., Wright, J. D., Cramer, B. S., Pekar, S. J. and Van Sickel, W. (2002), "174AX leg summary: sequences, sea level, tectonics, and aquifer resources: coastal plain drilling", *Proceedings of the Ocean Drilling Program, Leg 174AX (supplement): College Station, Texas, Ocean Drilling Program* , 207: College Station, TX (Ocean Drilling Program), pp. 1–40.

Miller, K. G., Kominz, M. A., Browning, J. V., Wright, J. D., Mountain, G. S., Katz, M. E., Sugarman, P. J., Cramer, B. S., Christie-Blick, N. and Pekar, S. F. (2005), "The Phanerozoic record of global sea-level change", *science* , Vol. 310(5752), American Association for the Advancement of Science, pp. 1293–1298.

Miller, K. G., Sugarman, P. J., Browning, J. V., Kominz, M. A., Olsson, R. K., Feigenson, M. D. and Hernández, J. C. (2004), "Upper Cretaceous sequences and sea-level history, New Jersey coastal plain", *Geological Society of America Bulletin* , Vol. 116(3-4), Geological Society of America, pp. 368–393.

Miller, K. G., Sugarman, P. J., Browning, J. V., Olsson, R. K., Pekar, S. F., Reilly, T. J., Cramer, B. S., Aubry, M.-P., Lawrence, R. P., Curran, J., Stewart, M., Metzger, J. M., Uptegrove, J., Bukry, D., Burckle, L. H., Wright, J. D., Feigenson, M. D., Brenner, G. J. and Dalton, R. F. (1998), "Bass River Site", *Proc. Ocean Drill. Program Initial Rep., 174AX* , 174AX: College Station, TX (Ocean Drilling Program), pp. 5–43.

Monteiro, F., Pancost, R., Ridgwell, A. and Donnadieu, Y. (2012), "Nutrients as the dominant control on the spread of anoxia and euxinia across the Cenomanian-Turonian oceanic anoxic event (OAE2): Model-data comparison", *Paleoceanography* , Vol. 27(4), Wiley Online Library, p. 17.

Nagalingum, N., Drinnan, A., Lupia, R. and McLoughlin, S. (2002), "Fern spore diversity and abundance in Australia during the Cretaceous", *Review of Palaeobotany and Palynology* , Vol. 119(1), Elsevier, pp. 69–92.

Nichols, G. (2009), *Sedimentology and Stratigraphy*, Wiley Desktop Editions, Wiley.

Nystuen, J. P., Mü ller, R., Mø rk, A. and Nø ttvedt, A. (2008), From desert to alluvial fan - from land to sea, *in* I. Ramberg, ed., 'The Making of a Land: Geology of Norway', Geological Society Publishing House.

Pacton, M., Gorin, G. E. and Vasconcelos, C. (2011), "Amorphous organic matter - Experimental data on formation and the role of microbes", *Review of Palaeobotany and Palynology* , Vol. 166(3), Elsevier, pp. 253–267.

Peyrot, D., Barroso-Barcenilla, F., Barrón, E. and Comas-Rengifo, M. J. (2011), "Palaeoenvironmental analysis of Cenomanian–Turonian dinocyst assemblages from the Castilian Platform (Northern-Central Spain)", *Cretaceous Research* , Vol. 32(4), Elsevier, pp. 504–526.

Pflug, H. D. (1953), "Zur Entstehung und Entwicklung des angiospermiden Pollens in der Erdgeschichte", *Palaeontographica Abteilung B* , Vol. 95(4-6, Schweizerbart'sche Verlagsbuchhandlung, pp. 60–171.

Pierce, R. L. (1961), *Lower upper Cretaceous plant microfossils from Minnesota*, Vol. 42, University of Minnesota Press.

Potonié, R. (1931), "Zur Mikroskopie der Braunkohlen.Tertiäre Blütenstabformen", *Braunkohle* , Vol. 30(16), pp. 325–333.

Potonié, R. (1956), "Synopsis der Gattungen der Sporae dispersae: I. Sporites", *Beih. Geol. Jahrb.* , Vol. 23, Geologische Landesanstalten der Bundesrepublik Deutschland, pp. 1–103.

Potonié, R. (1958), "Synopsis der Gattungen der Sporae dispersae: II. Sporites (Nachträge), Saccites, Aletes, Praecolpates, Polyplicates, Monocolpates", *Beih. Geol. Jahrb.* , Vol. 31, Geologische Landesanstalten der Bundesrepublik Deutschland, pp. 1–114.

Potonié, R. and Gelletich, J. (1933), "Über pteridophyten-sporen einer eozänen braunkohle aus dorog in ungarn", *SB Ges. Nat. Freunde (1932)* , Vol. 33, Gesellschaft Naturforschender Freunde zu Berlin, pp. 517–528.

Potonié, R. and Venitz, H. (1934), "Zur Mikrobotanik des miozänen Humodils der niederrheinischen Bucht", *Arb. Inst. Paläob. Petrogr. Brennsteine* , Vol. 5, Preuß. Geolog. Landesanst., pp. 5–54.

Powell, A., Dodge, J. and Lewis, J. (1990), "Late Neogene To Pleistocene Palynological Facies Of The Peruvian Continental Margin Upwelling, LEG 1121", *Proceedings of the Ocean Drilling Program, Scientific Results* , Vol. 112, 174AX: College Station, TX (Ocean Drilling Program), pp. 297–321.

Price, G. D. (2009), Mesozoic climates, *in* V. Gornitz, ed., 'Encyclopedia of Paleoclimatology and Ancient Environments', Springer, pp. 554–558.

Rachold, V. and Brumsack, H.-J. (2001), "Inorganic geochemistry of Albian sediments from the Lower Saxony Basin NW Germany: palaeoenvironmental constraints and orbital cycles", *Palaeogeography, Palaeoclimatology, Palaeoecology* , Vol. 174(1), Elsevier, pp. 121–143.

Sageman, B. (2009), Oceanic Anoxic Events, *in* V. Gornitz, ed., 'Encyclopedia of Paleoclimatology and Ancient Environments', Springer, pp. 554–558.

Sageman, B. B., Meyers, S. R. and Arthur, M. A. (2006), "Orbital time scale and new C-isotope record for Cenomanian-Turonian boundary stratotype", *Geology* , Vol. 34(2), Geological Society of America, pp. 125–128.

Saward, S. A. (1992), A global view of cretaceous vegetation patterns, *in* P. MacCabe and J. Parrish, eds, 'Controls on the Distribution and Quality of Cretaceous Coals', number 267 *in* 'Controls on the distribution and quality of Cretaceous coals', Geological Society of America, pp. 17–35.

Schlanger, S. and Jenkyns, H. (1976), "Cretaceous oceanic anoxic events: causes and consequences", *Geologie en mijnbouw* , Vol. 55(3-4), Netherlands Journal of Geosciences, pp. 179–184.

Schlumberger (2013), 'Oilfield glossary', `http://www.glossary.oilfield.slb.com/`. Retrieved (25.09.13) from `http://www.glossary.oilfield.slb.com/en/Terms.aspx?LookIn=term%20name&filter=condensed%20section`.

Sinninghe Damsté, J. S., van Bentum, E. C., Reichart, G.-J., Pross, J. and Schouten, S. (2010), "A CO^2 decrease-driven cooling and increased latitudinal temperature gradient during the mid-Cretaceous oceanic anoxic event 2", *Earth and Planetary Science Letters* , Vol. 293(1), Elsevier, pp. 97–103.

Spicer, R. A., Rees, P. M., Chapman, J. L., Jarzembowski, E. and Cantrill, D. (1993), "Cretaceous phytogeography and climate signals [and discussion]", *Philosophical Transactions of the Royal Society of London. Series B: Biological Sciences* , Vol. 341(1297), The Royal Society, pp. 277–286.

Stanford, S. D., Sugarman, P. J. and Owens, J. P. (2004), 'Bedrock geology of the camden and philadelphia quadrangles, camden, gluecester, and burlington counties, new jersey', Online. Retrieved (31.05.13) from `www.state.nj.us/dep/njgs/pricelst/ofmap/ofm61.pdf?`

Stover, L. E. (1962), "Taurocusporites, a new trilete spore genus from the Lower Cretaceous of Maryland", *Micropaleontology* , Vol. 8(1), Micropaleontol Project, pp. 55–59.

Sugarman, P., Miller, K., Olsson, R., Browning, J., Wright, J., De Romero, L., White, T., Muller, F. and Uptegrove, J. (1999), "The Cenomanian/Turonian carbon burial event, Bass River, NJ, USA; geochemical, paleoecological, and sea-level changes", *The Journal of Foraminiferal Research* , Vol. 29(4), CFFR, pp. 438–452.

Takashima, R., Nishi, H., Hayashi, K., Okada, H., Kawahata, H., Yamanaka, T., Fernando, A. G. and Mampuku, M. (2009), "Litho-, bio-and chemostratigraphy across the Cenomanian/Turonian boundary (OAE 2) in the Vocontian Basin of southeastern France", *Palaeogeography, Palaeoclimatology, Palaeoecology* , Vol. 273(1), Elsevier, pp. 61–74.

Takashima, R., Nishi, H., Huber, B. T. and Leckie, R. M. (2006), "Greenhouse world and the Mesozoic Ocean", *Oceanography* , Vol. 19(4), The Oceanography Society, pp. 82–92.

Tarduno, J., Brinkman, D., Renne, P., Cottrell, R., Scher, H. and Castillo, P. (1998), "Evidence for extreme climatic warmth from Late Cretaceous Arctic vertebrates", *Science* , Vol. 282(5397), American Association for the Advancement of Science, pp. 2241–2243.

Thomson, P. W. and Pflug, H. D. (1953), "Pollen und Sporen des mitteleuropäischen Tertiärs", *Palaeontographica Abteilung B* , Vol. 94(1-4), Schweizerbart'sche Verlagsbuchhandlung, pp. 1–138.

Trabucho Alexandre, J., Tuenter, E., Henstra, G. A., van der Zwan, K. J., van de Wal, R. S., Dijkstra, H. A. and de Boer, P. L. (2010), "The mid-Cretaceous North Atlantic nutrient trap: Black shales and OAEs", *Paleoceanography* , Vol. 25(4), Wiley Online Library, pp. n/a–n/a.

Traverse, A. (2007), *Paleopalynology*, Topics in Geobiology, Springer London, Limited.

Turgeon, S. C. and Creaser, R. A. (2008), "Cretaceous oceanic anoxic event 2 triggered by a massive magmatic episode", *Nature* , Vol. 454(7202), Nature Publishing Group, pp. 323–326.

Tyson, R. (1995), *Sedimentary organic matter: organic facies and palynofacies*, Chapman & Hall.

U.S. Geological Survey (2013), 'Atlantic coastal plain', `http://www.usgs.gov/`. Retrieved (31.05.13) from `http://3dparks.wr.usgs.gov/nyc/coastalplain/coastalplain.htm`.

van Helmond, N. (2013), "Ocean biogeochemistry in the mid-Cretaceous: reconstructing the nutrient-biosphere-climate link", PhD thesis, Utrecht University. In press.

Weyland, H. and Krieger, W. (1953), "Die Sporen und Pollen der Aachener Kreide und ihre Bedeutung für die Charakterisierung des mittleren Senons",

Palaeontographica Abteilung B , Vol. 95(1-3), Schweizerbart'sche Verlagsbuchhandlung, pp. 2–29.

Wolfe, J. A. and Upchurch, G. R. (1987), "North American nonmarine climates and vegetation during the Late Cretaceous", *Palaeogeography, Palaeoclimatology, Palaeoecology* , Vol. 61, Elsevier, pp. 33–77.

Zobaa, M. K., Oboh-Ikuenobe, F. E. and Ibrahim, M. I. (2011), "The Cenomanian/Turonian oceanic anoxic event in the Razzak Field, north Western Desert, Egypt: Source rock potential and paleoenvironmental association", *Marine and petroleum geology* , Vol. 28(8), Elsevier, pp. 1475–1482.

A. Plates

Plate 1

1. *Alsophilidites kerguelensis* Cookson, 1947
2. *Cyathidites minor* Couper, 1953
3. *Cyathidites minor* Couper, 1953
4. *Cyathidites australis* Couper, 1953
5. *Appendicisporites* sp.
6. *Appendicisporites* sp.
7. *Concavisporites* sp.
8. *Concavisporites* sp.
9. *Taurocusporites* sp.
10. *Cicatricosisporites* sp.
11. *Cicatricosisporites* sp.
12. *Lycopodiumsporites* sp.

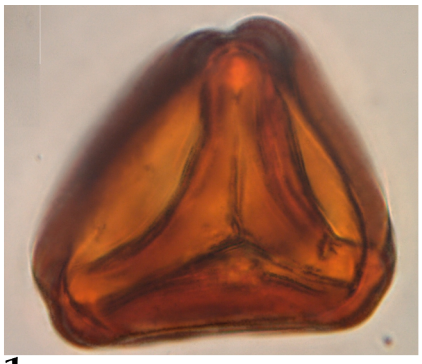

1

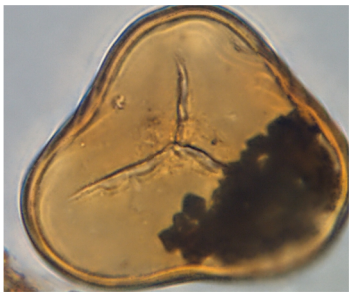

2

3

4

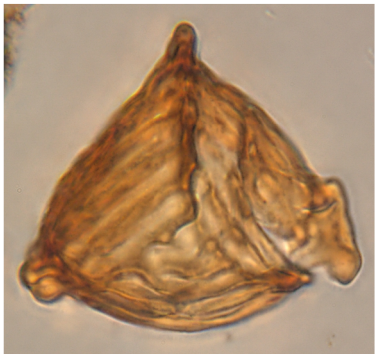

5

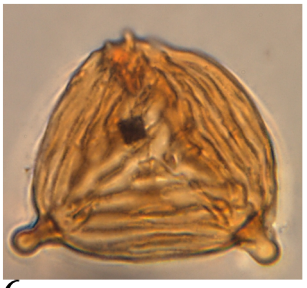

6

7

8

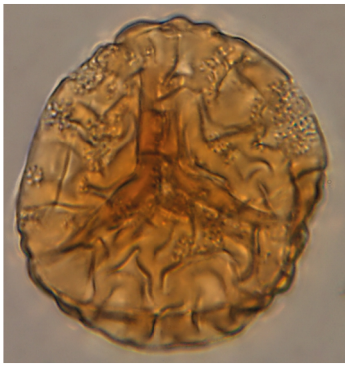

9

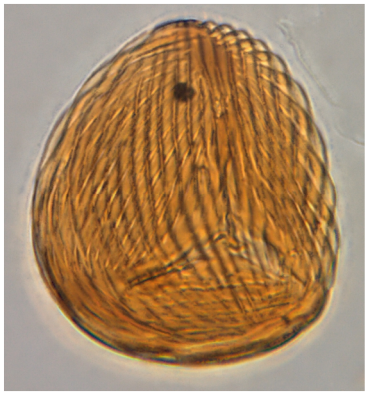

10

11

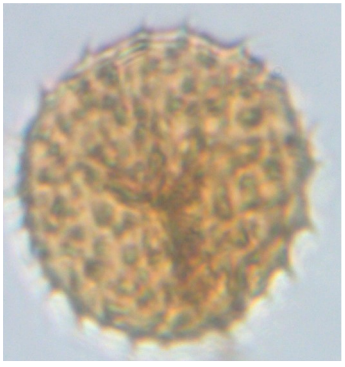

12

10 µm

Plate 2

1. *Abietineaepollenites grandialatus* Groot and Penny, 1960
2. *Phyllocladidites* sp.
3. *Dacrydiumpollenites rarus* Groot, Penny and Groot, 1961
4. *Dacrydiumpollenites rarus* Groot, Penny and Groot, 1961
5. *Rugubivesiculites rugosus* Pierce, 1961
6. *Rugubivesiculites rugosus* Pierce, 1961
7. *Abietineaepollenites microreticulatus* Groot and Penny, 1960

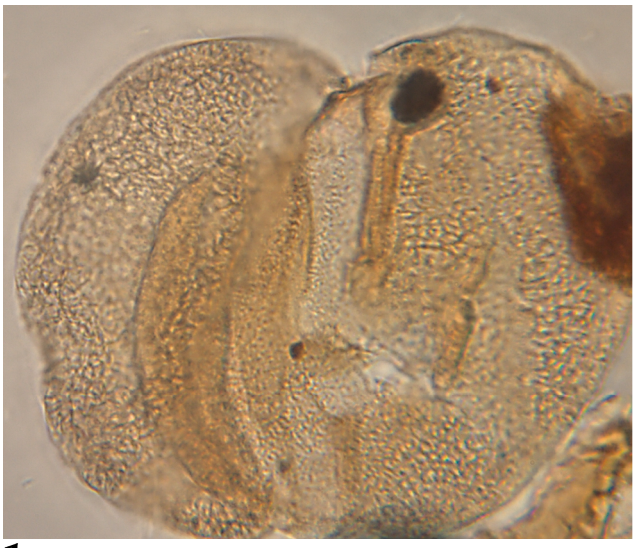

1

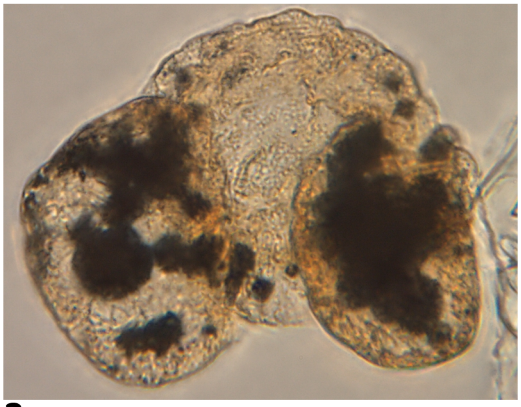

2

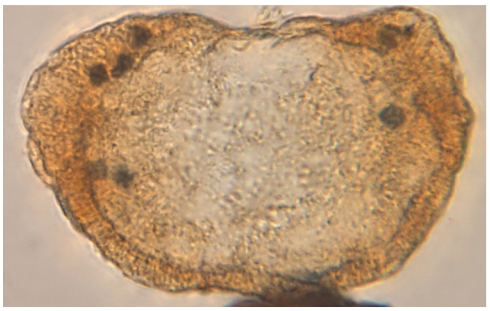

3

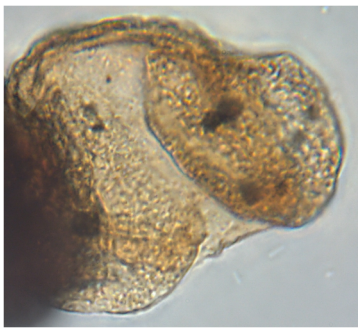

4

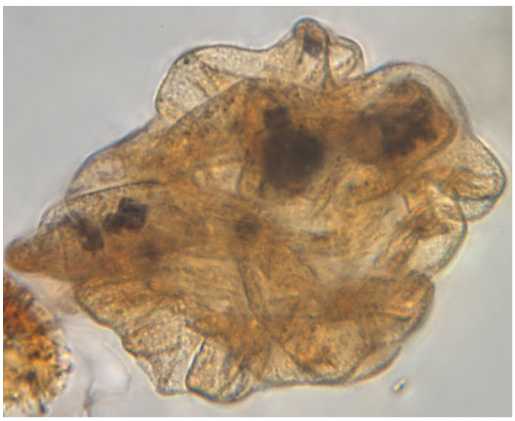

5

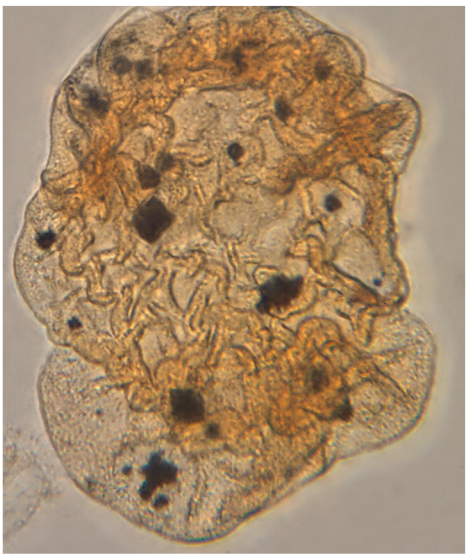

6

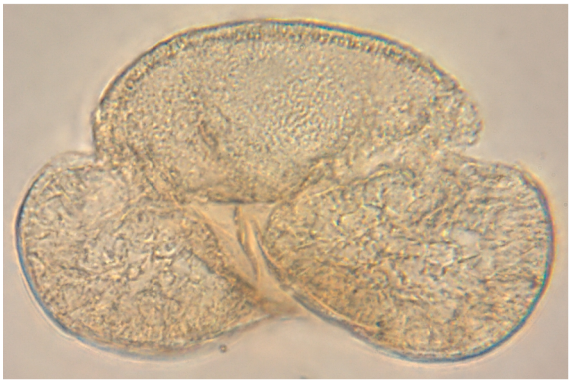

7

10 µm

Plate 3

1. *Complexiopollis* sp. 1
2. *Complexiopollis* sp. 2
3. *Complexiopollis* sp. 3
4. *Complexiopollis* sp. 4
5. *Complexiopollis* sp. 5
6. *Complexiopollis* sp. 6
7. *Atlantopollis verrucosa* (Groot and Groot, 1962) Góczán, Groot, Krutzsch and Pacltová, 1967
8. *Atlantopollis verrucosa* (Groot and Groot, 1962) Góczán, Groot, Krutzsch and Pacltová, 1967
9. Tetrad pollen
10. *Tricolpopollenites* sp.
11. *Tricolpopollenites* sp.
12. *Tricolporopollenites* sp. 1

1

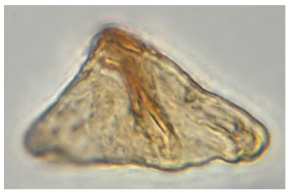

2

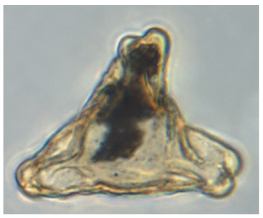

3

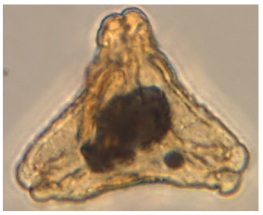

4

5

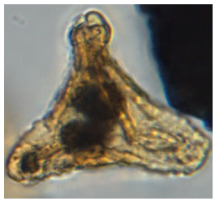

6

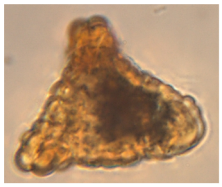

7

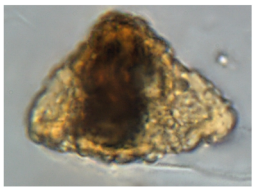

8

9

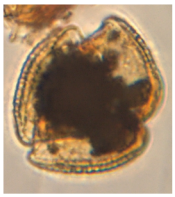

10

11

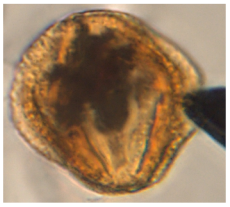

12

10 µm

Plate 4

1. *Inaperturopollenites dubius* Thomson and Pflug, 1953
2. *Inaperturopollenites atlanticus* Groot, Penny and Groot, 1961
3. *Clavatipollenites* sp.
4. *Clavatipollenites* sp.
5. Monosulcate sp

1

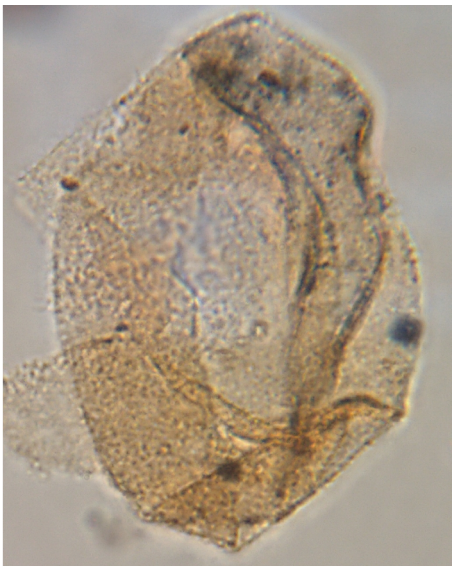

2

3

4

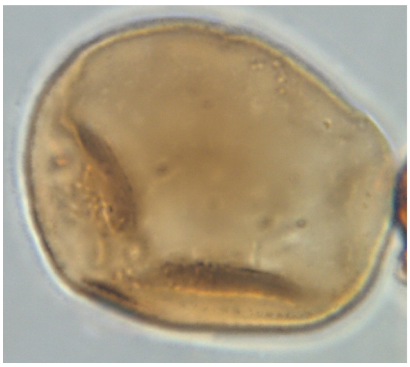

5

10 µm

B. Sample data

Sample nr.	Core	Depth interval (ft)	Depth (ft)	Weight (g)	Lycobatch no	Lycopodium # /batch	L-factor (#/g)
1	ODP174AX	1817-1817.1	1817.05	13.3003	483216	18583	1397.18653
2	ODP174AX	1821.05-1821.15	1821.1	11.1544	483216	18583	1665.979344
3	ODP174AX	1825.6-1825.7	1825.65	7.5381	483216	18583	2465.210066
4	ODP174AX	1828.1-1828.2	1828.15	12.4741	483216	18583	1489.726714
5	ODP174AX	1830.6-1830.7	1830.65	8.9021	483216	18583	2087.484975
6	ODP174AX	1833.3-1833.4	1833.35	12.0144	483216	18583	1546.727261
7	ODP174AX	1835.3-1835.4	1835.35	9.4974	483216	18583	1956.640765
8	ODP174AX	1838.6-1838.7	1838.65	13.4422	483216	18583	1382.437399
9	ODP174AX	1841.9-1842	1841.95	8.758	483216	18583	2121.831468
10	ODP174AX	1844.05-1844.15	1844.1	11.6589	483216	18583	1593.889647
11	ODP174AX	1846-1846.1	1846.05	9.8871	483216	18583	1879.519778
12	ODP174AX	1850.1-1850.2	1850.15	12.0287	483216	18583	1544.888475
13	ODP174AX	1854.1-1854.2	1854.15	12.0981	483216	18583	1536.026318
14	ODP174AX	1860.6-1860.7	1860.65	10.795	483216	18583	1721.445113
15	ODP174AX	1864.6-1864.7	1864.65	9.8983	483216	18583	1877.393088
16	ODP174AX	1868.6-1868.7	1868.65	11.8693	483216	18583	1565.635716
17	ODP174AX	1872-1872.1	1872.05	11.9527	483216	18583	1554.711488
18	ODP174AX	1874.6-1874.7	1874.65	14.169	483216	18583	1311.525161
19	ODP174AX	1877.3-1877.4	1877.35	8.0997	483216	18583	2294.282504
20	ODP174AX	1879.3-1879.4	1879.35	11.4515	483216	18583	1622.756844
21	ODP174AX	1884-1884.1	1884.05	10.9267	483216	18583	1700.696459
22	ODP174AX	1886.6-1886.7	1886.65	10.4683	483216	18583	1775.168843
23	ODP174AX	1890.6-1890.7	1890.65	11.0716	483216	18583	1678.438527
24	ODP174AX	1891.3-1891.4	1891.35	11.597	483216	18583	1602.397172
25	ODP174AX	1892.6-1892.7	1892.65	11.0425	483216	18583	1682.861671
26	ODP174AX	1897.3-1897.4	1897.35	11.7687	483216	18583	1579.018923
27	ODP174AX	1900.05-1900.15	1900.1	9.4781	483216	18583	1960.62502
28	ODP174AX	1901.3-1901.4	1901.35	11.6025	483216	18583	1601.637578
29	ODP174AX	1904-1904.1	1904.05	10.0346	483216	18583	1851.892452
30	ODP174AX	1906-1906.1	1906.05	12.4095	483216	18583	1497.481768
31	ODP174AX	1907.3-1907.4	1907.35	11.0018	483216	18583	1689.08724
32	ODP174AX	1909.3-1909.4	1909.35	11.2446	483216	18583	1652.615478
33	ODP174AX	1912.6-1912.7	1912.65	10.2343	483216	18583	1815.756818
34	ODP174AX	1915.3-1915.4	1915.35	10.6429	483216	18583	1746.04666
35	ODP174AX	1916.6-1916.7	1916.65	11.962	483216	18583	1553.502759
36	ODP174AX	1918-1918.1	1918.05	10.9364	483216	18583	1699.188033
37	ODP174AX	1920.6-1920.7	1920.65	10.6029	483216	18583	1752.633713
38	ODP174AX	1922.6-1922.7	1922.65	10.1201	483216	18583	1836.246677
39	ODP174AX	1924.6-1924.7	1924.65	11.6351	483216	18583	1597.150003
40	ODP174AX	1926.1-1926.2	1926.15	10.2801	483216	18583	1807.667241
41	ODP174AX	1927.3-1927.4	1927.35	10.2614	483216	18583	1810.961467

Sample nr.	Core	Depth interval (ft)	Depth (ft)	Weight (g)	Lycobatch no	Lycopodium # /batch	L-factor (#/g)
42	ODP174AX	1928.05-1928.15	1928.1	10.1416	483216	18583	1832.353869
43	ODP174AX	1930.1-1930.2	1930.15	10.9583	483216	18583	1695.792231
44	ODP174AX	1932.3-1932.4	1932.35	9.7962	483216	18583	1896.960046
45	ODP174AX	1934-1934.1	1934.05	7.4962	483216	18583	2478.989355
46	ODP174AX	1934.6-1934.7	1934.65	8.0465	483216	18583	2309.451314
47	ODP174AX	1935.3-1935.4	1935.35	5.7585	483216	18583	3227.055657
48	ODP174AX	1935.9-1936	1935.95	9.9735	483216	18583	1863.23758
49	ODP174AX	1936.6-1936.7	1936.65	8.9697	483216	18583	2071.752678
50	ODP174AX	1937.3-1937.4	1937.35	9.202	483216	18583	2019.452293
51	ODP174AX	1937.9-1938	1937.95	10.3403	483216	18583	1797.143216
52	ODP174AX	1938.5-1938.6	1938.55	11.4085	483216	18583	1628.873209
53	ODP174AX	1939.3-1939.4	1939.35	9.2349	483216	18583	2012.257848
54	ODP174AX	1940-1940.1	1940.05	6.6458	483216	18583	2796.202113
55	ODP174AX	1940.6-1940.7	1940.65	8.1555	483216	18583	2278.585004
56	ODP174AX	1941.2-1941.3	1941.25	11.3538	483216	18583	1636.720745
57	ODP174AX	1942.0-1942.1	1942.05	9.7158	483216	18583	1912.657733
58	ODP174AX	1943.3-1943.4	1943.35	10.0858	483216	18583	1842.491424
59	ODP174AX	1944.5-1944.6	1944.55	12.958	483216	18583	1434.094768
60	ODP174AX	1945.2-1945.3	1945.25	11.0609	483216	18583	1680.062201
61	ODP174AX	1946-1946.1	1946.05	9.8752	483216	18583	1881.784673
62	ODP174AX	1947.3-1947.4	1947.35	10.1697	483216	18583	1827.290874
63	ODP174AX	1948.1-1948.2	1948.15	8.9306	483216	18583	2080.823237
64	ODP174AX	1948.6-1948.7	1948.65	8.6801	483216	18583	2140.873953
65	ODP174AX	1950-1950.1	1950.05	6.5183	483216	18583	2850.896706
66	ODP174AX	1951.3-1951.4	1951.35	14.2434	483216	18583	1304.674446
67	ODP174AX	1952-1952.1	1952.05	6.0365	483216	18583	3078.439493
68	ODP174AX	1952.5-1952.6	1952.55	10.6759	483216	18583	1740.6495
69	ODP174AX	1953.3-1953.4	1953.35	6.411	483216	18583	2898.611761
70	ODP174AX	1954-1954.1	1954.05	11.8828	483216	18583	1563.857003
71	ODP174AX	1954.6-1954.7	1954.65	3.2218	483216	18583	5767.893724

C. Geochemical data

Sample depth (ft)	TOC (wt%)*	$CaCO_3$ (wt%) *	$\delta^{13}C_{org}$ (wt%)*	TeX_{86}*	SST (TEX_{86}^{H}) . Kim et al.. 2010 (°C)	Ti/Al*	Reconstructed palaeo-pH *
*van Helmond. 2013							
1817						0.062	
1817.05				0.88	34.82		6.78
1818.6							
1818.7	0.5	21.2	-23.9				
1818.65				0.89	35.22		6.77
1821.05						0.076	
1821.1				0.70	28.09		7.02
1822.3						0.051	
1822.35				0.89	35.16		6.55
1823.6						0.044	
1823.7	1.2	11.4	-24.0				
1823.65				0.89	35.16		6.85
1825.6						0.051	
1825.65				0.88	34.95		6.82
1828.1						0.050	
1828.2	1.5	8.8	-23.8				
1828.15				0.84	33.58		6.90
1830.6						0.045	
1830.65				0.88	34.74		6.83
1833.3						0.044	
1833.35				0.84	33.53		7.02
1835.3						0.046	
1835.4	1.2	8.7	-24.1				
1835.35				0.89	35.12		6.95
1838.1						0.049	
1838.15				0.89	35.12		6.79
1838.6						0.064	
1838.65				0.86	34.03		7.00
1841.9						0.075	
1841.95				0.90	35.38		7.04
1844.05						0.061	
1844.1	0.9	6.9	-24.5				
1844.1				0.78	31.38		6.94

Sample depth (ft)	TOC (wt%)*	$CaCO_3$ (wt%) *	$\delta^{13}C_{org}$ (wt%)*	TeX_{86}*	SST (TEX_{86}^{H}) . Kim et al.. 2010 (°C)	Ti/Al*	Reconstructed palaeo-pH *
1846						0.059	
1846.05				0.84	33.50		6.57
1849.3						0.067	
1849.35				0.90	35.34		6.68
1850.1						0.074	
1850.2	0.6	12.2	-24.3				
1850.15				0.89	35.29		6.70
1854.1						0.066	
1854.2	0.9	12.3	-23.9				
1854.15				0.91	35.85		6.62
1860.6						0.054	
1860.7	1.1	9.6	-24.0				
1860.65				0.91	35.76		6.69
1864.6						0.075	
1864.7	0.4	13.9	-23.7				
1864.7	0.5	13.4	-23.7				
1864.65				0.91	35.79		6.86
1868.6						0.054	
1868.7	1.3	9.5	-23.9				
1868.65				0.90	35.47		6.74
1870.6						0.070	
1870.7	0.4	24.9	-23.7				
1872						0.065	
1872.1	0.7	11.1	-23.7				
1872.05				0.91	35.73		6.82
1873.3						0.067	
1873.4	0.6	11.8	-23.6				
1873.35				0.92	36.22		7.03
1874.6						0.054	
1874.7	1.1	10.2	-24.0				
1874.65				0.93	36.42		6.89
1876.6						0.061	
1876.7	0.7	15.8	-23.6				
1879.3						0.055	

Sample depth (ft)	TOC (wt%)*	$CaCO_3$ (wt%) *	$\delta^{13}C_{org}$ (wt%)*	TeX_{86}*	SST (TEX_{86}^{H}) . Kim et al.. 2010 (°C)	Ti/Al*	Reconstructed palaeo-pH *
1879.4	0.8	10.4	-23.7				
1879.35				0.93	36.37		7.03
1881.3						0.061	
1881.4	0.7	15.0	-23.6				
1882.6						0.052	
1882.7	1.0	12.8	-23.8				
1884						0.056	
1884.1	0.9	10.9	-23.6				
1884.05				0.93	36.42		6.89
1885.3						0.050	
1885.4	1.0	15.9	-23.9				
1886.6						0.060	
1886.7	0.7	14.2	-23.9				
1886.65				0.92	36.19		7.03
1888						0.051	
1888.1	0.8	16.2	-23.8				
1888.1	0.8	16.3	-24.1				
1889.3						0.056	
1889.4	0.7	17.1	-23.4				
1890.6						0.054	
1890.7	0.9	11.6	-23.6				
1890.65				0.93	36.30		6.89
1891.3						0.049	
1891.4	1.0	15.8	-23.7				
1891.35				0.93	36.38		7.15
1892.6						0.051	
1892.7	0.8	14.0	-23.6				
1892.65				0.92	36.24		7.28
1896						0.057	
1896.1	0.6	16.8	-23.4				
1897.3						0.053	
1897.4	0.9	7.7	-24.0				
1897.35				0.95	36.93		7.17
1898.3						0.048	

Sample depth (ft)	TOC (wt%)*	$CaCO_3$ (wt%) *	$\delta^{13}C_{org}$ (wt%)*	TeX_{86}*	SST (TEX_{86}^{H}) . Kim et al.. 2010 (°C)	Ti/Al*	Reconstructed palaeo-pH *
1898.4	1.1	9.7	-23.8				
1900.05						0.054	
1900.1	0.9	13.1	-23.9				
1900.1				0.94	36.80		7.12
1901.3						0.051	
1901.35				0.94	36.91		7.21
1904						0.050	
1904.05				0.93	36.30		7.08
1906						0.045	
1906.05				0.95	36.99		7.24
1907.3						0.056	
1907.35				0.92	36.19		7.22
1908						0.053	
1908.1	1.1	12.2	-23.2				
1909.3						0.050	
1909.35				0.93	36.30		7.27
1912.6						0.053	
1912.7	1.0	20.0	-22.8				
1912.65				0.92	36.00		7.13
1914.6						0.047	
1914.7	1.2	15.0	-22.9				
1915.3						0.053	
1915.35				0.93	36.52		7.17
1916.6						0.053	
1916.7	0.9	16.6	-23.1				
1916.65				0.91	35.82		7.23
1918						0.052	
1918.1	1.1	25.9	-22.6				
1918.05				0.92	36.08		7.04
1918.6						0.053	
1918.65				0.90	35.56		7.30
1919.3						0.049	
1919.35				0.92	36.25		7.16
1920						0.055	

Sample depth (ft)	TOC (wt%)*	$CaCO_3$ (wt%) *	$\delta^{13}C_{org}$ (wt%)*	TeX_{86}*	SST (TEX_{86}^{H}) . Kim et al.. 2010 (°C)	Ti/Al*	Reconstructed palaeo-pH *
1920.1	1.3	10.4	-22.6				
1920.1	1.3	10.1	-22.6				
1920.05				0.92	36.01		7.04
1920.6						0.057	
1920.65				0.93	36.30		7.04
1921.3						0.051	
1921.35				0.90	35.52		7.06
1922						0.056	
1922.05				0.91	35.82		7.29
1922.6						0.056	
1922.7	1.1	14.5	-22.6				
1922.65				0.91	35.79		7.04
1923.3						0.050	
1923.35				0.91	35.72		7.11
1924						0.049	
1924.05				0.91	35.71		6.97
1924.6						0.049	
1924.65				0.92	36.13		7.34
1925.3						0.052	
1925.35				0.91	35.72		7.22
1926.1						0.052	
1926.15				0.92	36.18		7.18
1926.6						0.053	
1926.65				0.91	35.70		7.10
1927.3						0.056	
1927.35				0.91	35.84		7.05
1928.05						0.058	
1928.1	1.1	11.4	-23.4				
1928.1				0.94	36.81		7.13
1928.6						0.052	
1928.65				0.94	36.90		7.25
1929.3						0.050	
1929.35				0.93	36.44		7.18
1930.1						0.054	

Sample depth (ft)	TOC (wt%)*	$CaCO_3$ (wt%) *	$\delta^{13}C_{org}$ (wt%)*	TeX_{86}*	SST (TEX_{86}^{H}) . Kim et al.. 2010 (°C)	Ti/Al*	Reconstructed palaeo-pH *
1930.15				0.92	36.21		7.05
1931						0.054	
1931.05				0.93	36.48		7.22
1932.3						0.053	
1932.35				0.93	36.43		7.35
1934						0.049	
1934.1	1.4	15.5	-22.7				
1934.05				0.93	36.36		7.10
1934.6						0.048	
1934.65				0.92	36.27		6.83
1935.3						0.046	
1935.35				0.95	36.94		7.20
1935.9						0.055	
1936.0	1.1	17.3	-22.5				
1935.95				0.84	33.57		7.38
1936.6						0.047	
1936.7	1.5	25.5	-22.6				
1936.7	1.5	25.7	-22.9				
1936.65				0.91	35.85		6.99
1937.3						0.055	
1937.35				0.85	33.87		7.54
1937.9						0.054	
1937.95				0.90	35.55		7.40
1938.5						0.060	
1938.55				0.87	34.36		7.11
1939.3						0.059	
1939.4	0.6	26.1	-23.3				
1939.35				0.84	33.44		7.48
1940						0.064	
1940.05				0.88	34.64		7.32
1940.6						0.057	
1940.65				0.89	35.04		7.05
1941.2						0.059	
1941.25				0.90	35.54		7.09

Sample depth (ft)	TOC (wt%)*	$CaCO_3$ (wt%) *	$\delta^{13}C_{org}$ (wt%)*	TeX_{86}*	SST (TEX_{86}^{H}) . Kim et al.. 2010 (°C)	Ti/Al*	Reconstructed palaeo-pH *
1942						0.051	
1942.1	1.1	12.7	-25.0				
1942.05				0.88	34.91		7.32
1942.6						0.054	
1942.65				0.91	35.69		7.20
1943.3						0.055	
1943.35				0.91	35.86		7.10
1944						0.053	
1944.05				0.92	36.28		7.13
1944.5						0.053	
1944.6	1.1	16.0	-24.7				
1944.55				0.93	36.34		7.00
1945.2						0.050	
1945.3	1.1	12.9	-24.9				
1945.3	1.0	12.7	-24.8				
1945.25				0.94	36.70		7.25
1946						0.051	
1946.1	1.1	12.4	-25.3				
1946.05				0.92	36.27		7.29
1946.6						0.057	
1946.65				0.92	36.19		7.47
1947.3						0.057	
1947.35				0.93	36.40		7.53
1948.1						0.058	
1948.2	0.8	11.9	-25.2				
1948.15				0.93	36.37		7.45
1948.6						0.056	
1948.65				0.92	36.09		7.37
1949.3						0.053	
1949.35				0.92	36.09		7.42
1950						0.052	
1950.1	1.0	16.7	-24.7				
1950.05				0.92	36.16		7.55
1951.3						0.060	

Sample depth (ft)	TOC (wt%)*	$CaCO_3$ (wt%) *	$\delta^{13}C_{org}$ (wt%)*	TeX_{86}*	SST (TEX_{86}^{H}) . Kim et al.. 2010 (°C)	Ti/Al*	Reconstructed palaeo-pH *
1951.4	0.8	17.8	-25.2				
1951.35				0.89	35.00		7.37
1952						0.062	
1952.1	0.8	13.4	-25.4				
1952.05				0.93	36.30		7.61
1952.5						0.059	
1952.6	0.9	12.3	-25.2				
1952.55				0.91	35.76		7.44
1953.3						0.060	
1953.4	0.9	11.6	-25.2				
1953.4	0.9	11.9	-25.2				
1953.35				0.92	36.01		7.49
1954						0.059	
1954.1	0.8	14.0	-25.0				
1954.05				0.89	35.26		7.65
1954.6						0.063	
1954.65				0.85	33.80		7.38

D. Palynofacies data

Sample depth	Amorphoues OM	Wood remains	Cuticle remains	Plant tissue	Lath-shaped opaques	Equidimensional opaques	Foram linings	Bisaccate pollen	Other pollen	Spores	Dinoflagellate cysts	Prasinophytes	Acritarchs	Total sum
1817.05	43	75	33	10	24	111	7	3	6	3	17	9	0	341
1821.1	64	91	21	7	34	92	9	4	6	0	8	2	0	338
1825.65	66	53	11	8	14	125	3	10	3	5	14	4	0	316
1828.15	55	88	26	17	28	71	9	8	4	4	11	8	0	329
1830.65	44	68	24	3	34	101	6	7	9	5	12	5	2	320
1833.35	19	75	24	21	43	82	6	16	7	3	30	5	0	331
1835.35	39	63	16	6	45	117	3	17	8	5	9	3	0	331
1838.65	62	52	20	26	18	86	11	5	14	5	45	4	3	351
1841.95	39	95	17	13	22	81	12	7	5	9	31	4	0	335
1844.1	92	93	9	11	11	74	7	6	14	6	15	14	0	352
1846.05	70	64	37	13	35	103	6	4	11	7	13	3	0	366
1850.15	55	83	27	9	13	115	8	2	12	5	11	1	1	342
1854.15	37	105	21	19	18	111	7	13	7	3	16	2	0	359
1860.65	59	100	27	15	34	83	10	4	4	6	22	3	2	369
1864.65	32	69	17	9	42	109	16	11	7	1	22	2	3	340
1868.65	74	76	24	10	21	106	3	7	9	6	13	3	0	352
1872.05	45	89	21	6	30	114	11	5	8	3	9	1	0	342
1874.65	45	73	21	6	8	122	7	7	10	5	24	6	0	334
1877.35	77	55	24	12	32	103	8	3	5	0	12	5	0	336
1879.35	51	66	27	19	39	93	9	3	17	4	19	0	0	347
1884.05	50	91	7	6	41	157	12	6	11	4	15	6	1	407
1886.65	43	45	21	12	29	108	9	5	12	5	29	4	0	322
1890.65	33	98	19	12	30	114	7	7	4	3	12	3	0	342
1891.35	53	84	20	15	15	67	13	9	8	2	24	7	0	317
1892.65	44	60	14	11	23	123	3	10	10	3	19	1	0	321
1897.35	54	57	11	11	39	100	7	4	5	3	24	3	0	318
1900.05	46	81	21	13	32	110	8	2	13	0	33	3	0	362
1901.35	76	62	17	10	24	65	13	7	19	6	35	3	0	337
1904.05	69	85	40	12	13	45	28	11	14	2	14	11	0	344
1906.05	49	73	16	3	26	113	21	10	10	4	7	4	0	336
1907.35	30	42	15	4	56	139	10	11	9	0	13	3	0	332
1909.35	40	107	18	5	36	101	15	6	8	2	6	4	1	349
1912.65	36	106	14	9	24	118	26	12	10	2	1	6	1	365
1915.35	67	53	8	10	14	125	19	10	5	1	12	2	0	326
1916.65	20	77	3	3	26	133	22	10	3	4	5	1	1	308
1918.05	89	88	21	11	11	81	20	4	3	1	6	5	0	340
1922.65	41	109	18	7	35	132	21	9	4	2	5	14	0	397
1924.65	58	68	10	6	20	82	54	7	7	5	31	7	1	356
1926.15	67	67	9	10	42	119	45	17	6	2	36	7	0	427
1927.35	74	66	9	17	22	126	46	14	5	4	5	6	0	394
1928.1	87	57	7	8	28	106	23	9	4	2	11	4	0	346
1930.15	63	44	6	11	22	136	26	10	4	2	14	3	0	341

Sample depth	Amorphoues OM	Wood remains	Cuticle remains	Plant tissue	Lath-shaped opaques	Equidimensional opaques	Foram linings	Bisaccate pollen	Other pollen	Spores	Dinoflagellate cysts	Prasinophytes	Acritarchs	Total sum
1932.35	42	105	15	7	57	154	15	7	6	4	8	2	0	422
1934.05	50	51	11	14	24	124	21	18	10	1	9	10	0	343
1934.65	72	89	9	29	35	98	11	12	6	0	8	5	1	375
1935.35	66	71	9	17	22	127	18	20	9	4	28	8	1	400
1935.95	54	66	10	10	22	153	15	10	16	12	27	9	0	404
1936.65	83	80	8	21	14	88	15	23	15	3	32	13	0	395
1937.35	50	67	7	5	18	132	57	21	16	5	24	8	1	411
1937.95	49	29	4	6	11	145	21	18	8	7	18	11	0	327
1938.55	75	81	6	18	13	114	56	10	6	5	17	10	1	412
1939.35	26	42	2	2	24	113	40	32	4	3	24	8	2	322
1940.05	33	66	10	5	21	141	5	19	8	5	13	7	1	334
1940.65	94	94	8	15	32	102	2	9	3	4	15	6	1	385
1941.25	72	85	9	27	7	125	28	7	2	1	32	8	0	403
1943.35	53	68	11	13	29	115	16	4	2	2	12	5	0	330
1944.55	72	68	4	16	30	123	17	7	6	2	19	4	1	369
1945.25	42	79	15	20	25	105	5	10	0	3	24	5	0	333
1946.05	50	82	5	10	42	96	18	5	10	3	14	2	1	338
1947.35	26	67	16	7	43	124	18	7	2	3	28	3	3	347
1948.65	34	58	5	3	32	125	18	11	4	1	22	3	4	320
1951.35	39	26	7	14	27	142	8	18	4	2	32	7	2	328
1952.55	20	29	9	9	29	170	20	27	5	3	28	7	0	356

E. Palynological data

Sample depth	Lycopodium spike	Undifferentiated trilete spores	Cicatricosisporites spp.	Taurocusporites spp.	Lycopodiumsporites sp.	Todisporites sp.	Appendicisporites spp.	Cyathidites spp.	A. Kerguelensis	Concavisporites sp.	Monosulcate spp.	Clavatipollenites sp.	Undifferentiated bisaccates	D. rarus	Phyllocladidites sp.	Undifferentiated Abietineaepollenites	A. grandialatus	A. microreticulatus	A. microsaccus	R. rugosus	Tsugapollenites sp.	Undifferentiated Inaperturopollenites	I. dubius	I. hiatus	I. rugosus	I. atlanticus	Undifferentiated tricolpates, tricolporates	Undifferentiated tricolpates	Undifferentiated tricolporates	Undifferentiated triporates	Undifferentiated normapolles	Complexiopollis spp.	A. verrucosus	Total sum
1817.05	-	25	17	10	0	0	0	2	6	0	7	3	56	21	17	4	6	2	3	40	11	17	20	9	5	5	16	10	2	0	9	3	1	327
1821.1	-	15	17	2	0	0	3	1	3	0	10	3	64	13	6	0	9	5	6	19	12	8	14	6	0	1	11	5	3	5	2	4	3	250
1825.65	-	12	31	1	0	0	0	1	3	0	7	0	78	13	20	0	13	9	4	34	12	18	13	7	2	6	3	2	1	0	4	0	0	294
1828.15	-	19	25	5	0	0	1	2	4	0	7	3	74	12	11	1	2	4	5	33	13	16	8	9	1	9	14	8	4	3	5	3	2	303
1830.65	-	45	17	1	0	0	5	1	6	0	2	1	129	13	19	0	7	1	2	29	14	24	7	4	2	2	5	3	2	0	1	0	0	342
1833.35	-	33	26	2	0	0	9	1	0	0	3	3	130	13	11	0	8	5	5	21	6	26	6	4	0	10	5	7	2	8	4	0	4	352
1835.35	-	38	22	1	0	0	4	3	8	0	1	2	130	11	23	0	5	4	3	25	3	25	12	5	1	4	2	1	1	1	3	2	1	341
1838.65	-	50	14	2	0	0	1	1	9	1	6	0	113	0	6	0	1	0	1	7	3	50	9	6	1	7	7	6	0	1	5	1	13	321
1841.95	-	49	17	3	0	0	4	1	4	2	2	0	24	2	2	0	0	0	0	3	4	84	11	5	3	9	19	1	3	3	28	13	47	343
1844.1	-	80	16	4	0	0	1	1	3	0	3	1	59	5	2	0	0	0	1	10	8	49	8	4	3	7	9	4	1	1	8	1	13	302
1846.05	-	97	24	6	0	0	2	1	8	0	3	0	32	4	0	1	0	0	0	7	5	44	10	9	1	4	17	2	2	1	11	5	28	324
1850.15	-	54	16	2	0	0	0	1	6	0	6	2	31	3	0	0	1	0	0	7	2	41	3	6	0	4	21	6	3	5	39	11	31	301
1854.15	-	50	19	3	0	0	0	0	5	1	10	2	123	7	3	0	1	4	1	13	4	21	4	2	1	3	13	4	0	4	9	1	13	321
1864.65	-	51	17	0	0	0	4	0	6	0	7	1	68	3	3	1	1	2	1	17	7	42	10	3	3	18	14	2	2	8	7	5	26	329
1872.05	-	46	16	5	1	1	8	1	1	6	11	2	75	7	3	1	7	10	2	32	10	27	4	2	1	4	13	2	1	6	1	5	1	312
1877.35	-	38	14	0	2	1	2	3	6	1	5	2	37	2	1	0	0	1	0	17	3	45	13	3	1	6	27	3	5	1	16	17	44	316
1879.35	-	32	9	0	1	0	4	1	3	1	3	2	9	1	0	0	0	0	0	15	4	48	16	2	3	10	16	6	1	3	41	25	55	311
1884.05	-	70	7	3	1	0	7	3	10	7	1	1	45	6	4	0	4	4	3	24	9	28	8	5	1	3	14	4	4	4	4	17	9	310
1886.65	-	83	5	2	3	0	3	2	8	5	6	1	51	1	1	0	1	0	0	9	5	51	12	5	1	4	15	4	0	0	1	2	20	301
1890.65	-	64	8	2	0	0	5	2	1	1	7	0	76	3	1	0	2	2	1	19	17	43	7	4	0	8	10	0	1	0	3	3	11	301

Sample depth	Lycopodium spike	Undifferentiated trilete spores	Cicatricosisporites spp.	Tarocusporites spp.	Lycopodiumsporites sp.	Todisporites sp.	Appendicisporites spp.	Cyathidites spp.	A. Kerguelensis	Concavisporites sp.	Monosulcate spp.	Clavatipollenites sp.	Undifferentiated bisaccates	D. rarus	Phyllocladidites sp.	Undifferentiated Abietineaepollenites	A. grandialatus	A. microreticulatus	A. microsaccus	R. rugosus	Tsugapollenites sp.	Undifferentiated Inaperturopollenites	I. dubius	I. hiatus	I. rugosus	I. atlanticus	Undifferentiated tricolpates, tricolporates	Undifferentiated tricolpates	Undifferentiated tricolporates	Undifferentiated triporates	Undifferentiated normapolles	Complexiopollis spp.	A. verrucosus	Total sum
1891.35	-	45	5	2	0	0	4	1	2	2	4	0	94	4	2	1	0	5	4	40	13	33	5	0	0	6	14	6	0	0	1	0	5	298
1892.65	480	58	13	8	4	0	19	1	5	0	22	0	59	11	6	6	0	1	1	40	7	16	2	1	0	1	8	2	0	0	1	2	9	303
1897.35	522	44	15	8	1	0	24	3	5	4	3	0	28	7	1	1	1	0	0	14	3	26	9	1	0	2	6	0	0	0	31	8	21	266
1900.1	470	62	12	5	0	0	14	1	0	1	8	0	14	2	1	1	1	0	0	13	5	16	3	0	0	1	10	0	0	0	40	13	34	257
1901.35	430	57	17	4	0	0	18	2	0	3	7	0	29	1	0	0	0	0	0	18	0	28	3	0	0	0	15	1	0	0	42	17	41	303
1904.05	160	51	15	13	0	0	9	6	0	7	4	0	7	2	0	1	0	0	1	14	3	18	6	2	1	1	11	0	1	0	49	51	30	303
1906.05	246	53	12	15	0	0	15	0	1	5	15	0	74	10	2	0	1	0	1	45	7	16	7	0	0	1	9	0	0	0	4	2	5	300
1907.35	233	46	11	6	0	0	22	2	0	3	19	0	65	7	1	0	3	2	1	51	3	29	1	0	1	1	12	0	0	0	3	4	7	300
1909.35	504	54	19	3	0	0	12	0	1	0	16	0	53	7	0	0	0	1	0	55	3	27	5	1	3	3	15	0	0	0	2	4	11	295
1912.65	320	74	23	15	0	1	17	0	0	4	16	0	52	7	1	0	0	1	0	59	10	14	1	0	1	1	11	0	0	0	0	1	1	310
1915.35	200	54	10	13	0	0	16	0	0	3	4	0	76	11	5	0	6	2	1	58	4	14	5	1	0	4	23	2	0	0	3	0	0	315
1916.65	290	41	9	21	0	0	12	1	1	3	16	0	70	11	3	1	1	1	0	49	6	33	5	1	0	1	15	0	0	0	2	0	1	304
1918.05	340	60	9	9	0	0	15	1	0	4	22	0	59	11	2	0	1	3	0	50	5	21	6	0	0	3	12	4	0	0	1	1	1	300
1920.65	316	87	24	18	0	0	8	0	2	4	7	0	33	9	0	0	0	1	0	20	4	34	10	2	1	5	16	0	1	0	7	3	4	300
1922.65	210	76	29	13	0	1	12	0	0	4	18	0	25	6	2	2	1	1	1	46	10	17	3	2	0	3	23	0	0	0	2	1	2	300
1924.65	375	45	11	5	0	0	11	1	0	10	31	0	49	14	8	1	4	1	4	68	12	10	4	1	0	1	16	1	0	0	3	0	1	312
1926.15	227	68	26	6	1	0	17	2	0	0	9	1	34	6	1	0	0	1	0	59	5	26	3	2	0	0	22	1	0	0	8	0	2	300
1927.35	184	31	21	8	1	0	9	1	0	0	35	0	16	6	3	0	0	1	1	86	6	7	3	0	1	2	30	8	1	0	12	7	5	301
1928.1	340	25	19	2	0	0	3	1	5	0	18	0	10	2	0	1	2	1	0	26	5	17	13	4	3	2	15	0	0	0	51	37	38	300
1930.15	310	56	23	7	0	0	6	4	5	3	12	0	22	4	3	0	5	0	0	53	7	20	7	2	2	2	6	0	0	0	22	18	12	301

Sample depth	Lycopodium spike	Undifferentiated trilete spores	Cicatricosisporites spp.	Taurocusporites spp.	Lycopodiumsporites sp.	Todisporites sp.	Appendicisporites spp.	Cyathidites spp.	A. Kerguelensis	Concavisporites sp.	Monosulcate spp.	Clavatipollenites sp.	Undifferentiated bisaccates	D. rarus	Phyllocladidites sp.	Undifferentiated Abietineaepollenites	A. grandialatus	A. microreticulatus	A. microsaccus	R. rugosus	Tsugapollenites sp.	Undifferentiated Inaperturopollenites	I. dubius	I. hiatus	I. rugosus	I. atlanticus	Undifferentiated tricolpates, tricolporates	Undifferentiated tricolpates	Undifferentiated tricolporates	Undifferentiated triporates	Undifferentiated normapolles	Complexiopollis spp.	A. verrucosus	Total sum
1932.35	451	50	26	7	1	2	14	2	3	3	18	2	16	4	1	0	1	2	0	79	4	11	7	4	0	4	12	1	1	0	13	3	13	304
1934.05	210	54	12	9	0	1	9	0	5	1	15	1	42	7	0	0	3	2	1	78	6	15	3	3	0	2	16	1	1	0	7	4	8	306
1934.65	149	37	18	6	0	0	15	1	3	4	18	0	33	5	4	0	2	6	3	61	4	26	6	2	2	6	11	2	1	0	13	8	19	316
1935.35	211	34	10	5	0	0	1	0	3	2	12	0	55	7	3	1	1	4	1	79	5	22	1	0	0	8	11	0	0	0	39	17	7	328
1935.95	110	40	15	3	0	0	11	1	3	4	17	0	39	7	3	0	1	1	2	53	6	22	4	3	2	1	15	2	1	0	27	8	11	302
1936.65	70	13	20	6	2	0	0	8	0	3	10	1	64	11	8	5	2	1	0	97	4	25	8	2	1	6	9	1	0	0	15	7	5	334
1937.35	360	36	6	3	1	0	11	0	3	2	35	4	43	5	2	5	2	2	1	71	6	14	1	2	0	1	10	5	0	0	14	35	7	327
1937.95	386	55	26	5	0	0	5	0	5	5	10	4	39	8	5	2	5	10	2	65	5	15	6	2	1	1	3	7	0	0	9	2	8	310
1938.55	226	53	27	5	1	0	3	0	9	4	18	0	49	10	3	0	6	3	2	56	10	4	5	3	2	6	9	2	4	0	7	21	9	331
1939.35	331	54	11	4	1	0	14	1	6	1	26	2	78	20	13	0	3	4	4	28	14	5	4	0	1	8	10	10	4	0	7	2	2	337
1940.05	372	50	24	3	0	0	23	1	8	1	13	1	46	13	4	0	7	1	4	15	9	9	2	1	0	2	12	8	2	0	12	32	24	327
1940.65	236	37	20	1	1	0	10	6	5	0	16	1	52	16	7	2	0	8	1	20	16	17	9	4	0	5	12	3	1	0	2	20	28	320
1941.25	230	38	44	1	0	0	16	0	7	2	15	1	36	14	4	1	2	5	0	12	3	9	3	4	1	10	7	5	3	0	8	22	29	302
1942.05	189	19	14	0	0	0	8	2	5	0	4	0	33	11	6	0	3	1	2	12	7	16	13	6	1	1	10	8	1	0	20	32	70	305
1943.35	166	20	9	1	0	0	9	6	1	1	7	2	29	18	5	0	2	4	4	16	10	12	2	4	1	5	7	8	1	0	26	30	66	306
1944.55	139	35	14	1	0	0	6	1	5	3	12	0	27	13	4	0	4	3	1	18	8	9	1	9	5	0	3	14	0	0	19	56	40	311
1945.25	365	52	10	0	0	0	15	6	7	1	5	0	34	5	3	0	3	5	1	16	19	19	5	4	2	5	8	1	0	0	22	35	25	308
1946.05	377	56	17	0	0	0	10	1	6	4	8	0	45	16	3	2	1	4	0	22	5	9	6	1	1	2	7	1	0	0	11	43	27	308
1947.35	609	41	6	3	0	0	14	2	1	0	5	0	16	6	2	0	1	1	0	9	3	4	2	0	0	4	5	1	1	0	35	87	61	310
1948.15	308	18	4	1	0	0	5	1	3	2	4	0	6	1	0	0	0	1	0	3	0	13	11	4	3	4	4	0	0	0	77	78	58	301

Sample depth	Lycopodium spike	Undifferentiated trilete spores	Cicatricosisporites spp.	Taurocusporites spp.	Lycopodiumsporites sp.	Todisporites sp.	Appendicisporites spp.	Cyathidites spp.	A. Kerguelensis	Concavisporites sp.	Monosulcate spp.	Clavatipollenites sp.	Undifferentiated bisaccates	D. rarus	Phyllocladidites sp.	Undifferentiated Abietineaepollenites	A. grandialatus	A. microreticulatus	A. microsaccus	R. rugosus	Tsugapollenites sp.	Undifferentiated Inaperturopollenites	I. dubius	I. hiatus	I. rugosus	I. atlanticus	Undifferentiated tricolpates, tricolporates	Undifferentiated tricolpates	Undifferentiated tricolporates	Undifferentiated triporates	Undifferentiated normapolles	Complexiopollis spp.	A. verrucosus	Total sum
1948.65	405	43	9	4	0	0	23	3	11	2	8	0	27	8	3	3	0	3	0	16	2	13	8	4	3	4	16	0	0	0	50	30	34	327
1950.05	400	49	16	8	0	0	7	2	11	4	7	4	28	6	9	2	2	5	0	20	8	21	13	3	1	8	10	10	1	0	18	17	16	306
1951.35	168	54	22	7	0	0	10	1	10	3	16	0	56	14	10	2	2	9	2	34	8	14	6	3	1	3	6	3	1	0	14	3	5	319
1952.05	602	49	22	2	0	0	17	0	5	1	6	0	70	13	5	3	1	5	3	13	8	13	1	0	1	0	9	2	0	0	18	19	17	303
1952.55	389	79	17	8	0	0	27	3	5	5	16	0	52	7	3	0	1	1	2	20	10	16	2	2	0	2	11	3	0	0	12	3	6	313
1953.35	560	81	20	9	0	0	21	3	5	2	12	0	53	4	3	0	0	1	2	11	3	17	2	0	0	1	9	3	0	0	18	9	13	302
1954.05	450	90	18	12	0	0	23	1	5	2	1	0	56	8	1	0	0	1	1	6	4	10	1	2	1	2	14	2	0	0	25	6	15	307
1954.65	1200	69	7	10	20	0	17	2	3	2	11	0	61	7	4	1	1	7	2	26	3	12	1	0	0	3	19	5	0	0	21	1	9	324

F. Sources of botanical affinities for identified taxa

Sporomorph	Botanical affinity	References
Anthocerotophyta		
Taurocusporites	cf. Anthocerotophyta	Gary et al., 2009
Pteridophyta		
Appendicisporites spp.	Schizaeaceae	Peyrot et al., 2011, see article for further references
Alsophilidites	Cyatheaceae	Groot et al., 1961
Cicatricosisporites spp.	Schizaeaceae	Kimyai, 1966
Concavisporites	Matoniaceae	Abbink et al., 2004
Cyathidites spp.	Cyatheaceae	Groot et al., 1961; Kimyai, 1966
Todisporites sp.	Osmundaceae	Gary et al., 2009
Undifferentiated trilete spores	cf. Pteridophyta	Gary et al., 2009
Lycophyta		
Lycopdodiumsporites	Lycopodiaceae	Groot et al., 1961
Coniferophyta		
Abietineaepollenites spp.	Pinaceae	Groot et al., 1961
D. rarus	Podocarpaceae	Groot et al., 1961
I. atlanticus	Araucariaceae	Groot et al., 1961
Inaperturopollenites spp.	Taxodiaceae-Cupressaceae	Eldrett et al., 2009
Phyllocladidites sp.	Podocarpaceae	Groot et al., 1961
Rugubivesiculites rugosus	Podocarpaceae	Groot et al., 1961; Kimyai, 1966
Tsugapollenites sp.	Tsuga (Pinaceae)	Eldrett et al., 2009
Undifferentiated bisaccates	Coniferophyta	Gary et al., 2009
Anthophyta		
A. verrucosus	Fagales	Friis et al., 2003
Clavatipollenites sp.	Chloranthaceae	Friis et al., 2011
Complexiopollis spp.	Fagales	Friis et al., 2003
Undifferentiated normapolles	Fagales	Friis et al., 2003